

ACTIVITY REPORT 2020



ACTIVITY REPORT 2020

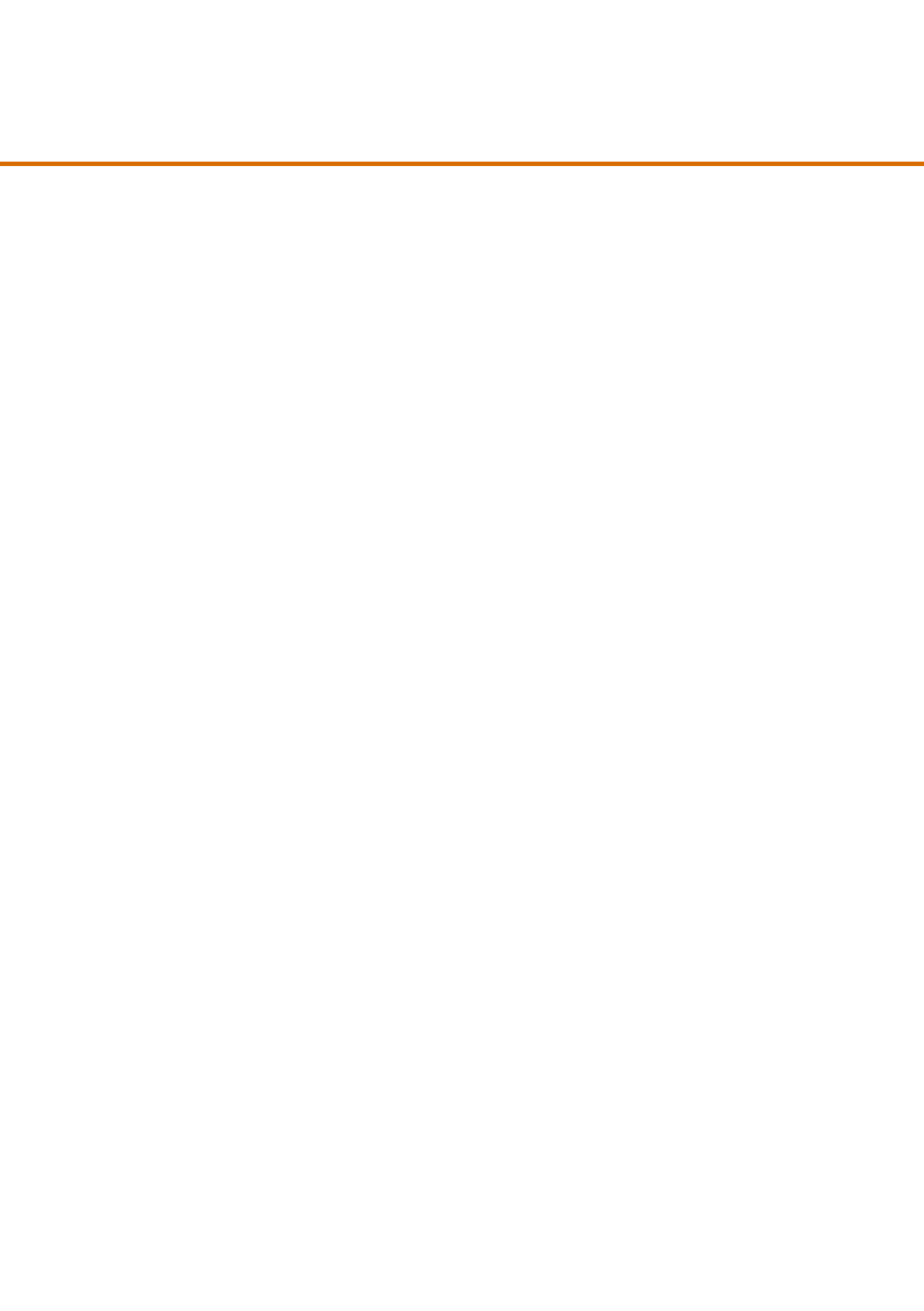


Table of contents

3	FOREWORD
5	HIGHLIGHTS
87	PROJECTS AND GRANTS
103	PUBLICATIONS
113	CNR NANO LIFE
127	PEOPLE

Institute director

Lucia Sorba

Coordinators of units

Modena: Elisa Molinari*

Modena: Massimo Rontani

Pisa: Lucia Sorba

Administrative director

Giovanna Diprima

Executive board

Cnr researchers

Giorgia Brancolini,

Stefan Heun, Paola Luches,

Gian Michele Ratto,

Massimo Rontani

Cnr technical/administrative staff

Luisa Neri

Affiliated researchers

Andrea Alessandrini, Elisa Molinari,

Dario Pisignano, Alessandro Tredicucci

CONTACTS

Piazza San Silvestro, 12

I-56127 Pisa, Italy

ph. +39 050 509418

website: www.nano.cnr.it

e-mail: segreteria.nest@nano.cnr.it

Modena unit

via Campi, 213A

I-41125 Modena, Italy

ph. +39 059 2055629

website: www.nano.cnr.it

e-mail: segreteria.s3@nano.cnr.it

* until 30/09/2018

Foreword



This is the fifth biennial report of the Institute Nanoscience of the National Research Council (Cnr Nano).

The highlights of the years 2018–2019, collected in this Activity Report, have been divided into five strategic areas: solid-state quantum technology, fundamental and translational nanobiophysics, nanoscale theory modelling and computation, physics and technology of light at the nanoscale, and surfaces and interfaces: nanofabrication, imaging, and spectroscopy.

As a result of the stabilization process and the new competitions, the Institute Nanoscience is strongly consolidated. Nineteen new young researchers were recruited in the 2018–2019 period.

An element of excellence of the Institute continues to be the large number of highly competitive projects earned. In particular, in 2019 several European projects started under the Horizon 2020 program: two FET-Open projects, the Centre of excellence MAX, coordinated by Cnr Nano, and an Innovation Action Project H2020-NMBP-to-IND, also coordinated by Cnr Nano. The Institute Nanoscience is also part of the ARTES project - Industry 4.0, and it is one of the laboratories of the High Technology Network of the Emilia Romagna Region. The large number of granted projects is also seen at the local level, where a FAS project of the Tuscany region and one with the Emilia Romagna region have been granted in 2019. Furthermore, in 2020, four projects “Bando Ricerca Salute” of the Tuscany Region, a project with the Fondazione Carilucca, one with ELA International, the project Core3 (continuation of the Graphene Flagship), and an ERC POC will start.

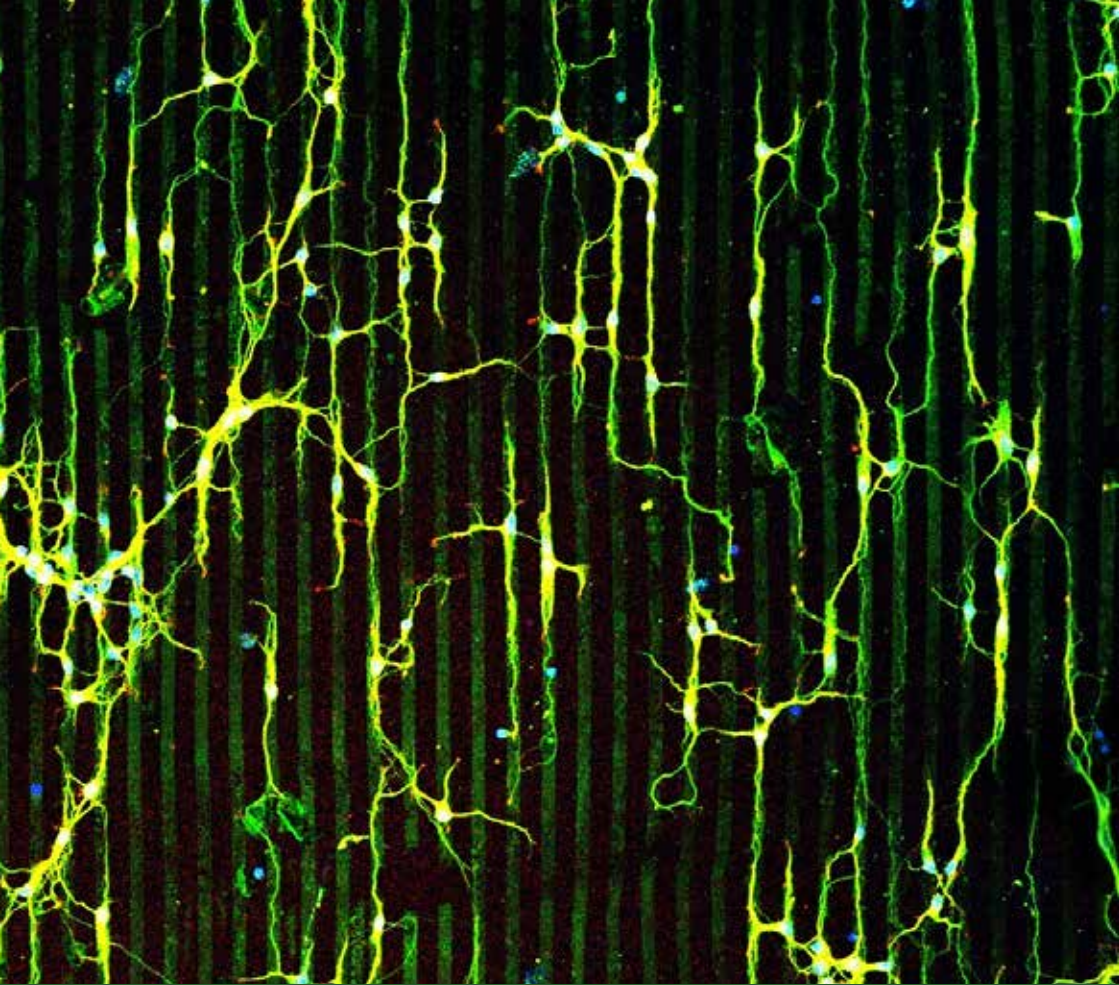
The large impact of Cnr Nano in the national and international context is demonstrated by the large number of publications in high impact factor journals. In the following pages, information on published papers, funded projects, and the events in the period 2018–2019 are presented.

I would like to thank Luisa Neri, Maddalena Scandola, Giorgia Brancolini, Andrea Camposeo, Stefan Heun, Paola Luches, Matteo Carrega, and Andrea Ferretti for their help in making this Report.


Lucia Sorba

Director of the Institute Nanoscience of Cnr





Highlights

-

**Fundamental
and translational
nanobiophysics**

Fundamental and translational nanobiophysics

The research activities are devoted to the understanding at different levels of complexity of the pathogenesis of diseases with high social impact or aging, the development of innovative drugs, and methodologies for detecting pathogens and cell diagnostics. These activities range from the characterization of the interaction between biological moieties and nanostructures materials to studies on the development of novel scaffolds for cell cultures suitable for regenerative medicine. Five main topics are outlined in the following.

Novel Therapeutic Tools. A novel computational strategy is presented to augment experimental studies that aim to optimize the size and surface chemistry of the nanoparticles for the therapeutic use. The activity represents an important step in the delivery of a general coarse-grained strategy which opens the way to the rational design of new tools in biomaterial sciences, nanobiotechnology and nanomedicine.

A study on brain-targeted enzyme-loaded nanoparticles overcomes the limitation of blood-brain barrier crossing for the treatment of Krabbe disease. The smart nanocarriers are developed by specifically engineering nanoparticles with targeting peptides. Enzymes are encapsulated into biocompatible and biodegradable polymeric nanoparticle, active against lysosomal storage disorder. The results open new therapeutic perspectives.

Ubiquitin protein ligase E3A (UBE3A) is studied in neuronal contact guidance as well as the neuronal morphological aspects relevant to Angelman syndrome. The results support the view that UBE3A-related deficits in early neuronal morphogenesis may lead to defective neuronal connectivity and plasticity.

Optical tweezers experiments unravel the calcium-dependent modulation of the misfolding pathways of the human neuronal calcium sensor-1, ultimately highlighting its biological function.

Lab-on-a-chip devices for personalized medicine. A label-free sub-nanomolar biosensor based on Rayleigh surface acoustic waves (R-SAWs) is demonstrated to be an ultra-sensitive, fully electrical, SAW-based nano resonator for sensing applications. The biosensor is benchmarked against biotin-streptavidin binding, providing an enhanced limit of detection with respect to standard commercial gravimetric sensors and generally better than that of common Love-SAW biosensors. The measured sensitivity and dynamic range are promising for a variety of health-related assays, such as cancer biomarker detection.

Biophysics of membrane and cells. New routes based on the interaction of stem cells with novel classes of substrates and smart materials are selected for regenerative medicine. Results highlight the correlation of wetting anisotropy and protein adsorption capacity of different surfaces, ultimate cell conformational changes reflected by skeletal and nuclear elongation, and directed cell commitment. These findings establish rules for the design of next, specifically instructive scaffolds based on nanomaterials for the deterministic reprogramming of stem cells.

Other studies are not represented in this sample, but are worth mentioning since they open new lines of investigation that promise to bring about fallout in the field of theranostic. A line of research is contributing to the rational design of Green Fluorescence Proteins with reversibly switching, a property that has paved the way to novel applications in cell imaging, such as many super-resolution techniques. Another research line uses optical microscopy for revealing the dynamic interplay between chemical stimuli and chromatin organization in normal as well as dysfunctional cells, by using a new toolbox of biomarkers.

Modeling the Interaction between Amyloidogenic Proteins and Functionalized Metal Nanoparticles

Coarse-graining (CG) methodologies offer a trade-off between computational speed and accuracy. The activity represents an important step in the delivery of a general CG strategy for studying protein-inorganic nanoparticles interactions being central to the rational design of new tools in biomaterial sciences, nanobiotechnology and nanomedicine. We have developed a low-resolution CG model to describe the β 2-microglobulin interaction with coated gold nanoparticles. The parameterization strategy relies on atomistic simulations thus it is easily extensible to NPs of different surface chemistry and size. The computational strategy opens the way to a fast and systematic study of the effect of size and functionalization of NPs over therapeutic efficiency.

Metal nanoparticles (NP) of tunable surface properties are studied as therapeutic agents against amyloidogenic diseases [1]. Phenyl functionalized NPs have a double nature due to the hydrophilic gold core and hydrophobic side chain which allows them to strongly interact with amyloidogenic proteins, possibly preventing their aggregation. The potential therapeutic efficiency of these NPs depends on several factors. The need of affinity of the NP with the proteins generally requires functionalizing with hydrophobic groups; on the other hand, this also implies the tendency on

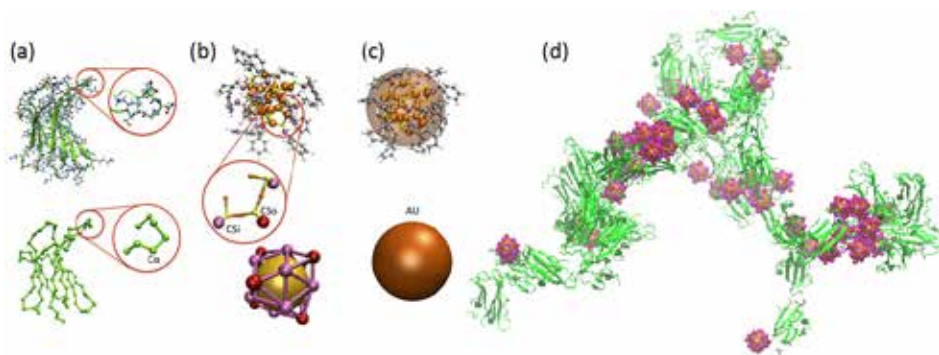


Fig. 1

Coarse graining procedures and simulations: (a) atomistic and CG-minimalist model of the β 2 μ (b) atomistic and CG model for the NP. The detail reports the Au (orange) coordinated S atoms (yellow) with the first C atom of the functionalizing chain, colored according to the two possible different coordinations of their bound S, and named CSo (outer) and CSi (inner), (c) the meso-scale model for the NP, i.e., a single larger bead; (d) multiple solute simulations of the CG model providing the structure of aggregates after 1 μ s, and showing that the NP-protein binding is able to interfere with the protein-protein binding, blocking protein sites for the binding with another protein, thus leading to a potential protein-protein aggregation inhibition. Formation of larger protein-NP aggregates is occurring via NP-NP hydrophobic interactions. Our study suggests that the relative concentrations between proteins and NPs would have an important role on amyloid aggregation. Protein all-atom reconstruction is performed with PULCHRA.

self-aggregation of NPs, which must be limited to increase the availability of the NPs. NP aggregations can in turn be counterbalanced using charged-core particles, whose repulsion depends on the temperature, the ionic strength of the solution, and the concentration of NPs and proteins.

The comprehension of the phase diagram of the NPs-proteins systems as a function of environmental variable (temperatures/concentrations) and of the NPs features (size, charge, functionalization) is necessary in order to optimize their therapeutic action. Computer simulations are a fundamental tool to study these aspects. A full atomistic representation is certainly insightful [1], but has a computational cost that strongly limits the efficient exploration of the phase space. We recently addressed the problem by means of low-resolution representations of the systems components. The amyloid proteins, exemplified by the β 2-microglobulin [2], are represented by means of a single-residue based (minimalist) model, whose parameterization is capable of representing the secondary structure fluctuations and transitions [3] and aggregation. The NPs are represented both at the mesoscale level with a single sphere with double hydrophobic-polar nature, and a finer level with a hydrophilic metal core and hydrophobic functionalizing “beads” [4]. The behavior of mixtures of the two components is studied with different methodologies, including stochastic dynamics and efficient sampling algorithms [5]. Our results give indications on how to improve the structural physical and chemical properties of the NP to optimize their potential therapeutic action.

Contact person

Giorgia Brancolini (giorgia.brancolini@nano.cnr.it)

References

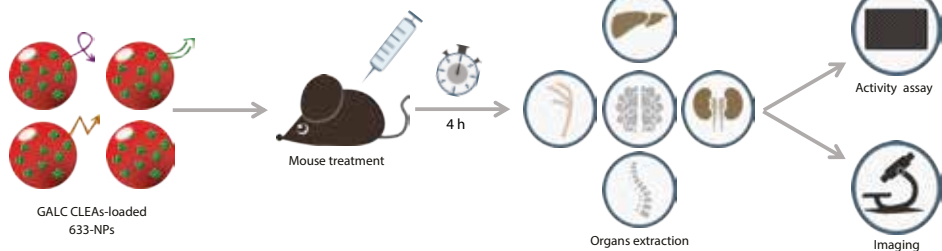
- [1] Citrate stabilized Gold Nanoparticles interfere with Amyloid Fibril formation: D76N and DN6 Variants. G. Brancolini, M. C. Maschio, C. Cantarutti, A. Corazza, F. Fogolari, S. Corni, and G. Esposito. *Nanoscale* 10, 4793 (2018).
- [2] Low-Resolution Models for the Interaction Dynamics of Coated Gold Nanoparticles with β 2-microglobulin. G. Brancolini, H. Lopez, S. Corni, and V. Tozzini. *Int. J. Mol. Sci.* 20 (16), 3866 (2019).
- [3] Structural Transition States Explored With Minimalist Coarse Grained Models: Applications to Calmodulin. F. Delfino, Y. Porozov, E. Stepanov, G. Tamazian, and V. Tozzini. *Front. Mol. Biosci.* 6, 104 (2019).
- [4] Building Minimalist Models for Functionalized Metal Nanoparticles. G. Brancolini and V. Tozzini. *Front. Mol. Biosci.* 6, 50 (2019).
- [5] Multi-scale modeling of Proteins interaction with Functionalized Nanoparticles. G. Brancolini and V. Tozzini. *Curr. Opin. Colloid Interface Sci.* 41, 66-73 (2019).

Brain-targeted enzyme-loaded nanoparticles: A breach through the blood-brain barrier for enzyme replacement therapy in Krabbe disease

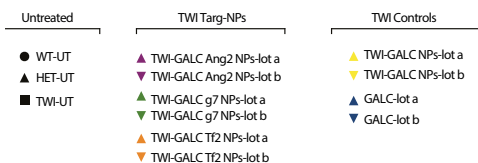
An enzyme brain-delivery system based on the encapsulation of cross-linked enzyme aggregates (CLEAs) into poly-(lactide-co-glycolide) (PLGA) nanoparticles (NPs) functionalized with brain targeting peptides (Ang2, g7 or Tf2) is demonstrated for Krabbe disease, a neurodegenerative lysosomal storage disorder (LSD) caused by galactosylceramidase (GALC) deficiency. We report enzymatic activity measurements in the nervous system and in accumulation districts upon intraperitoneal injections *in vivo*, demonstrating activity recovery in the brain of affected mice up to the unaffected mouse level. Together, these results open new therapeutic perspectives for all LSDs with major brain-involvement.

Krabbe disease [KD] is a fatal neurodegenerative LSD caused by deficiency of the enzyme GALC. GALC's loss of function causes increased levels of the cytotoxic sphingolipid psychosine (PSY) in neural tissues, leading to devastating demyelination [Del Grosso 2016]. The best therapeutic option would be a systemic enzyme replacement therapy (ERT) [Safari 2018], but the presence of the blood-brain barrier (BBB) forbids the translocation of proteins like GALC (77 kDa) into the central nervous system (CNS). In recent years, a lot of interest arose from the development of enzyme-loaded nanosystems, which may enhance the efficacy of ERTs and minimize side effects. We recently described [1] a new encapsulation strategy based on CLEAs into PLGA NPs that allows loading enzymes with excellent efficiency and activity retention. In the present work, we focused on GALC for testing enzyme delivery into the brain *in vivo*. We synthesized and fully characterized new formulations of GALC CLEA-loaded PLGA NPs. These NPs were functionalized with targeting peptides Angiopep-2 (Ang2) [Demeule 2008], g7 [Tosi 2011], or transferrin binding (Tf2) [Santi 2017] peptides, aimed to allow NPs to pass the BBB. We studied NP cell uptake and trafficking and their capability to reinstate enzymatic activity in murine model cells and in fibroblasts from patients with KD [2]. Then, we tested NPs *in vivo* in the spontaneous mouse model of KD (Fig. 1). After intraperitoneal injection we evaluated the presence of NPs and enzymatic activity recovery in different nervous system organs, as well as in typical accumulation districts. We demonstrated the capability of our targeted NPs to vehiculate a large protein into the brain of an LSD murine model, overcoming the BBB and delivering functional enzyme in a therapeutically relevant amount [2]. This approach opens new exciting therapeutic opportunities not only for all CNS-involved LSDs with no cure available to date but also for all disorders, which could benefit from the passage of specific proteins through the BBB to reach CNS.

A Experimental plan



B Legend



C

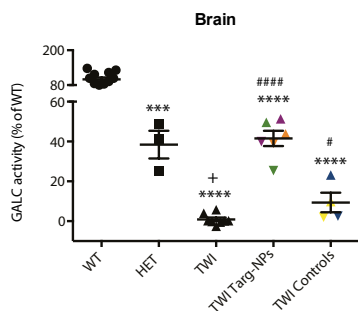


Fig. 1

(A) TWI mice were treated with targeted GALC CLEA ATTO 633NPs (GALC Ang2 NPs, GALC g7 NPs, or GALC Tf2 NPs), non-targeted GALC CLEA ATTO 633 NPs (GALC CLEA NPs), or with the free rm-GALC (GALC). Four hours later mice were euthanized, and GALC activity was assayed in extracted brain, sciatic nerves, spinal cord, kidneys, and liver by HMU-bGal assay.

(B) Untreated: WT (WT-UT), heterozygous (HET-UT), and TWI (TWI-UT). Targeted GALC CLEA ATTO 633 NPs (TWI Targ-NPs): TWI-GALC Ang2 NPs (lot a and lot b), TWI-GALC g7 NPs (lot a and lot b), and TWI-GALC Tf2 NPs (lot a and lot b). Control treatments (TWI Controls): GALC CLEA ATTO633 NPs (TWI-GALC NPs lot a and lot b) and free rm-GALC (GALC-lot a and lot b).

(C) Brain GALT activity. ***P < 0.001 HET versus WT; ****P < 0.0001 TWI, TWI Targ-NPs, and TWI Controls versus WT; + P < 0.05 TWI versus HET; # P < 0.05 TWI Controls versus TWI; ##### P < 0.0001 TWI Targ-NPs versus TWI one-way ANOVA (Tukey's test). Means ± SEM (n = 3 to 12 per group).

Contact persons

Marco Cecchini (marco.cecchini@nano.cnr.it)
Ambra Del Grosso (ambra.delgrosso@nano.cnr.it)

References

- [1] Cross-Linked enzyme aggregates as versatile tool for enzyme delivery: Application to polymeric nanoparticles. M. Galliani, M. Santi, A. Del Grosso, A. Cecchetti, F. M. Santorelli, S. L. Hofmann, J.-Y. Lu, L. Angella, M. Cecchini, and G. Signore. *Bioconj. Chem.* 29, 2225–2231 (2018).
- [2] Brain-targeted enzyme-loaded nanoparticles: A breach through the blood-brain barrier for enzyme replacement therapy in Krabbe disease. A. Del Grosso, M. Galliani, L. Angella, M. Santi, I. Tonazzini, G. Parlanti, G. Signore, and M. Cecchini. *Science Advances* 5, 11, eaax7462 (2019).

The Complex Conformational Dynamics of Neuronal Calcium Sensor-1: A Single Molecule Perspective

The human neuronal calcium sensor-1 (NCS-1) is a multispecific two-domain EF-hand protein expressed predominantly in neurons. Here we review recent studies describing at the single molecule level the structural and mechanistic details of the folding and misfolding processes of NCS-1. The conformational equilibria of the Ca^{2+} -bound, Mg^{2+} -bound and apo states of NCS-1 were investigated by employing optical tweezer assays, revealing a complex folding mechanism underlain by a rugged and multidimensional energy landscape. We discuss the role of inter-domain interactions in shaping the energy landscape of NCS-1, the significance of the misfolding events induced by pathologically high Ca^{2+} concentrations and ultimately the biological function of NCS-1.

Optical tweezers were used to manipulate NCS-1 in the presence and absence of divalent ions [1,2], Fig. 1. In the presence of activating Ca^{2+} concentration, unfolded NCS-1 molecules (U) fold into their native states (N) through a sequence of events coordinated by calcium binding, which involve two intermediate states ($U > I2 > I1 > N$) [2]. Fluctuations of NCS-1 between N, I1, I2 and U were monitored and analysed to reconstruct its energy landscape. Sometimes, in a Ca^{2+} dependent manner, NCS1 can take misfolding pathways leading to two distinct misfolded conformations [2]. In the presence of Mg^{2+} , NCS-1 folds into its native conformation by populating a single intermediate state ($U > I > N$), while in absence of divalent ions the N domain remains always unstructured while the C-domain folds into a compact but loosely folded conformation [2], Fig. 2.

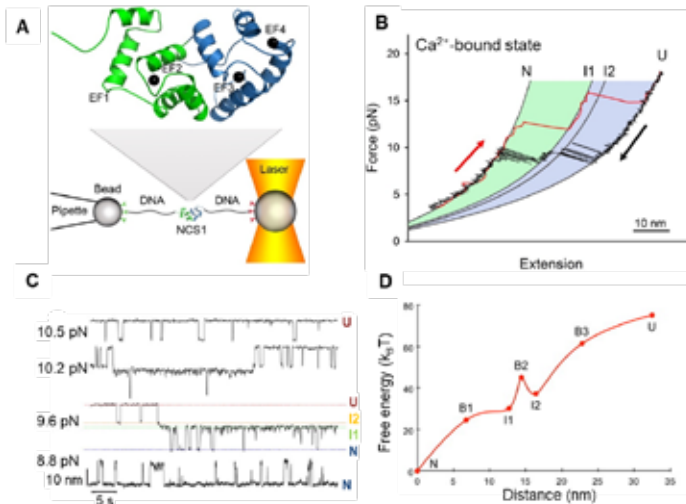


Fig. 1
 A) Mechanical manipulation of NCS-1 with optical tweezers. B) In the presence Ca^{2+} , NCS-1 folds (black trace) into its native state by populating the intermediate states I2 and I1. C) At constant forces, the protein can be observed fluctuating at equilibrium between U, I1, I2 and N, allowing the reconstruction of its energy landscape (D) in terms of activation energy barriers and position of the transition states (indicated with the letter B) along the reaction coordinate [2].

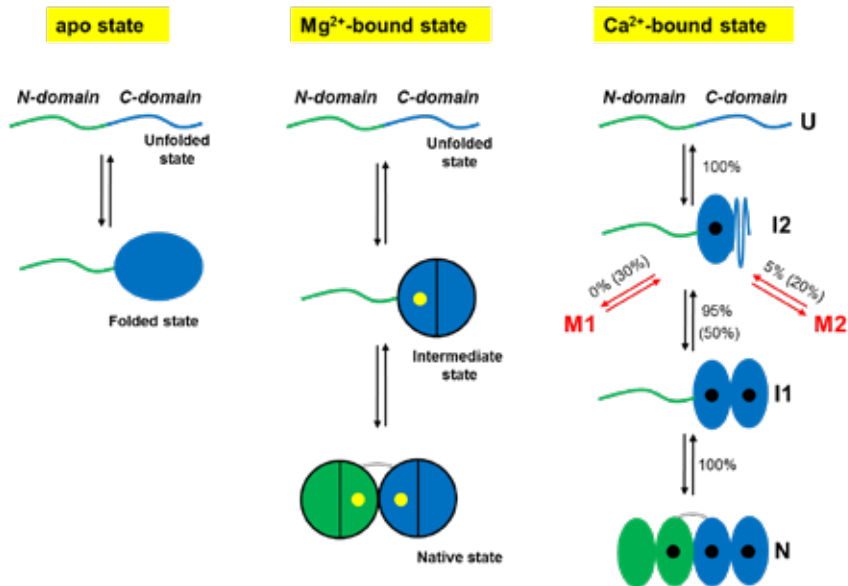


Fig. 2

Folding mechanisms of NCS-1. In the absence of divalent ions, only the C-domain fluctuates between a folded and an unfolded state. In the presence of Mg^{2+} (yellow dots), NCS1 folds through an intermediate state, while in the presence of Ca^{2+} , NCS-1 folds into N through a four-state process. Once populated I_2 , NCS1 can either proceed towards N or take misfolding pathways in a Ca^{2+} dependent manner.

Contact person

Ciro Cecconi (ciro.cecconi@unimore.it)

References

- [1] Bio-Molecular Applications of Recent Developments in Optical Tweezers. D. Choudhary, A. Mossa, M. Jadhav, and C. Cecconi. *Biomolecules* 9, 23 (2019).
- [2] The Complex Conformational Dynamics of Neuronal Calcium Sensor-1: A Single Molecule Perspective. D. Choudhary, B. B. Kragelund, P. O. Heidarsson, and C. Cecconi. *Frontiers in Molecular Neuroscience* 11 (468), 1-8 (2018).

The role of ubiquitin ligase E3A in polarized contact guidance, and rescue strategies in UBE3A-deficient hippocampal neurons

Ubiquitin protein ligase E3A (UBE3A) plays a key role in neurodevelopment: its lack leads to Angelman Syndrome (AS), while its increase to autism (Dup15q syndrome). Here, we investigated the role of UBE3A in neuronal contact guidance, with the aim to identify morphological and molecular aspects relevant for neuronal development in AS and Dup15q syndrome. We studied axon and dendrite growth by using micrograting substrates (GRs) that can induce specific directional stimuli to cells. We found a loss of axonal contact guidance along GRs that is specific for AS neurons and correlates with defective axonal branching and focal adhesions activation. We finally tested different rescue strategies, by either UBE3A protein re-expression or by pharmacological treatments acting on cytoskeleton contractility.

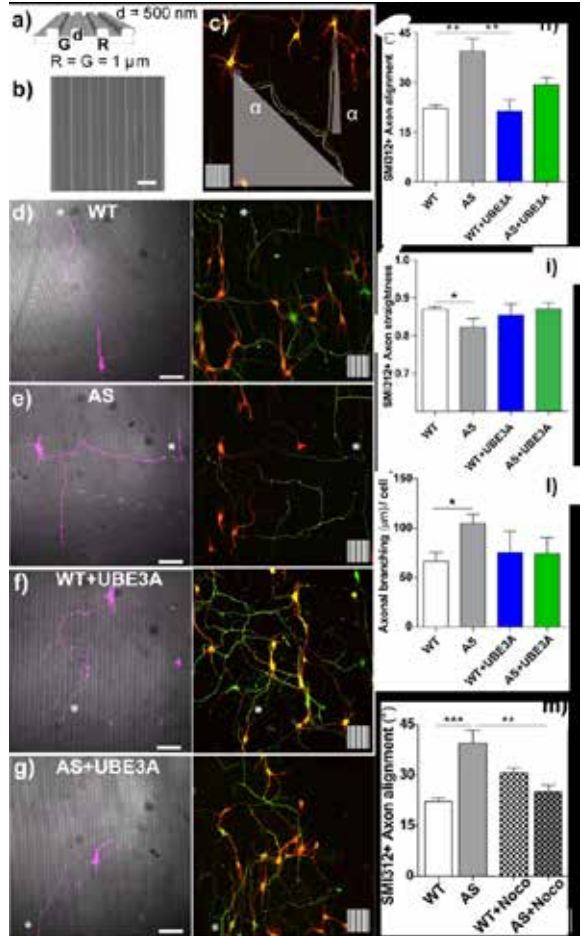
Here, we studied selectively axon and dendrite contact guidance and morphological features of Wild-Type, AS and UBE3A-overexpressing neurons (Dup15q autism model) on GRs (1 μ m ridge, 1 μ m groove, 0.5 μ m depth), with the aim to clarify UBE3A role in neuronal topographical guidance.

We found that AS HNs have a specific deficit in axonal guidance in response to GR directional stimuli *in vitro* (Fig. 1), and show an increased axonal alignment angle to GRs (Fig. 1h) in parallel with reduced straightness (Fig. 1i) and increased secondary axonal branching (Fig. 1l). This deficit is specific to loss of UBE3A, as overexpression of UBE3A has no influence on axon topographical guidance. Deficits at the level of growth cone orientation and actin fiber content, focal adhesion effectors and actin-binding proteins were also observed in AS neurons on GRs (data not shown here). We then tested different rescue strategies for restoring correct topographical guidance in AS neurons on GRs. We tested the effects of pharmacological treatments acting on cytoskeleton. Importantly, Nocodazole, a drug that depolymerizes microtubules and increases cell contractility, rescued AS axonal alignment along GRs (Fig. 1m). We further demonstrated that the defective axonal guidance can be only partially rescued by UBE3A protein reinstatement (Fig. 1h).

Conclusions: We exploited GRs substrates allowing the *in vitro* examination of specific topographical stimuli for neurons. We identified a specific *in vitro* deficit in axonal contact guidance due selectively to the loss of UBE3A and we further demonstrate that this defective guidance can be rescued by pharmacological treatment with Nocodazole, thus acting on cell contractility. Overall, cytoskeleton dynamics emerge as important partners in UBE3A-mediated contact guidance responses. These results support the view that UBE3A-related deficits in early neuronal morphogenesis may lead to defective neuronal connectivity and plasticity.

Fig. 1

a) Scheme of micrograting substrates (GRs): the pattern has 1 μm ridge (R) and 1 μm groove (G) lines, and depth (d) = 500 nm. b) Scanning Electron Microscopy image of thermoplastic GRs, scale bar= 1 μm . c) Scheme of axon tracings for 2 neurons: axon= white continuous line; (α) is the alignment angle between each neuritic trace and the underlying GRs direction (inset, side 50 μm). d-g) Representative confocal images of WT (d), AS (e), WT+UBE3A (f) and AS+UBE3A (g) hippocampal neurons (HNs). WT and AS neurons were cultured on GRs, transfected with empty-Tomato vector (d-e) or with UBE3A 2/3-Tomato vector (f-g) (WT+UBE3A, model of UBE3A overexpression) and immunostained for axonal marker (SMI312, green) and dendrite marker (MAP2, red) (at div4); * indicates axons; the underlying GRs pattern is reported as inset. Scale bars= 50 μm . h) Axonal alignment angle to GRs pattern ($^\circ$); i) Axonal straightness (i.e. ratio between the distance from the initial and end point of the axon and its length); l) Axonal secondary branching (axonal branches in μm / neuron); m) Axonal alignment angle of WT and AS HNs cultured on GRs in the presence of Nocodazole 40 nM (squared): * Bonferroni test; $n \geq 3$, at least 15 HNs/sample.



Contact persons

Ilaria Tonazzini (ilaria.tonazzini@nano.cnr.it)
 Marco Cecchini (marco.cecchini@nano.cnr.it)

Reference

[1] The role of ubiquitin ligase E3A in polarized contact guidance and rescue strategies in UBE3A-deficient hippocampal neurons. I. Tonazzini, G. M. Van Woerden, C. Masciullo, E. Mientjes, Y. Elgersma, and M. Cecchini. *Molecular Autism* 10, 41 (2019).

Functionalized polymer nanostructures for biophysical studies of cell adhesion and lineage commitment

The nanostructuring of bioactive composite polymers offers the interesting opportunity to realize novel classes of smart substrates able to provide specific biophysical cues and direct the stem cell fate. Here, combinatorial surfaces with various fibrous morphology and functionalization with graphene oxide (GO) are employed as cell growth substrates for the culture of primary neurospheres from dental pulp stem cells (DPSCs). The developed materials provide lineage-specific cues that lead to the selective commitment of DPSCs toward osteoblasts, glial cells, fibroblasts, and neurons even in basal medium conditions, suggesting noticeable potentialities for tissue engineering.

Graphene and its derivatives such as graphene oxide (GO) have attracted an unequalled interest in several scientific and technological fields, including regenerative medicine. Indeed, their carrier transport mechanisms and their ultrahigh active surface can potentially influence the cell behavior by directing adhesion, proliferation, and differentiation of stem cells into specific lineages.

We here propose a hybrid approach in which polymer nanofibers of polycaprolactone (PCL) realized by electrospinning are surface functionalized with GO by means of a layer-by-layer method schematized in Fig. 1a. Fibrous scaffolds are particularly interesting for tissue engineering applications, as their nanofilaments structurally mimic the hierarchical organization of the natural extracellular matrix.

We realized four types of PCL scaffolds: fibers with random and aligned orientation functionalized with GO and fibers with random and aligned orientation which undergo the same layer-by-layer processing except for the treatment with GO (Fig. 1b and 1c respectively). The employed method guarantees uniform and homogeneous GO adsorption on the fiber surface, and the overall functionalization significantly affects the surface wettability by increasing the hydrophilicity of PCL. Such effect is fundamental for an efficient cell–substrate interaction.

Finally, we cultured primary neurospheres from DPSCs on the fibrous surfaces and assessed the substrates biocompatibility thus revealing no remarkable cytotoxic effects. In addition, the fiber orientation was found to influence the cell morphology through a cytoskeletal reorganization and a superior cell elongation on aligned fibers scaffolds when compared to the random oriented ones. Through the evaluation of the expression of several differentiation markers, we found that the different scaffolds selectively direct the fate of neurospheres toward four different lineages, such as osteoblastic, glial, fibroblastic, and neuronal as schematized in Fig. 1d. The confocal imaging of specific markers confirms these findings (Fig. 1e). In conclusion, the combination of wetting properties, protein adsorption capacity and effects on cell morphology of the substrate is able to specifically direct the cell commitment without the use of exogenous factors thus unveiling new potentialities for cellular programming.

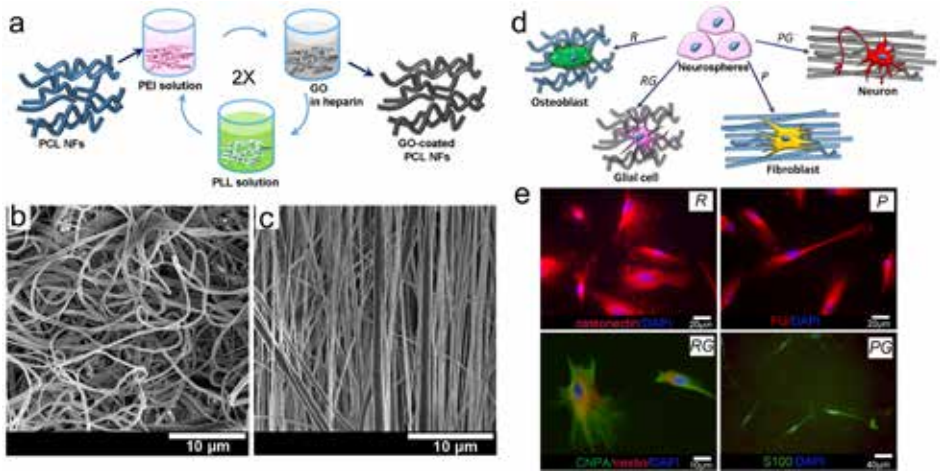


Fig. 1

a) Schematics of the stepwise coating of nanofibers by GO. Briefly, the surface of the scaffolds was activated by soaking in polyethyleneimine dissolved in PBS, then fibers were immersed into heparin with GO, followed by soaking in poly-L-lysine. After every step, fibers were washed in PBS. The immersion, washing, and soaking steps were repeated two times. b,c) SEM images of random (b) and aligned (c) fibers. d) Schematics of the different cell commitment: neurospheres from DPSCs show a differentiation propensity for osteoblastic, glial, fibroblastic, and neuronal cells on random fibers (R), random GO-coated fibers (RG), uniaxially aligned fibers (P) and uniaxially aligned GO-coated fibers (PG), respectively. e) Immunofluorescence staining against osteonectin (red)/DAPI (blue), CNPase (green)/nestin (red)/DAPI (blue), FU (red)/DAPI (blue), and S100 (green)/DAPI (blue) respectively on neurosphere grown on substrate R, RG, P, and PG fibers.

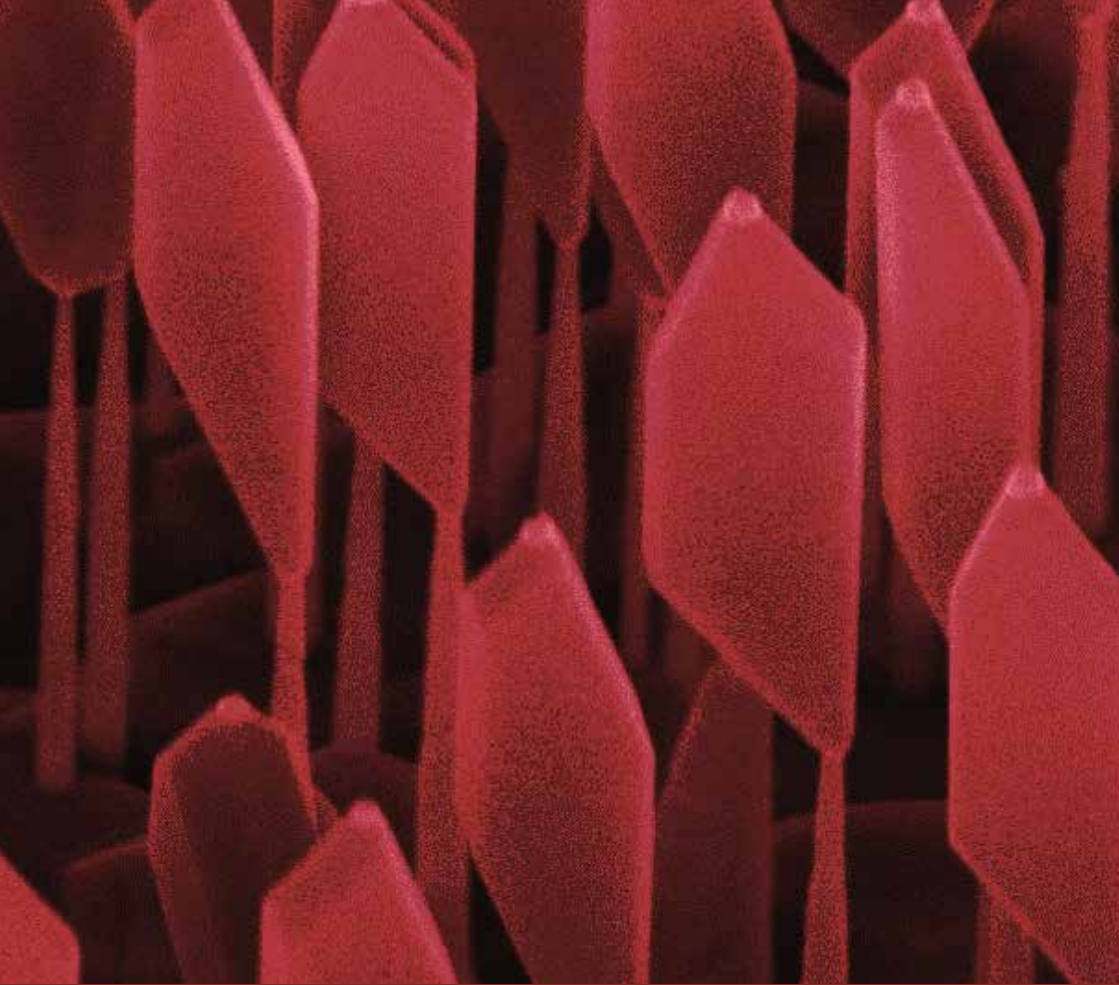
Contact person

Alberto Portone (alberto.portone@nano.cnr.it)

References

- [1] Lineage-Specific Commitment of Stem Cells with Organic and Graphene Oxide-Functionalized Nanofibers. A. Portone, M. Moffa, C. Gardin, L. Ferroni, M. Tatullo, F. Fabbri, L. Persano, A. Piattelli, B. Zavan, and D. Pisignano. *Adv. Funct. Mater.* 29, 1806694 (2019).
- [2] Quasi-3D morphology and modulation of focal adhesions of human adult stem cells through combinatorial concave elastomeric surfaces with varied stiffness. A. Portone, A. G. Sciancalepore, G. Melle, G. S. Netti, G. Greco, L. Persano, L. Gesualdo, and D. Pisignano. *Soft Matter* 15, 5154 (2019).
- [3] Micropatterning control of tubular commitment in human adult renal stem cells. A. G. Sciancalepore, A. Portone, M. Moffa, L. Persano, M. De Luca, A. Paiano, F. Sallustio, F. P. Schena, C. Bucci, and D. Pisignano. *Biomaterials* 94, 57 (2016).





Highlights

-

**Physics and
technology of light
at the nanoscale**

Introduction to Physics and technology of light at the nanoscale

The thematic area of **physics and technologies of light at the nanoscale** investigates phenomena that characterize the interaction of electromagnetic radiation with nanostructured materials. This field encompasses research activities aimed at the realization of innovative inorganic and organic nanomaterials (2-dimensional materials, nanowires, metasurfaces, and nanofibers), the experimental study and modelling of the optical properties of the obtained nanostructures, and the design and realization of photonic and optoelectronic devices, such as continuous wave (cw) and pulsed coherent light sources, photodetectors, optomechanical components, and 3-dimensional (3D) waveguides.

The synthesis and fabrication of elongated nanostructures with high aspect ratio provides a novel class of materials with anisotropic optical properties and the capability of guiding and transporting light at various length scales. Recently, InP-InAs-InP multi-shell NWs were fabricated with emission at multi-wavelengths, attributed to different quantum emitters realized in individual nanowires. Semiconductor nanowires are interesting also for their collective optical properties, as the polarized reflectance of random assemblies of vertical nanowires, which shows well-defined modulation of the intensity by varying the angle of incidence. In addition, polymer nanofibers were reported as flexible elongated nanostructures capable of long-distance transport of the light generated by the nanoscale light sources incorporated in them. Nanofibers can be also assembled in complex nanopho-

tonic networks featuring optical gain, light scattering and lasing tailored by the network architecture.

Nanostructured materials were also designed for the control of the properties of light, such as the intensity, polarization and propagation direction. In this framework, light-responsive 3D structures are being developed by additive manufacturing technologies, which allow light-by-light modulation of the intensity and polarization. In the field of optomechanical systems, GaAs suspended metasurfaces were realized, enabling the arbitrary control of the polarization properties of light interacting with such nanostructured membranes. In these suspended metasurfaces dynamical polarization modulation was reported through the excitation of the mechanical modes of the membrane.

The use of nanopatterned layers and 2D materials is currently being exploited for light generation, and detection, and for the control of beam properties in frequency ranges of the electromagnetic spectrum, such as the terahertz radiation. Here, the integration of 2D nanomaterials (graphene and selenium-doped black phosphorus) in photodetectors with advanced design of the device allowed the detection of THz radiation with high sensitivity and fast response times. Various architectures of quantum cascade lasers (QCLs) have been developed and studied, which allowed the realization of cw electrically pumped random lasers and the QCLs with a low divergence beam, cw operation and single mode emission. Recently, saturable absorbers relevant for passively mode-locked QCLs and quantum cascade lasers combs were reported.

Overall, the combination of nanomaterials with targeted optical properties and of innovative architectures of the devices are opening new directions for applications in technologies such as optical diagnostics, high-resolution microscopy, additive manufacturing, quantum optical sensing and metrology, quantum communication and quantum information.

Photonic Engineering of Terahertz Quantum Cascade Lasers

Quantum cascade lasers (QCLs) operating at THz frequencies have undergone rapid development since their first demonstration. Typically, continuous-wave (CW) operation is required to target application needs, combined with a low divergent spatial profile in the far-field, and a fine spectral control of the emitted radiation. This, however, is very difficult to achieve in practice both when single-mode emission and multimode emission are required. We have recently conceived and devised different approaches to address the aforementioned performance improvements. We demonstrate broadband, electrically pumped continuous-wave quasi-periodic and random QCL and record dynamic range, high-power, fully stabilized, QCL frequency-combs opening the route for novel applications in speckle-free imaging and quantum-metrology.

We develop distributed feedback THz wire QCLs, in which feedback is provided by a sinusoidal corrugation of the cavity, defining the frequency, while light extraction is ensured by an array of surface holes (Fig. 1a). This new architecture, extendable to a broad range of far-infrared frequencies, has led to the achievement of low-divergent beams (10°), single-mode emission, high slope efficiencies (250 mW/A), and stable CW operation.

By exploiting a broadband heterostructure, we furthermore demonstrate the first one-dimensional quasi-crystal distributed feedback laser by lithographically patterning a series of air slits of different widths, following the Octonacci sequence, on the top metal layer of a THz QCL. We tuned the emission from single-mode to multimode over a 530 GHz bandwidth, achieving a maximum peak optical power of 240 mW (190 mW) in multimode (single-mode) lasers with record slope efficiencies up to ≈ 570 mW/A at 78 K and ≈ 700 mW/A at 20 K, wall-plug efficiencies of $\eta \approx 1\%$ and low divergent emission (Fig. 1b).

To push the concept of disordered resonators further, we also developed the first electrically pumped CW random laser (Fig. 1c). By combining this concept with the QCL gain media we obtain a highly collimated vertical emission at ~ 3 THz, with a 430 GHz bandwidth, device operation up to 110 K, peak (pulsed) power of 21 mW, CW emission of 1.7 mW, and continuous frequency tuning over 11 GHz.

The same broadband heterostructure can be also exploited to develop miniaturized frequency comb (FC) sources across hard-to-access spectral regions, as the far-infrared. Four-wave-mixing based QCL-combs are ideal candidates, in this respect, due to the unique possibility to tailor their spectral emission by proper nanoscale design of the quantum wells. We demonstrate full-phase-stabilization of record dynamic range, high power QCL-comb against the primary frequency standard, proving independent and simultaneous control of the two comb degrees of freedom (modes spacing and frequency offset) at a metrological level (Fig. 1d). Each emitted mode exhibits a sub-Hz relative frequency stability, while a correlation analysis on the modal phases confirms the high degree of coherence in the device emission, proving that

this technology is mature for metrological-grade uses, as well as for an increasing number of scientific and technological applications. Finally, by integrating an on-chip tightly coupled mirror with the QCL cavity (Gires Tournois interferometer) we demonstrate tunable, lithographically independent, control of the free-running coherence properties of THz QCL FCs.

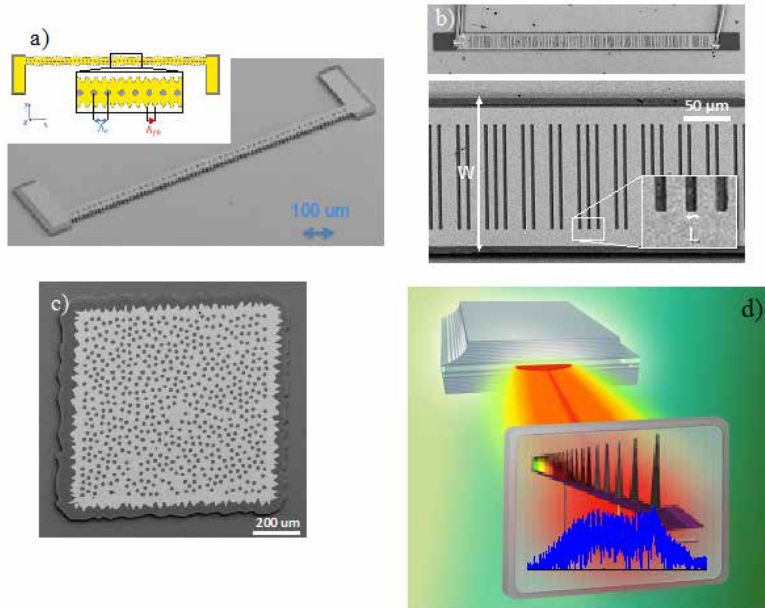


Fig. 1 a) Schematic diagram of the laterally corrugated wire laser and related SEM picture; b) SEM image of an Octonacci quasi crystal THz laser; c) SEM image of a random 2D THz QCL resonator; d) Quantum cascade laser emitting a discrete set of equally spaced modes, each corresponding to the tooth of an optical frequency comb. The semiconductor heterostructure embedded in the QCL active core is schematically shown as a sequence of striped lines.

Contact person

Miriam Serena Vitiello (miriam.vitiello@nano.cnr.it)

References

- [1] Continuous-wave highly-efficient low-divergence terahertz wire lasers. S. Biasco, K. Garrasi, F. Castellano, L. Li, H. E. Beere, D. A. Ritchie, E. H. Linfield, A. Giles Davies, and M. S. Vitiello. *Nat Comm* 9, 1122 (2018).
- [2] Frequency-tunable continuous-wave random lasers at terahertz frequencies. S. Biasco, H. E. Beere, D. A. Ritchie, L. Li, A. Giles Davies, E. H. Linfield, and M. S. Vitiello. *Light: Science & Applications* 8, 43 (2019).
- [3] Fully phase-stabilized quantum cascade laser frequency comb. L. Consolino, M. Nafa, F. Cappelli, K. Garrasi, F. P. Mezzapesa, L. Li, A. Giles Davies, E. H. Linfield, M. S. Vitiello, and P. De Natale. *Nat Comm* 10, 2938 (2019).
- [4] High dynamic range, heterogeneous, terahertz quantum cascade lasers featuring thermally tunable frequency comb operation over a broad current range. K. Garrasi, F. P. Mezzapesa, L. Salemi, L. Li, L. Consolino, S. Bartalini, P. De Natale, A. G. Davies, E. H. Linfield, and M. S. Vitiello. *ACS Photonics* 6, 73 (2019).
- [5] Tunable and compact dispersion compensation of broadband THz quantum cascade laser frequency combs. F. P. Mezzapesa, V. Pistore, K. Garrasi, L. Li, A. G. Davies, E. H. Linfield, S. Dhillon, and M. S. Vitiello. *Optics Express* 27, 20231 (2019).

Near-field THz nanophotonics

Imaging at THz frequencies is severely restricted by diffraction. We here demonstrate nanoscale probe based on semiconductor nanowires and 2D layered materials, providing sub-wavelength resolution at room temperature (RT) in a compact THz imaging system without the need for mode-locked table-top femtosecond pulse lasers, atomic force interaction or demodulation techniques. Furthermore, a novel scattering-type near-field optical microscopy (s-SNOM) system based on a terahertz (THz) quantum cascade laser operating in self-detection mode is here demonstrated providing background-free near-field imaging and nanoscale spatial resolution. The possibility to unveil the plasmonic properties of 2D-materials and heterostructures and probing resonant phonon-polariton modes of layered materials will push forward the development of plasmonic devices, offering unique opportunities to provide fully integrated on-chip high-Q elements with a wide tunability.

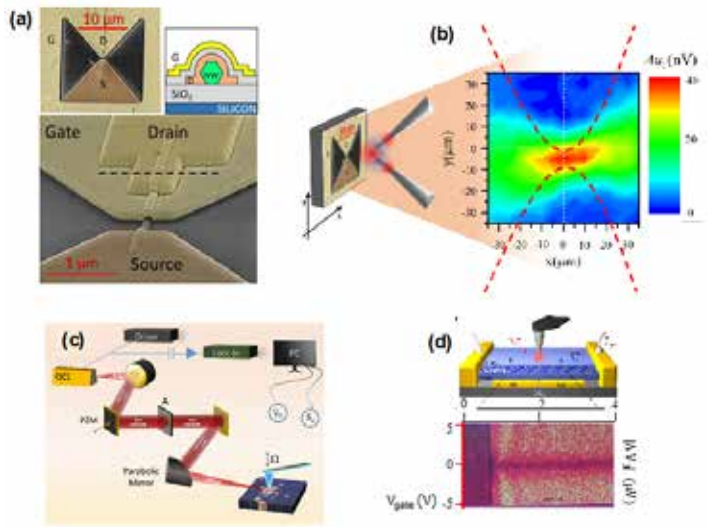
Near-field imaging with terahertz (THz) waves is emerging as a powerful technique for fundamental research in photonics and across physical and life sciences. Spatial resolution beyond the diffraction limit can be achieved either by collecting THz waves from an object through a small aperture placed in the near-field or via scattering near field optical microscopy. However, both approaches suffer from severe limitations in the far infrared.

Light transmission through a sub-wavelength size aperture is fundamentally limited by the wave nature of light. To overcome the above limit, we conceived a novel architecture that exploits the inherently strong evanescent THz field arising within the aperture to mitigate the problem of vanishing transmission. The sub-wavelength aperture is originally coupled to asymmetric electrodes, which activate the thermo-electric THz detection mechanism in a transistor channel made of flakes of black-phosphorus or InAs nanowires (Fig. 1a). The proposed novel THz near-field probes enable room-temperature sub-wavelength resolution coherent imaging with a 3.4 THz quantum cascade laser, paving the way to compact and versatile THz imaging systems and promising to bridge the gap in spatial resolution from the nanoscale to the diffraction limit (Fig. 1b). At THz frequencies, scattering-type scanning near-field optical microscopy (s-SNOM) mostly relies on cryogenic and bulky detectors, which represents a major constraint for its practical application. Amplitude- and phase-resolved near-field imaging is particularly appealing to enable access to the spatial variation of complex-valued dielectric responses of THz frequency resonant 2D materials, heterostructures and low dimensional systems.

We devised the first THz s-SNOM system that provides both amplitude and phase contrast, and achieves nanoscale (60-70nm) in-plane spatial resolution. It features a quantum cascade laser that simultaneously emits THz frequency light and senses the backscattered optical field through a voltage modulation induced inherently through the self-mixing technique (Fig. 1c). We demonstrated its performance by probing a phonon-polariton-resonant CsBr crystal, doped black phosphorus flakes, ink jet printed graphene and propagation of THz acoustic plasmons in graphene (Fig. 1d).

Fig. 1

a) Upper left and lower left: Scanning electron microscope (SEM) images of the near-field probe with an embedded FET-based THz nano-detector (view angles of 0° and 70°). A top gate contact (G) defines the aperture; the aperture size is $18 \mu\text{m} \times 18 \mu\text{m}$; the InAs nanowire detector is at the aperture centre; and the source (S) and drain (D) contacts are isolated from the gate with a layer of SiO_2 (upper right) Schematic diagram of the cross-sectional view of the device. b) Left: schematics of two needles employed for focusing the THz beam to a sub-wavelength spot. The needles are placed in front of the NW nanodetector probe. Right: spatial distribution of the near-field probe photovoltage; the red dotted lines mark the simulated confinement provided by the drain and gate contact. c) Self-detection scattering type near field optical microscope with nanometer resolution at terahertz frequencies: schematic diagram showing the experimental arrangements; d) Propagating THz acoustic plasmons in graphene. Upper: Schematics of the employed device; bottom: third harmonic self-mixing near field signal collected as a function of the gate voltage (V_{gate}).



Contact person

Miriam Serena Vitiello (miriam.vitiello@nano.cnr.it)

References

- [1] Phase-sensitive terahertz imaging using room-temperature near-field nanodetectors. M. C. Giordano, L. Viti, O. Mitrofanov, and M. S. Vitiello. *Optica* 5, 651-657 (2018).
- [2] Phase-resolved terahertz self-detection nearfield microscopy. M. C. Giordano, S. Mastel, C. Liewald, L. L. Columbo, M. Brambilla, L. Viti, A. Politano, K. Zhang, L. Li, A. G. Davies, E. H Linfield, R. Hillenbrand, F. Keilmann, G. Scamarcio, and M. S. Vitiello. *Optics Express* 26, 18423-18435 (2018).

Dielectric metasurfaces for static and dynamic polarization control in the near infrared range

Exploiting the powerful field control capabilities of artificial photonic materials, we developed GaAs suspended nano-structured metasurfaces for an arbitrary control of the polarization state of light. Using a chiral pattern, we showed the possibility of controlling the reflected or transmitted polarization state of light by inverse-designing the system [1]. The static flexibility by design is enriched by the dynamical modulation of the output polarization enabled by the excitation of fundamental mechanical mode of the suspended membrane itself [2]. Acting as a fast (350 kHz) polarization modulator and as a fast polarimeter by exploiting a thermal direct optical spring effect [3], our device represents a novel technology for polarization-based telecom applications with the potential of ultrafast operations when high order mechanical modes are considered.

The first successes in mocking the optical properties of natural materials through nano-structuration quickly led to a rapid research effort which defined metamaterials and metasurfaces as powerful tools for photonic applications; their tunability-by-design with recent computational tools made it possible to develop photonic systems which outperform the natural materials they were inspired from.

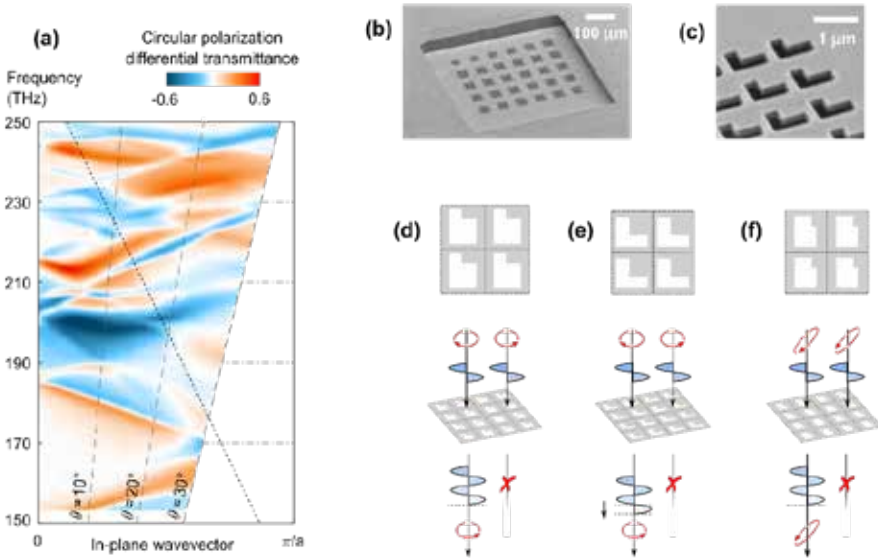


Fig. 1

Static polarization operations of chiral dielectric metasurfaces. (a) Photonic band structure reveals itself in the circular polarization differential transmittance (i.e., circular dichroism for transmitted intensities) measured at oblique incidence. The sample is a dielectric membrane metasurface (b-c), patterned with L-shaped holes. By means of an inverse-design technique we have shown that general wave operations can be performed by specially designed L-shaped holes (d-f).

In our research we exploit this powerful platform to get advanced control on the polarization state of near infrared light for advanced optical components and modulators. In particular, we are interested in working with minimal metasurfaces, composed by patterned single GaAs layers: a typical set of devices is shown in Fig. 1 (b). By defining a chiral geometry, as a simple “L-shape” (Fig. 1 (c)), we can obtain strong linear or circular dichroism, as shown by the measured differential transmittance reported in Fig. 1 (a) [1]. The polarization state, intensity and phase of the reflected and transmitted waves can be arbitrarily controlled by changing the shape of the holes, as demonstrated by numerical simulations based on inverse-design of which special cases are reported in Fig. 1 (d)-(e)-(f).

A further tuning knob of the metasurface properties stems from the mechanical actuation of the suspended membrane that hosts the chiral pattern. We demonstrated that, due to the high phase sensitivity of the metasurface, tiny displacements from equilibrium position lead to strong modification of the light polarization and phase state (Fig. 2 (a)). Using the ~350 kHz fundamental membrane mode (Fig. 2 (b)), we can obtain a fast, dynamic modulation along non-trivial paths on the Poincaré sphere, as shown by the colored lines in Fig. 2 (c), which indicate the response at different laser wavelengths [2]. Exploiting the back-action of light on the mechanics induced through thermal effects (Fig. 2 (d)), we can use the same device as a fast polarimeter, where we can uniquely associate to each input polarization state an amplitude and frequency of the mechanical resonance (the latter shown in Fig. 2 (e)) [3]. The potential of increasing the operating frequencies exploiting higher order modes makes our system particularly appealing for fast light modulation technology.

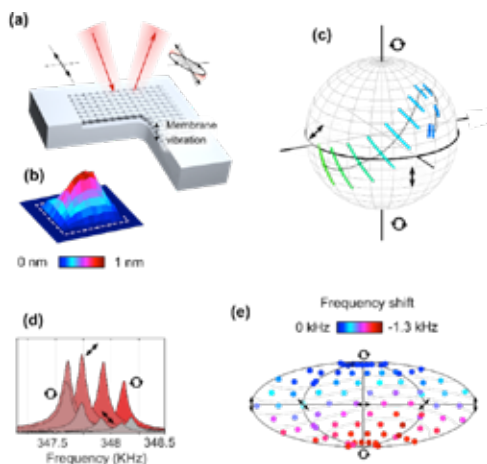


Fig. 2

Dynamic polarization operation and back-action. A dielectric membrane is fabricated in close vicinity to a bulk substrate with a monolithic technique (a); thanks to a form of optomechanical interaction the membrane vibration is translated into amplitude and polarization modulation of the reflected light beam. The membrane vibrates with drum-like motion (b). Details of the polarization modulation paths represented on the Poincaré sphere (c). If the structure is illuminated with light of different polarization, the mechanical resonance frequency and transduction amplitude are affected (d); this effect has a peculiar fingerprint when plotted on the projected Poincaré sphere (e).

Contact persons

Alessandro Pitanti (alessandro.pitanti@nano.cnr.it)

Simone Zanutto (simone.zanutto@nano.cnr.it)

References

- [1] Photonic bands, superchirality, and inverse design of a chiral minimal metasurface. S. Zanutto, G. Mazzamuto, F. Riboli, G. Biasiol, G. C. La Rocca, A. Tredicucci, and A. Pitanti. *Nanophot.* 8, 2291–2301 (2019).
- [2] S. Zanutto and A. Pitanti, US Provisional Patent Application: Optomechanical Modulator, Patent Pending
- [3] Optomechanics of chiral dielectric metasurfaces. S. Zanutto, A. Tredicucci, D. Navarro-Urrios, M. Cecchini, G. Biasiol, D. Mencarelli, L. Pierantoni, and A. Pitanti. *Adv. Opt. Mat.* 1901507 (2019).

Semiconductor nanowires for light emission, reflection and guiding

Semiconductor nanostructures with large dielectric constant and high aspect ratio, such as nanowires (NWs), represent a formidable playground for the study of light-matter interactions, nanophotonics and nano-optics. Building on our expertise in the InAs/InP NW growth technology, we engineered InP-InAs-InP multi-shell NWs that behave as polychromatic emitters in the energy range from 0.7 to 1.6 eV. Besides, we proposed ensembles of GaAs/AlGaAs core/shell NWs as an effective medium for light manipulation in reflection geometry. Finally, we investigated the waveguiding properties of multi-branched SnO₂ NWs.

We investigated the photoluminescence (PL) emission from InP-InAs-InP multi-shell NWs, observing different PL features ascribable to distinct emitting domains: InAs quantum dot and well, and InP crystal-phase quantum disks arising from the co-existence of zincblende (ZB) and wurtzite (WZ) segments in the same InP NW [1]. Moreover, we studied the anisotropy of the g-factor tensor and diamagnetic coefficient in WZ/ZB crystal-phase quantum dots (QDs) realized in single InP nanowires [2] (see Fig. 1). The WZ and ZB alternating axial sections in the NWs were identified by high-angle annular dark-field scanning transmission electron microscopy (HAADF-STEM). The electron (hole) g-factor tensor and the exciton diamagnetic coefficients in WZ/ZB crystal-phase QDs were determined through micro-PL measurements at 4.2 K with different magnetic field configurations, and rationalized by invoking the spin-correlated orbital current model.

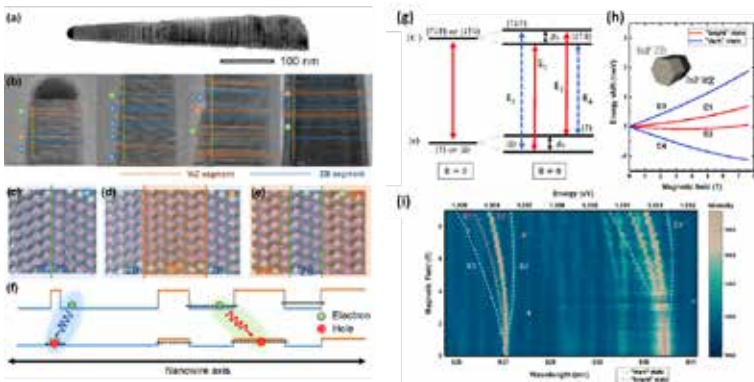


Fig. 1

(a) Dark field STEM image of an InP NW. (b) STEM-HAADF images of different InP NW segments. Different symbols correspond to different structures depicted in Fig. (c)-(e), where the ball-and-stick model of different segments and atomic resolution STEM images are reported. (f) Schematic energy level of the WZ/ZB sequence in the InP NW. (g) Energy diagram of the negatively-charged-exciton with B perpendicular to the growth axis. (h) Energy shift of the four possible transitions of charged exciton, as a function of B. (i) Magneto-PL spectra of X- and XX- with $B_{\text{out-of-plane}}$ from 0 to 9 T.

Arrays of scatterers with subwavelength size and periodicity enable light manipulation and an extraordinary control of the light-matter interaction at the nanoscale. We demonstrated that random assemblies of vertically aligned core-shell GaAs-AlGaAs NWs display an optical response dominated by periodic modulations of the polarization-resolved reflected light as a function of the incident angle [3] (see Fig. 2). Numerical simulations link the observed oscillatory effects to the core and shell thickness and the tapering of the nanostructure. Our results suggest the use of III-V NW arrays as optical meta-mirrors with perspective for sensing applications.

Mesoscale and nanoscale systems with a topology characterized by bends or crossings - such as V-, T- or Y-shaped, crosswise or multi-armed structures - provide a fascinating playground for the study of guiding and interference phenomena. We focused on individual multibranching SnO₂ nanostructures with “nodes,” i.e. locations where two or more branches originate, and we studied how light propagates when a laser source is focused onto a node [4]. Combining scanning electron microscopy and optical analysis, Raman and Rayleigh scattering, we unveil the mechanism behind the light-coupling occurring at the node.

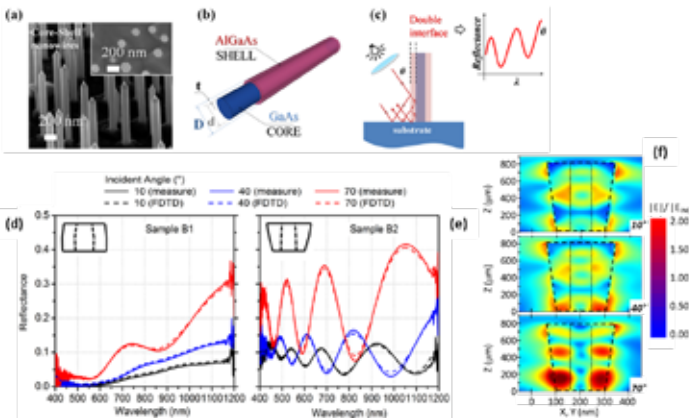


Fig. 2 (a) 45° tilted SEM image of GaAs-AlGaAs core-shell (C-S) NWs. (b) Sketch of a C-S NW. (c) Shining light onto the lateral surface of a C-S NW. Measured (solid line) and simulated (dashed line) reflectance for a (d) non-tapered and (e) tapered C-S NW sample. (f) Near-field electric field expansion for tapered C-S sample (incident angle is indicated).

Contact person

Francesco Rossella (francesco.rossella@sns.it)

References

[1] Polychromatic emission in a wide energy range from InP-InAs-InP multi-shell nanowires. S. Battiato, S. Wu, V. Zannier, A. Bertoni, G. Goldoni, A. Li, S. Xiao, X. D. Han, F. Beltram, L. Sorba, X. Xu, and F. Rossella. *Nanotechnology* 30, 194004 (2019).

[2] Anisotropies of the g-factor tensor and diamagnetic coefficient in crystal-phase quantum dots in InP nanowires. S. Wu, K. Peng, S. Battiato, V. Zannier, A. Bertoni, G. Goldoni, X. Xie, J. Yang, S. Xiao, C. Qian, F. Song, S. Sun, J. Dang, Y. Yu, F. Beltram, L. Sorba, A. Li, B.-i Li, F. Rossella, and X. Xu. *Nano Research* 12, 2842-2848 (2019).

[3] Strong modulations of optical reflectance in tapered core-shell nanowires. F. Floris, L. Fornasari, V. Bellani, A. Marini, F. Banfi, F. Marabelli, F. Beltram, D. Ercolani, S. Battiato, L. Sorba, and F. Rossella. *Materials* 12, 3572 (2019).

[4] 3D Multi-branched SnO₂ semiconductor nanostructures as optical waveguides. F. Rossella, V. Bellani, M. Tommasini, U. Gianazza, E. Comini, and C. Soldano. *Materials* 12, 3148 (2019).

Fast and sensitive nanodetectors at Terahertz frequency

Two-dimensional (2D) materials and related heterostructures are emerging as potential building blocks for devising photonic and nanoelectronic devices and components spanning from the X-ray to the visible, telecom, infrared and microwave frequency ranges, owing to their flexibility in terms of electro-mechanical properties, absorption bands, platform integrability and large-scale production capability. We recently broadened the frequency coverage of 2D-materials based ultrafast devices to the terahertz (THz) frequency range allowing state-of-the-art performance in terms of detection and manipulation of THz light and showing the intriguing possibility of integration with existing THz sources to shed new light on the physical mechanisms underlying their operation and to address applications still not exploited so far.

Uncooled Terahertz (THz) photodetectors (PDs) showing fast (ps) response and high sensitivity (noise equivalent power (NEP) $< \text{nW/Hz}^{1/2}$) over a broad (0.1-10 THz) frequency range are needed for applications in high-resolution spectroscopy (precisions of 10⁻¹¹), metrology, quantum information, security, imaging, optical communications. However, present THz receivers cannot provide the required balance between sensitivity, speed, operation temperature, and frequency range.

We recently exploited 2D materials as photoactive nanosystem to overcome all of these limitations in one device.

We developed novel THz-frequency detectors exploiting hBN/graphene/hBN heterostructures that exploit the photo-thermoelectric effect. The core structure relies on a novel architecture that employs a dual-gated, dipolar antenna with a gap of 100 nm. We demonstrate that this new detector has excellent sensitivity, with a noise-equivalent power of 80 pW/Hz^{1/2} at room temperature, a response time below 30 ns (setup-limited), a high dynamic range (linear power dependence over more than 3 orders of magnitude) and broadband operation (measured range 1.8 - 4.2 THz, antenna-limited), which fulfills a combination that is currently missing in the state of the art (Fig. 1a-b).

We also demonstrate that by integrating our RT THz nano-receivers with lithographically-patterned high-bandwidth (~100 GHz) chips, we can further improve the detection speed to hundreds ps response times, preserving the high sensitivity (Fig. 1c). Remarkably, this can be achieved with various antenna and transistor architectures (single gate, dual gate) for any frequency in the 0.1-10 THz range, thus paving the way for the design of ultrafast graphene arrays in the far infrared, opening concrete perspective for targeting the aforementioned applications.

If graphene can be an interesting material system for THz oriented applications due to its high mobility and gapless nature, the inherent in-plane anisotropy of BP, combined with the tuneable bandgap, makes it an appealing and intriguing alternative for many applications in the far infrared.

We therefore exploited the intrinsic chemical stability of thin flakes of Se-doped BP, combined with the strong electrical and thermal anisotropy and the possibility to

control, via its thickness, the energy gap to develop high sensitive room-temperature photodetectors at 3.4 THz with state of the art performances and different layer thicknesses (Fig. 1d).

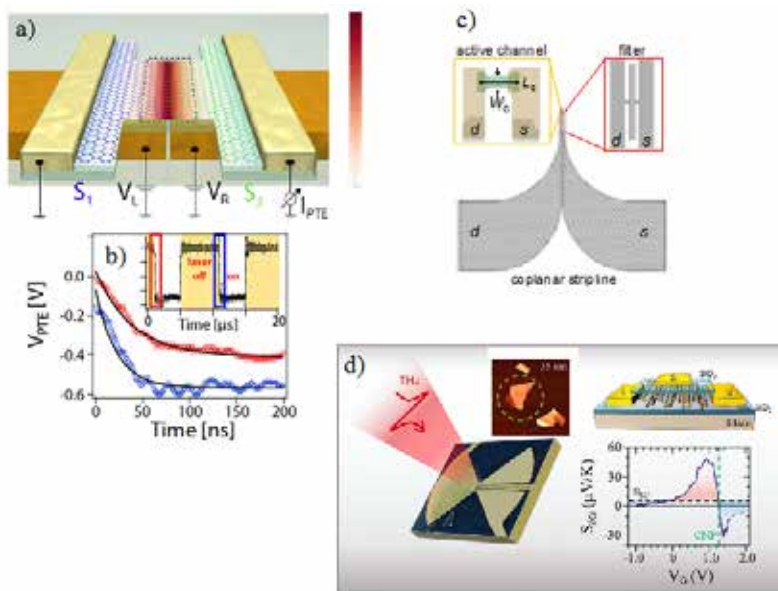


Fig. 1

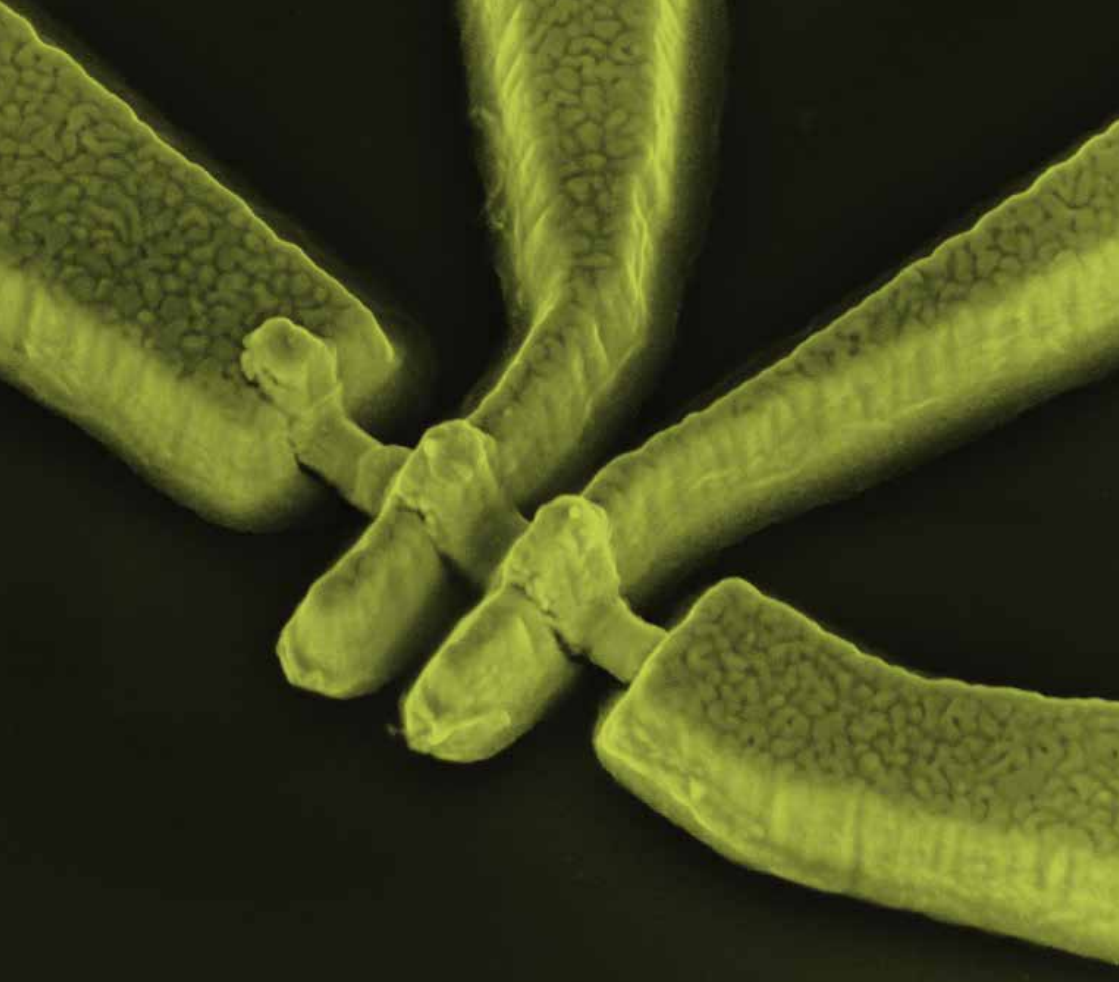
a) Schematic representation (right; not to scale) of the antenna-integrated pn-junction graphene photodetector; b) Results of the pulsed laser experiment, where the photocurrent was amplified by a fast-current pre-amplifier (Femto) and the data were acquired with a fast oscilloscope. The inset shows how the photovoltage V_{PTE} follows the switching of the pulsed laser; c) On-chip RF components. The S and D electrodes are shaped in a CPS geometry. Inset (left): the shape of the active LMH channel (green area) guarantees a lower contact resistance with respect to a rectangular geometry. The S and D contacts have a thickness of 45 nm in vicinity proximity of the GFET channel (yellow areas) and a thickness of 140 nm far from the GFET channel. Inset (right): planar low-pass filter, with cut-off frequency 300 GHz; d) Terahertz detection activated by photo-thermoelectric effect in selenium-doped thin (35 nm) black phosphorus flakes.

Contact persons

Miriam Serena Vitiello (miriam.vitiello@nano.cnr.it)
Leonardo Viti (leonardo.viti@nano.cnr.it)

References

- [1] Thermoelectric terahertz photodetectors based on selenium-doped black phosphorus flakes. L. Viti, A. Politano, K. Zhang, and M. S. Vitiello. *Nanoscale* 11, 1995 (2019).
- [2] Fast and Sensitive Terahertz Detection Using an Antenna-Integrated Graphene pn Junction. S. Castilla, B. Terrés, M. Autore, L. Viti, J. Li, A. Y. Nikitin, I. Vangelidis, K. Watanabe, T. Taniguchi, E. Lidorikis, M. S. Vitiello, R. Hillenbrand, K. Tielrooij, and F. H. L. Koppens. *Nano Letters* 19, 2765 (2019).
- [3] Plasmonics with two-dimensional semiconductors: from basic research to technological applications. A. Agarwal, M. S. Vitiello, L. Viti, A. Cupolillo, and A. Politano. *Nanoscale* 10, 8938 (2018).



Highlights

-

**Solid-state quantum
technology**

Introduction to Solid-state quantum technology

Research in solid state quantum technology focuses on the fabrication, investigation, and implementation of novel nanodevices. Joint experimental and theoretical activity is devoted to the study of quantum systems and phenomena, and aims at developing novel concepts and ideas, with potential impact on future applications. Advanced fabrication techniques and low-temperature magneto-transport measurements are developed along four main research lines, as described below.

Topologically protected quantum technology. The study of topological states of matter, intrinsically robust to external perturbations, is of great interest for new quantum computing architectures. Hybrid superconductor/semiconductor devices with strong-spin-orbit coupling represent an ideal platform to inspect this new physics. The quest for unambiguous signatures of the presence of topological quasiparticles, like Majorana fermions, has become a priority and is stimulating significant research efforts. Systems based on Josephson junctions, quantum Hall setups, topological insulators, and InAs nanowires are modelled and investigated by means of low-temperature quantum transport experiments.

Charge and thermal transport at the nanoscale. Precise control of charge and heat transport at the nanoscale is at the heart of new technological advances. High-quality semiconducting nanowires and quantum dots are currently investigated, showing outstanding thermoelectric performance with high figure of merit. Tailoring of energy flow and heat flux is also achieved in hybrid systems with superconducting elements, with possible applications as thermal routers, heat converters, and nanorefrigerators. Both charge and heat transport are manipulated by electrostatic means by properly patterned side gates on the nanostructures. Unexpected gating effects have been recently reported on fully metallic superconducting systems, rising several open issues both from a fundamental point of view and for potential applications in superconducting qubits manipulation.

Superconducting spintronics. Spintronics is a research field wherein two fundamental branches of physics, magnetism and electronics, are combined. One of the promising perspectives of spintronics is the possibility to control spin and charge at the nanometer scale, both at classical and quantum (qubit) level, limiting unwanted heating effects. Recent advances allowed to combine ferromagnetic insulators with superconductors, enabling control of spin polarization with high precision and possible applications in quantum sensing, like magnetometers and spin valves. Moreover, molecular spin systems can be engineered and coherently manipulated with unprecedented precision in combination with microwave planar resonators made of high-temperature superconductors.

Quantum metrology and simulation. Quantum features of nanosystems are exploited to achieve high-precision measurements and to set new metrological standards. Present work focuses on the development of graphene and other 2D materials for quantum Hall resistance standards. Other activities concern quantum magnetometry based on the use of thermal states of single and collective spins, and on the measurement of the spin projection along optimal directions. Precise manipulation of electrons in nanostructured environment and their interactions with optical beams offers interesting possibilities to simulate complex systems in a controlled fashion, building a toolbox to study quantum phenomena.

Investigation of hybrid Josephson junctions for topological applications

InAs-based devices are studied, in combination with superconductors, for new topological applications. Low-temperature magnetotransport measurements on suspended InAs nanowires revealed important information on the intrinsic spin-orbit coupling. Side-gate tuning can be used to control spin-orbit length. We have inspected Josephson junctions with a high-mobility InAs quantum-well bridging two Nb superconductors. We demonstrate supercurrent flow with critical temperature up to 8.1 K and high critical field. Low-temperature transport shows clear quantum Hall plateaus, allowing for the study of the coexistence of superconductivity and quantum Hall effect. Superconducting quantum interference patterns can be tuned by external gates.

Recent experimental and theoretical activities focused on hybrid semiconductor/superconductor systems, aiming at the emergence of new topological states of matter, like Majorana fermions or parafermions. Hybrid superconductor/semiconductors with strong spin-orbit coupling offer a promising platform in this direction. Low-temperature transport measurements with a vector magnet on a suspended InAs nanowire (Fig. 1a) allowed to report a weak anti-localization signal (Fig. 1b) and to extract polar maps of spin-orbit length and coherence length. We demonstrated that the spin-orbit interaction is isotropic and can be controlled by external side gates [1,2].

Hybrid Josephson junctions (Fig. 2a) formed by an InAs quantum-well placed between two Nb contacts have been investigated as well. Transport measurements revealed a critical temperature up to 8.1 K and a high critical field (of the order of 3 T). Modulation of supercurrent amplitude is achieved by acting on side gates. Well-developed quantum Hall plateaus have been also observed (Fig. 2b). These samples therefore allow to study the coexistence of topological edge states and superconductivity [2,3].

We fabricated and investigated a hybrid trenched Josephson junction in which the width, area, and supercurrent of the two arms of a SQUID-like geometry can be independently controlled with high precision. We demonstrate wide tunability of interference patterns by electrostatic means, from a SQUID with narrow arms to a Fraunhofer pattern in an extended JJ [4]. These results pave the way for new device architectures with potential topological applications.

In parallel, theoretical activities on parafermionic models have been conducted. Microscopic descriptions of parafermionic chains, based on a tight binding model and on generalized hydrodynamic approaches have been inspected, discussing both equilibrium thermodynamic properties and non-equilibrium dynamics under temperature gradients. A deep theoretical understanding of the fundamental properties of parafermions will be useful in view of new experiments aiming at the detection of these elusive quasiparticles [5,6].

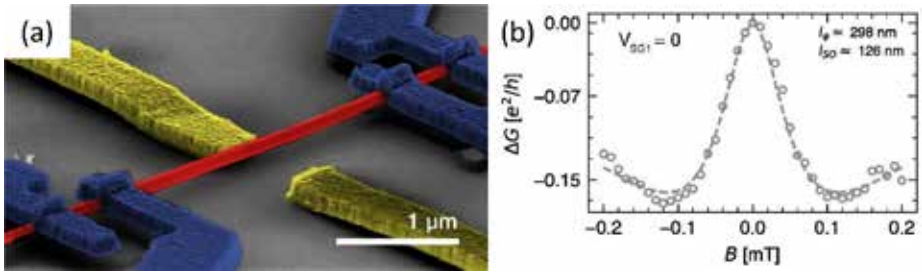


Fig. 1

(a) False-colored SEM image of a representative device with four-wire measurement setup. A suspended InAs nanowire (in red) is contacted with four ohmic contacts (in blue). Two lateral gate electrodes (in yellow) allow to induce tunable electric fields inside the wire and modulate the spin-orbit interaction. (b) The conductance correction $\Delta G(B) = G(B) - G(0)$ is shown as a function of magnetic field applied along the z-axis at zero external gate voltages $V_{SG1} = V_{SG2} = 0$. The peak at zero field is due to the weak anti-localization effect.

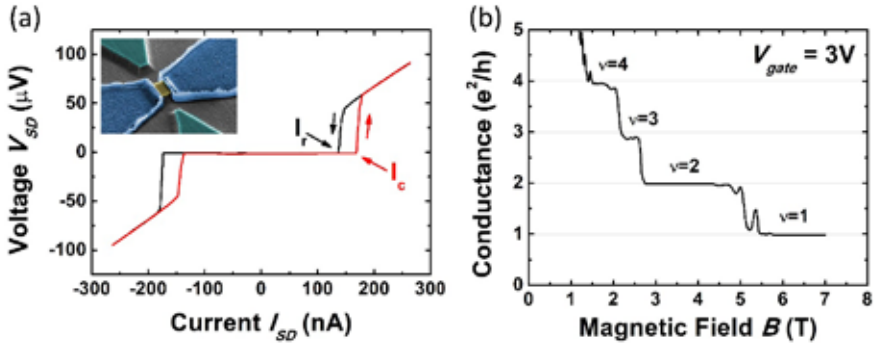


Fig. 2

(a) Source-drain voltage V_{SD} vs. source-drain current I_{SD} of InAs-based Josephson junction. The black (red) arrow shows the direction of the black (red) sweep. The inset shows a false color SEM image of the device. The mesa is yellow, side gates are green, niobium is blue. (b) Conductance (in units of e^2/h) as a function of magnetic field, showing well-developed quantum Hall plateaus already at 1.5 T.

Contact person

Matteo Carrega (matteo.carrega@nano.cnr.it)

References

- [1] Vectorial control of the spin-orbit interaction in suspended InAs nanowires. A. Iorio, M. Rocci, L. Bours, M. Carrega, V. Zannier, L. Sorba, S. Roddaro, F. Giazotto, and E. Strambini. *Nano Lett.* 2, 652 (2019).
- [2] Investigation of InAs based devices for topological applications. M. Carrega, S. Guiducci, A. Iorio, L. Bours, E. Strambini, G. Biasiol, M. Rocci, V. Zannier, L. Sorba, F. Beltram, S. Roddaro, F. Giazotto, and S. Heun. *Spintronic XII Proc. of SPIE 11090, 110903z* (2019).
- [3] Towards quantum Hall effect in a Josephson junction. S. Guiducci, M. Carrega, G. Biasiol, L. Sorba, F. Beltram, and S. Heun. *Phys. Status Solidi RRL* 13, 1800222 (2019).
- [4] Full electrostatic control of quantum interference in an extended trenched Josephson junction. S. Guiducci, M. Carrega, F. Taddei, G. Biasiol, H. Courtois, F. Beltram, and S. Heun. *Phys. Rev. B* 99, 235419 (2019).
- [5] Energy transport in an integrable parafermionic chain via generalized hydrodynamics. L. Mazza, J. Viti, M. Carrega, D. Rossini, and A. De Luca. *Phys. Rev. B* 98, 075421 (2018).
- [6] Anyonic tight-binding models of parafermions and of fractionalized fermions. D. Rossini, M. Carrega, M. Calvanese Strinati, and L. Mazza. *Phys. Rev. B* 99, 085113 (2019).

Field-effect control of metallic superconducting systems

The electric field is believed to have no influence on metallic superconductors. However, recent experiments have shown that the properties of a superconductor can be manipulated via field-effect. Here, we report on the electrostatic control of the supercurrent in superconducting wires, nano-constrictions, in superconductor-normal metal-superconductor (SNS) proximity transistors. Later, we discuss the action of the electrostatic field on the superconducting phase, by reporting on a gated SQUID and on the switching current probability distribution of a gated Josephson junction (JJ). We conclude discussing some device applications of this phenomenology.

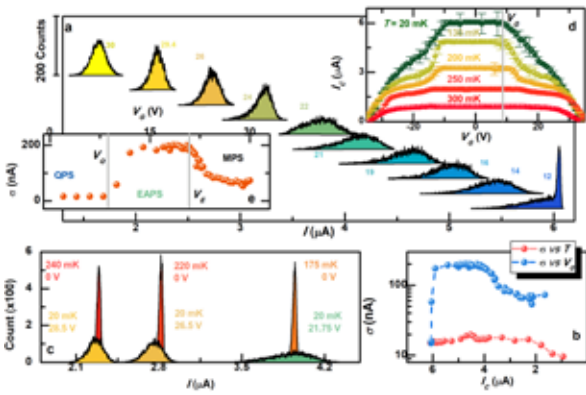
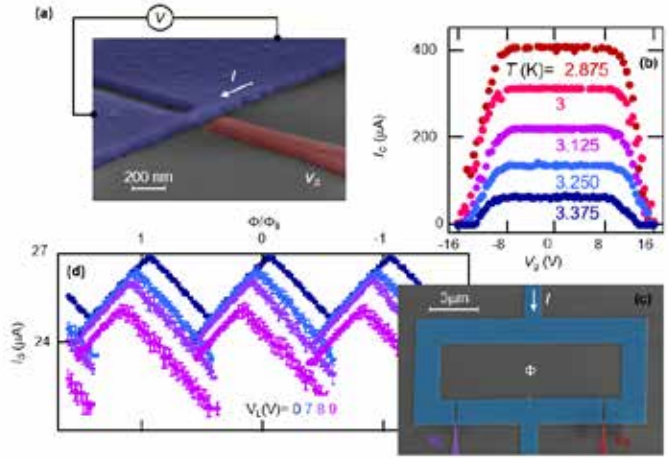
Following from the Bardeen-Cooper-Schrieffer (BCS) and Fermi liquid theory, the electric field (EF) should have no influence on metallic superconductors. However, recently, the impact of EFs on BCS metallic superconductors has been investigated [1-6] to demonstrate the suppression of the critical current (I_c) in gated metallic superconducting films, wires [1] and nano-constriction JJs (NC). Figure 1a shows a representative V gated NC. In such devices, by biasing the gate, it is possible to fully suppress I_c (Fig. 1b). This effect, was observed on several BCS metals, such as Al, Ti, NbN and Nb. Furthermore, field-effect remains effective in SNS devices [4]. This suggests the field-effect to be quite general, not even requiring a genuine superconductor but only the superconducting correlations.

Experiments on SQUID devices (Fig. 1c) [3] demonstrated that the EF also couples with the superconducting phase, resulting in a modified interference pattern (see Fig 1d): the EF applied to one of the JJ of the SQUID indirectly affects also the other JJ and, therefore, the entire interferometer. This behavior was described with a model imposing a gate-dependent suppression of the I_c and the creation of phase fluctuations of the gated JJ. This hypothesis is confirmed by measuring the switching current probability distribution (SCPD) of a gated NC, which provides information on the phase slippages in the JJ. SCPDs are largely affected by the EF: in particular, their standard deviation increases when the EF is present (see Fig. 2). This again suggests that the EF induces phase fluctuations into the superconductor; on the other side, it is an evidence of the non-thermal origin of the I_c suppression.

We highlight that it is possible to exploit this unconventional field-effect to realize classical superconducting logic ports in which the high and low states of I_c encode for logical 1 and 0 [6]. These devices are expected to take advantage from the high modulation bandwidth of a superconductor (in the 10 - 100GHz range) and from their low-dissipation operation.

Fig. 1

(a) False-color SEM image of a V-based DB-FET. The transistor channel (blue) is current biased. The gate voltage is applied to the lateral gate electrode (red, V_g). (b) Critical current (I_c) vs. gate voltage (V_g) for several temperatures (T). (c) False-color SEM image of a field-effect SQUID (blue). The left (V_L) and right (V_R) side gate electrodes are shown in purple and red, respectively. (d) Switching current (I_s) vs. magnetic flux Φ at $T=50$ mK.

**Fig. 2**

(a) SCPDs vs current (I) at different gate voltage values of a Ti DB. The curves are vertically offset for clarity. (b) Comparison of σ vs I_c obtained for SCPDs as a function of temperature at $V_c=0$ (light red), and of gate voltage at 20 mK (light blue). (c) Mode-matched SCPDs, red and orange distributions were obtained for $V_c=0$ at selected temperatures whereas yellow and green distributions were measured at $T=20$ mK for different gate voltage values. (d) I_c vs V_g for several temperatures. (e) Standard deviation σ of the SCPDs vs V_c .

Contact persons

Giorgio De Simoni (giorgio.desimoni@nano.cnr.it)
 Francesco Giazotto (francesco.giazotto@nano.cnr.it)

References

- [1] Metallic supercurrent field-effect transistor. G. De Simoni, F. Paolucci, P. Solinas, E. Strambini, and F. Giazotto. *Nature Nanotechnology* 13, 802 (2018).
- [2] Ultra-efficient superconducting Dayem bridge field-effect transistor. F. Paolucci, G. De Simoni, E. Strambini, P. Solinas, and F. Giazotto. *Nano Lett.* 18, 4195 (2018).
- [3] Field-Effect Controllable Metallic Josephson Interferometer. F. Paolucci, F. Vischi, G. De Simoni, C. Guarcello, P. Solinas, and F. Giazotto. *Nano Lett.* 19, 96263-6269 (2019).
- [4] Josephson Field-Effect Transistors Based on All-Metallic Al/Cu/Al Proximity Nanojunctions. G. De Simoni, F. Paolucci, C. Puglia, and F. Giazotto. *ACS Nano* 13, 77871-7876 (2019).
- [5] Magnetotransport Experiments on Fully Metallic Superconducting Dayem Bridge Field-Effect Transistors. F. Paolucci, G. De Simoni, P. Solinas, E. Strambini, N. Ligato, P. Virtanen, A. Braggio, and F. Giazotto. *Phys. Rev. Applied* 11, 024061 (2019).
- [6] Field-Effect Control of Metallic Superconducting Systems. F. Paolucci, G. De Simoni, P. Solinas, E. Strambini, C. Puglia, N. Ligato, and F. Giazotto. *Field-Effect, AVS Quantum Sci.* 1, 016501 (2019).

Hybrid quantum systems based on molecular spin centers coupled to confined microwave fields

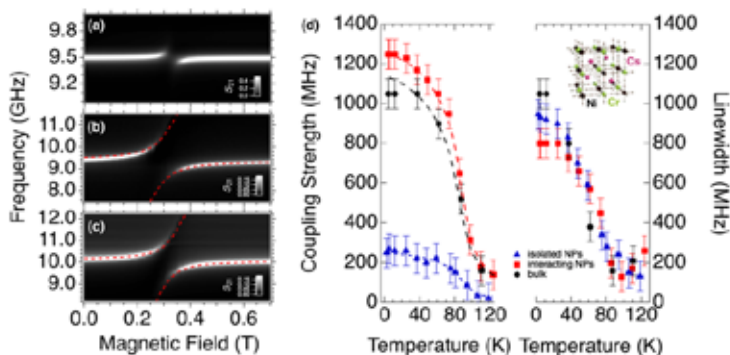
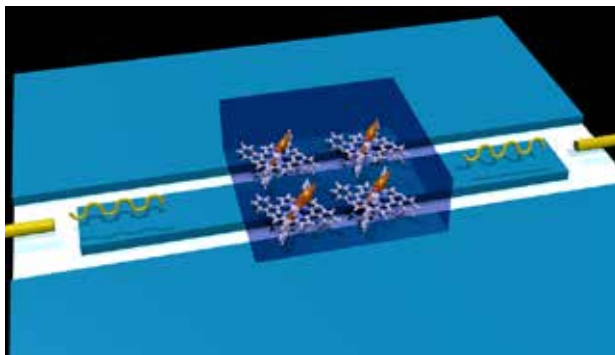
Molecular spins have shown genuine quantum properties, both as collection of independent units as well as individual objects. To show the viability of their integration in superconducting circuits for circuit quantum electrodynamics experiments, we have recently demonstrated the coherent coupling between confined electromagnetic radiation at microwave frequencies and ensembles of selected molecular spin centers. These studies have also been extended to collective spin excitations in magnetically ordered materials. The achievement of the strong coupling regime with ferromagnetic nanoparticles opens up new perspectives for spintronics and magnonics.

Molecular nanomagnets can be engineered at the molecular level, while advanced technologies to coherently manipulate magnetic systems and to address them with unprecedented spatial and energy resolution have emerged in the latest years. We have studied the coherent coupling between molecular spin centers and microwave fields in a cavity. Firstly, we have developed high TC superconducting planar resonators [1], including also dual mode resonators [2], and obtained excellent performances up to liquid nitrogen temperature and in magnetic fields up to 7 T. High spin-photon cooperativity has been achieved with molecular spins diluted in a non-magnetic matrix at 0.5 K [Sci. Rep. 7, 13096 (2017)], while strong coupling has been observed up to 50 K with concentrated samples of organic radicals [APL 106, 184101 (2015)]. The possibility to create coherent coupling among spatially separated spin ensembles has been further explored, showing that molecular spins can be efficiently integrated in quantum devices [1]. In [3] we argue that these results open up novel perspectives in the field of quantum sensing.

We have extended these studies to metallo-organic ferromagnetic materials with low damping of the magnetization dynamics. These systems provide a versatile platform for hybrid devices, yet the effect of nanostructuring needs to be controlled. We have investigated insulating CsNiCr Prussian blue analogue, including bulk samples or magnetically isolated and interacting nanoparticles (NPs) dispersed in different non-magnetic matrices. Ferromagnetic resonance spectroscopy has been performed over a wide temperature range across the ferromagnetic transition occurring at 90 K. We have found that the Gilbert damping parameter of 10 nm NPs compares well (10–3) with values reported for prototypical yttrium iron garnet. Strong coupling with confined microwave fields has been observed for bulk samples, as well as for interacting NPs. These results clarify the conditions for the coherent manipulation of collective spin degrees of freedom in nanostructured coordination materials.

Fig. 1

Pictorial representation of a molecular spin ensemble (purple) coupled to a superconducting coplanar resonator. Microwaves are injected in the planar resonator (cyan) by two small feed antennas positioned at the opposite sides of the chip (yellow). Coherent hybridization of spin and photons modes takes place through magnetic dipolar coupling at the position of the magnetic antinode in the middle of the resonator.

**Fig. 2**

Transmission spectroscopy data obtained at 60 K on CsNiCr Prussian blue analogue. Spectral maps measured for isolated NPs, interacting NPs and bulk sample are shown respectively in (a), (b) and (c). The temperature dependence of the extracted coupling strength and linewidth is shown in (d). Inset: structure of the CsNiCr(CN)₆ Prussian blue analogue.

Contact persons

Alberto Ghirri (alberto.ghirri@nano.cnr.it)
 Marco Affronte (marco.affronte@unimore.it)

References

- [1] Coherent coupling of molecular spins with microwave photons in planar superconducting resonators. C. Bonizzoni, A. Ghirri, and M. Affronte. *Adv. Phys.-X* 3, 1435305 (2018).
- [2] Microwave dual-mode resonators for coherent spin-photon coupling. C. Bonizzoni, F. Troiani, A. Ghirri, and M. Affronte. *J. Appl. Phys.* 124, 194501 (2018).
- [3] Towards quantum sensing with molecular spins. F. Troiani, A. Ghirri, M. G. A. Paris, C. Bonizzoni, and M. Affronte. *J. Magn. Magn. Mater.* 491, 165534 (2019).

Recent advances in fast Josephson thermal circuits

Phase-coherent caloritronics develop from the interplay between heat transport properties and phase-coherent behaviour of Josephson circuits. Acting on the Josephson phase, e.g., through the applied magnetic field, one can master thermal transport and, thus, manipulate the temperature of the system. The advent of phase-coherent caloritronics opened the door to the realization of a plethora of innovative solid-state devices, such as thermal interferometers and diffractors, thermal router [1] and rectifier, thermal diode and transistors, even a full-thermal logic architecture [2]. Missing elements in this scenario were superconducting solid-state devices capable of fast thermal evolution. We obtained them exploiting fluxons and fast solitons, thus establishing the basis for novel classes of circuits for quantum computation and quantum sensing.

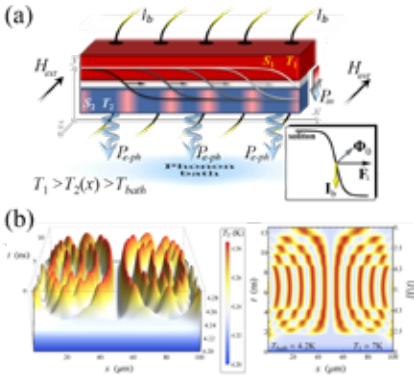
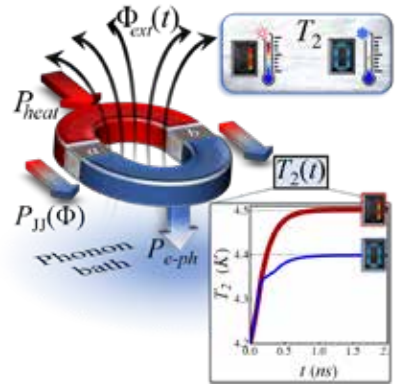
The recent theoretical achievements of the group concerning the effects of fluxons on the fast temperature evolution in Josephson devices brought to new proposals for caloritronics applications. We made a step forward in the panorama of existing thermal memories, introducing the concept of superconducting (Josephson) thermal memory [3], which uses the electronic temperature of an inductive superconducting quantum-interference device (SQUID) to define two distinct thermal states (Fig. 1). We studied the dynamics of a magnetic flux-controlled SQUID, and the hysteresis of its steady temperature states, to define the logic states of the memory.

We also explored how the thermal gradients can affect the critical current of Josephson junctions made by different superconductors. In particular, we identified regimes where, unexpectedly, the critical current is sharply increased with increasing the temperature, and thus we developed a Josephson threshold calorimeter based on this working principle [4,5].

Additionally, we explored the intriguing idea to exploit fluxons, i.e., solitons, for affecting locally the temperature of a long Josephson junction (Fig. 2), and its applicative potential in fast heat mastering. This kind of excitations can be controlled and handled in different manners, so paving the way for the realization of alternative coherent devices based on soliton-sustained thermal transport. The theoretical results of the group in this research area include both the original insight that a soliton can locally induce thermal effects in a temperature-biased junction [6], and the design of concrete applications, e.g., a thermal router [4,5] and a heat oscillator [7]. Since solitons can be moved by an electric bias current [8], these proposals readily lend themselves to a further advance in the flux-flow operation mode [9], which is a flow of continuously magnetically excited soliton along the junction, where the solitons mediate the control of dissipationless current over the averaged heat transport in the junction.

Fig. 1

Thermal fluxes in a magnetically driven SQUID formed by two superconductors residing at different temperatures T_1 and T_2 . The applied magnetic flux threading the SQUID loop, Φ_{ext} , drives the temperature T_2 . The heat current $P_{\text{JJ}}^{\text{ext}}$ flowing through the junctions depends on the temperatures and the total flux Φ through the SQUID ring. $P_{\text{e-ph}}$ represents the coupling between quasiparticles in the superconducting lead and the lattice phonons residing at T_{bath} , whereas P_{heat} denotes the power injected into the device through heating probes in order to impose a fixed quasiparticle temperature T_1 . The arrows indicate the direction of heat currents for $T_1 > T_2 > T_{\text{bath}}$. The temperature T_2 is the observable used to define the logic states 0 and 1 of the thermal memory.

**Fig. 2**

(a) A tunnel long Josephson junction driven by an external in-plane magnetic field $H_{\text{ext}}(t)$ and a homogeneously distributed bias current I_b . The temperature T_i of each electrode S_i is also indicated. A chain of solitons drifting along the junction under the action of I_b is depicted. The incoming P_{in} and outgoing $P_{\text{e-ph}}$ thermal powers in S_2 are also represented, for $T_1 > T_2(x) > T_{\text{bath}}$. In the inset: bias current-induced Lorentz force $F_L = I_b \times \Phi_0$ acting on a soliton. (b) Evolution of the temperature profile $T_2(x, t)$ of the floating electrode S_2 .

Contact persons

Francesco Giazotto (francesco.giazotto@nano.cnr.it)

Alessandro Braggio (alessandro.braggio@nano.cnr.it)

References

- [1] Phase-tunable Josephson thermal router. G. F. Timossi, A. Fornieri, F. Paolucci, C. Puglia, and F. Giazotto. Nano Letters 18, 1764 (2018).
- [2] Phase-tunable thermal logic: computation with heat. F. Paolucci, G. Marchegiani, E. Strambini, and F. Giazotto. Phys. Rev. Appl. 10, 024003 (2018).
- [3] Josephson Thermal Memory. C. Guarcello, P. Solinas, A. Braggio, M. Di Ventra, and F. Giazotto. Phys. Rev. Appl. 9, 014021 (2018).
- [4] Nonlinear Critical-Current Thermal Response of an Asymmetric Josephson Tunnel Junction. C. Guarcello, A. Braggio, P. Solinas, and F. Giazotto. Phys. Rev. Appl. 11, 024002 (2019).
- [5] Josephson-Threshold Calorimeter. C. Guarcello, A. Braggio, P. Solinas, G. P. Pepe, and F. Giazotto. Phys. Rev. Appl. 11, 054074 (2019).
- [6] Solitonic Josephson Thermal Transport. C. Guarcello, P. Solinas, A. Braggio, and F. Giazotto. Phys. Rev. Appl. 9, 0304014 (2018).
- [7] Phase-coherent solitonic Josephson heat oscillator. C. Guarcello, P. Solinas, A. Braggio, and F. Giazotto. Sci. Rep. 8, 12287 (2018).
- [8] Solitonic thermal transport in a current biased long Josephson junction. C. Guarcello, P. Solinas, A. Braggio, and F. Giazotto. Phys. Rev. B 98, 104501 (2018).
- [9] Thermal flux-flow regime in long Josephson tunnel junctions. C. Guarcello, P. Solinas, F. Giazotto, and A. Braggio. J. Stat. Mech. 084006 (2019).

Manipulating the free electron wavefunction for quantum measurements

Recent years have been characterized by a new twist in electron microscopy and in general in the science of particle optics thanks to the ability to use holograms and shaping techniques inspired by light optics. These techniques are now mature but it is time to demonstrate the practical use of these ideas in fundamental physics and in material science. The EU QSORT project aims in particular at demonstrating new complex electro-optics configurations capable of producing optimal measurement of magnetic phenomena and biological samples. Beyond this we show new fundamental ideas like quark structure investigation by neutron vortex beams and shaped interaction with surface plasmon-polaritons, demonstrating how many fields of physics can benefit from coherent beam manipulation.

Most of the group activity has been focused on the EU QSORT project (www.qsort.eu) that we lead. One of the project aims is to produce a new extension of a transmission electron microscope, named orbital angular momentum (OAM)-sorter, capable of measuring in a parallel and efficient way the component of the OAM in the direction of the main propagation. The new device is based on MEMS electrodes introduced along the electron beam path and opportunely biased. Figure 1 shows the OAM sorter schematically, the new electrodes devices and the experimental result: an OAM spectrum with two peaks corresponding to known components of the beam.

Since this observable had never been available before as a direct observable in microscopy, we think we can use it to access a large number of new sample properties [1,2]. Theoretical papers from our group show, in particular, that we should be able to measure the dichroism in both plasmon excitations and in the L-edge ionization edges of magnetic materials. Notably, the detection of the magnetic dichroism (EMCD) with the OAM-sorter represents the ideal technique to measure the magnetic effects on the density of states with serious advantages over X-ray technique (XMCD). For example, we show that the relation to physical properties like spin and orbital magnetic component of the material should be quite simplified through the use of sum rules independent from cumbersome dynamic effects.

Figure 2 is a demonstration of the possibility to characterize the symmetry of each excited plasmon modes in more complex plasmonic structures [1]. Analogously we demonstrated the possibility to excite plasmon-polariton vortex modes with light, and probe them using electrons by acquiring the OAM from the interaction [4]. The application of the sorter to this configuration would permit to directly probe the electron beam state after the interaction. The possibility to impart an OAM to particles is of even broader and fundamental interest as we could even imagine to study the inner degrees of freedom of nucleons (protons and neutron) by simply adding an extrinsic OAM to a nucleon [3,4].

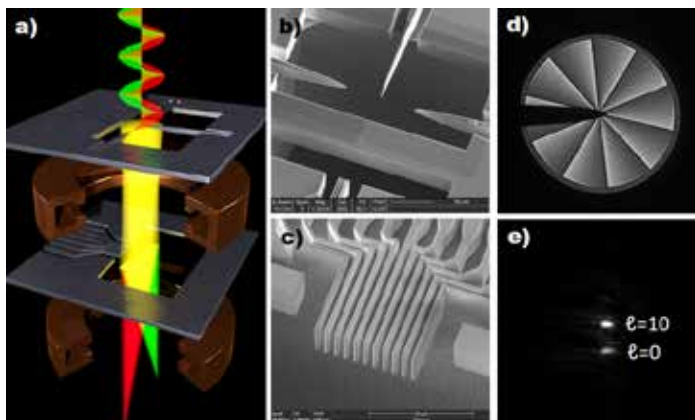


Fig. 1

a) Scheme of the experimental apparatus: the sample is located in the standard sample position, the first sorter element is located in the objective aperture plane and the second element the SAD aperture. b) and c) SEM images of the actual devices produced by optical mask lithography. Evolution of a vortex beam ($|\ell=10\rangle+|\ell=0\rangle$) from the generation (d) from the final OAM spectrum (e).

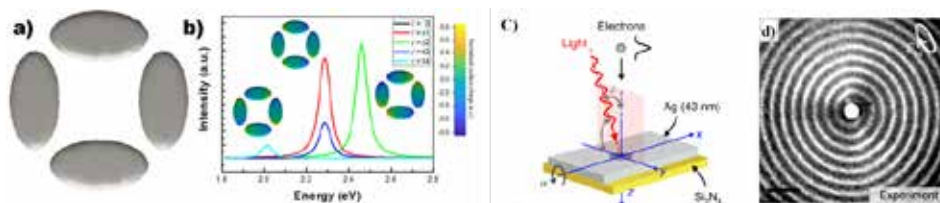


Fig. 2

a) Plasmonic structure composed of four Ag elliptical disks and b) its simulated OAM-resolved EEL spectra. The surface charge distribution of each plasmonic mode is reported as insets. c) scheme of the light excitation of the surface plasmon polarization (SPP) and d) the experimental field of the SPP.

Contact person

Vincenzo Grillo (vincenzo.grillo@nano.cnr.it)

References

- [1] Orbital angular momentum and energy loss characterization of plasmonic excitations in metallic nanostructures in TEM. M. Zanfagnini, E. Rotunno, S. Frabboni, A. Sit, E. Karimi, U. Hohenester, and V. Grillo. *ACS Photonics* 6, 620-627 (2019).
- [2] Orbital-angular-momentum-resolved EMCD. E. Rotunno, M. Zanfagnini, S. Frabboni, J. Ruzs, R. E. Dunin Borkowski, E. Karimi, and V. Grillo. *Phys Rev B* 100, 224409 (2019).
- [3] Ultrafast generation and control of an electron vortex beam via chiral plasmonic near fields. G. M. Vanacore, G. Berruto, I. Madan, E. Pomarico, P. Biagioni, R. J. Lamb, D. McGrouther, O. Reinhardt, I. Kaminer, B. Barwick, H. Larocque, V. Grillo, E. Karimi, F. J. Garcia de Abajo, and F. Carbone. *Nature Materials* 18, 573-579 (2019).
- [4] Twisting neutrons may reveal their internal structure. H. Larocque, I. Kaminer, V. Grillo, R. W. Boyd, and E. Karimi. *Nature Physics* 14, 1 (2018).

Ferromagnetic insulator-superconductor systems

Nowadays, a renewed interest in studying FI/S structures comes with the development of superconducting spintronics. Ferromagnetic insulators (FIs) attached to a superconductor are known to induce triplet superconducting pairing and an exchange energy splitting in the Bardeen–Cooper–Schrieffer (BCS) density of states proportional to the FI magnetization, and penetrating into the superconductor to a depth comparable with the superconducting coherence length.

Recent experimental findings of the SQEL group at Cnr Nano are presented for the implementation of promising spintronic technologies based on this material combination. These include a superconducting magnetic random access memory (RAM) and novel thermoelectric radiation detector based on EuS/Al bilayers.

Magnetism and superconductivity, two antagonist orders in bulk materials, can co-exist at the nanoscale and generate exotic states and/or improve device functionalities and performances. Seminal works from the 80's have demonstrated this strong hybridization in thin bilayers of ferromagnetic insulators (FI) and conventional superconductors (S) such as EuS and Al.

The unique characteristics of these bilayers, together with the evolution of modern nanofabrication techniques, renewed the interest in studying FI/S structures to develop new superconducting spintronics applications.

We investigate this magnetic proximity effect in EuS/Al bilayers tunnel coupled to an Al probing layer. Remarkably, the tunneling spectroscopy of our devices reveals

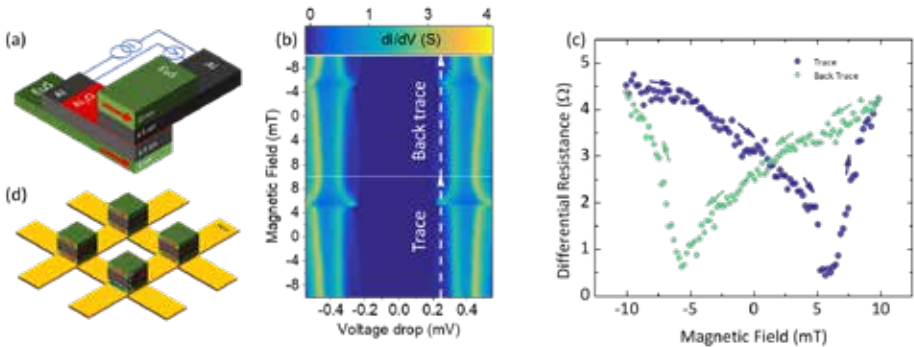


Fig. 1

Evolution of the Absolute Spin Valve (ASV) in the magnetic field. (a) Scheme of the EuS/Al/AlO_x/Al/EuS ASV together with the four wire measurement set-up. (b) Color plot of the tunneling differential conductance of the ASV measured at 50 mK as a function of the voltage drop V and of the external magnetic field. (c) Tunneling differential resistance extracted at $V = 248 \mu\text{V}$ (i.e., along the dashed white line in panels b) as a function of the magnetic field. (d) Example of superconducting magnetic RAM based on the ASV effect. Each EuS/Al cell is a logic element controlled by NbN word-write lines

exchange splitting of the BCS peaks even in the unpolarized state of the EuS, with enhancement when magnetizing the sample as a consequence of the characteristic magnetic domain structure of the EuS layer.

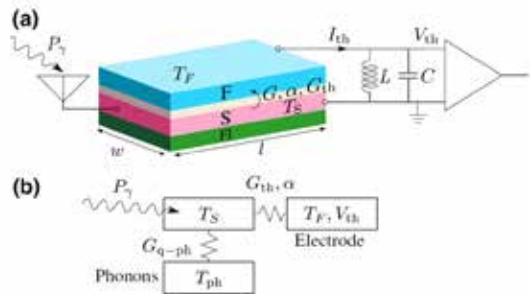
A technological application resulting from this hybrid material came with the absolute spin-valve effect obtained with a tunnel junction made with a two EuS/Al layers [1,2] shown in Fig. 1a. The high contrast in the tunneling magnetoresistance (TMR) measured at low temperature (<1 K), see Fig. 1b and c, demonstrate the promising capabilities of this valve to implement a superconducting magnetic RAM operating at cryogenic temperatures (Fig. 1d), then compatible with the new generation of superconducting high-frequency processors.

Furthermore, the hard gap and clear intrinsic spin-splitting observed in our measurements indicate that EuS/Al bilayers are an excellent platform for the development of large variety of quantum technologies requiring the coexistence of superconducting correlations and built-in spin-splitting exchange fields, as for example in the field of Majorana-based quantum computation [3].

Finally, the giant thermoelectric effect recently found in FI/S hybrid structures (sketched in Fig. 2) made this material combination ideal also for ultrasensitive thermoelectric radiation detectors [4]. We are studying to turn this idea into a near future technology thanks to the support of the European FET project SUPERTED.

Fig. 2

(a) The thermoelectric detector, where a temperature difference $T_S - T_F$ drives a thermoelectric current I_{th} and/or a thermovoltage V_{th} across a spin-polarized junction. The latter is composed of either a normal insulator and a ferromagnetic electrode (F) or a ferromagnetic insulator (FI) and a normal metal electrode. (b) Heat balance: incoming radiation power (P_{γ}) heats up the quasiparticles in the spin-split superconductor (S), and the amount of heating depends on the heat conductances to the main heat baths.



Contact persons

Elia Strambini (elia.strambini@nano.cnr.it)

Francesco Giazotto (francesco.giazotto@nano.cnr.it)

References

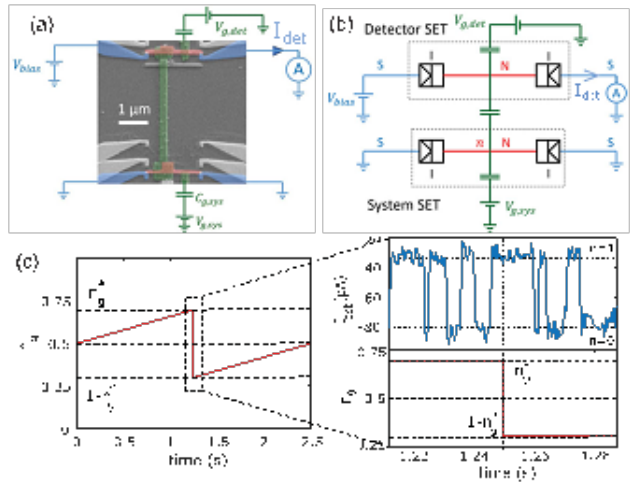
- [1] Toward the Absolute Spin-Valve Effect in Superconducting Tunnel Junctions. G. De Simoni, E. Strambini, J. S. Moodera, F. S. Bergeret, and F. Giazotto. *Nano Lett.* 18, 6369–6374 (2018).
- [2] Charge transport through spin-polarized tunnel junction between two spin-split superconductors. M. Rouco, S. Chakraborty, F. Aikebaier, V. N. Golovach, E. Strambini, J. S. Moodera, F. Giazotto, T. T. Heikkilä, and F. S. Bergeret. *Phys. Rev. B.* 100, 184501 (2019).
- [3] Majorana bound states in hybrid two-dimensional Josephson junctions with ferromagnetic insulators. P. Virtanen, F. S. Bergeret, E. Strambini, F. Giazotto, and A. Braggio. *Phys. Rev. B.* 98, 020501 (2018).
- [4] Thermoelectric Radiation Detector Based on Superconductor-Ferromagnet Systems. T. T. Heikkilä, R. Ojajärvi, I. J. Maasilta, E. Strambini, F. Giazotto, and F. S. Bergeret. *Phys. Rev. Appl.* 10, 034053 (2018).

Thermal transport, thermoelectricity, and thermodynamics in nanostructures and single-electron devices

We study various thermodynamic properties of single-electron devices, such as quantum dots and metallic islands. From the theoretical side, we study electronic thermal and thermoelectric (TE) transport in capacitively-coupled systems and apply our approach to model experiments on the thermovoltage and the statistics of work extraction. From an experimental side, on the one hand, we implement single-electron systems where the electronic configuration can be controlled down to the last conduction-band electron, while, on the other, we develop reliable methods, like the so-called 3-omega, to precisely assess the TE properties (such as the Seebeck coefficient) of individual nanostructures.

The advent of nanostructures is opening new perspectives for the fundamental investigation of thermodynamics at the nanoscale. From a theoretical side, we study the thermodynamic properties of single-electron devices. In particular, we discuss electronic thermal transport in such systems assuming that two metallic islands (MIs) or quantum dots (QDs) are electrically isolated and placed in the two circuits (the drive and the drag) of a three- or four-electrode setup. In the latter setup we study the thermal drag effect when the system is biased, for example by a temperature ΔT , on the drive circuit, while no biases are present on the drag circuit [1]. The three-electrode setup is analyzed as a simple implementation of an autonomous refrigerator, a system that uses heat as a resource to achieve refrigeration [2]. We apply our theoretical approach to model two different experiments, the first regarding the measurement of thermovoltage in MIs [3], and the second one regarding the occurrence of an apparent violation of the second law of thermodynamics in the statistics of work extraction from a MI (see Fig. 1) [4].

Fig. 1
 (a) Scanning electron micrograph of the single-electron transistor (SET) capacitively coupled to a voltage-biased detector SET. Leads (blue) made of superconducting aluminum are coupled through oxide (tunnel) barriers to the copper (red) island. (b) Electrical circuit representation. (c) Protocol used to maximize work extraction, with a zoom on the detector SET output current under system driving, around the quench event.



From an experimental side, we implement QD systems where the electronic configuration can be controlled down to the last conduction-band electron. This can be achieved using the technology of heterostructured nanowires (see “InAs/InP axial heterostructured nanowires: from the growth dynamics to quantum confined electronic devices”, p. 52). Devices are used to measure the thermoelectric response due to the tunneling through few electron orbitals. This allows a precise measurement of the Seebeck coefficient and – thanks to modelling – a precise estimate of the thermal transport and conversion efficiency (up to a figure of merit $ZT=35$ at 30K). A share of the experimental activities also focuses on the development of reliable methods to assess the TE properties of individual nanostructures [5]. In particular, we demonstrate a platform to measure thermal transport in suspended nanowire devices [6], using the so-called 3-omega method that exploits self-heating in the presence of an AC current modulation at frequency ω (see Fig. 2) [6].

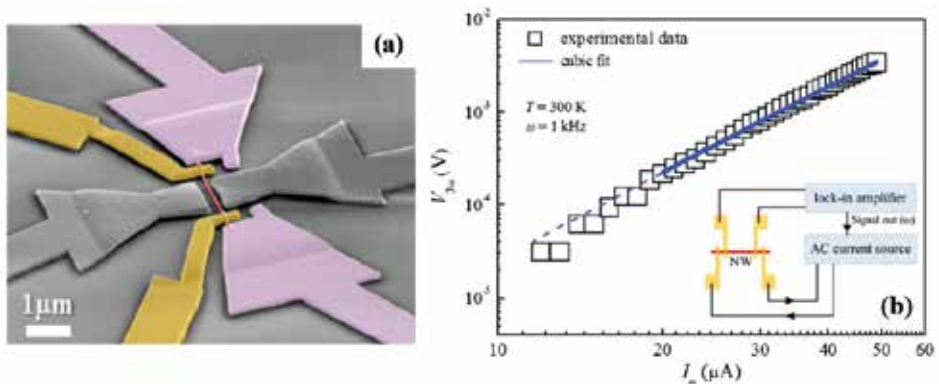


Fig. 2

(a) Scanning electron micrograph of a suspended nanowire structure for the measurement of thermal conductivity of an individual InAs nanowire. (b) Experimental data on the third harmonics voltage drop due to self-heating in the suspended nanostructure. The cubic dependence of the voltage on the drive current can be used to estimate the thermal conductivity of the nanostructure.

Contact persons

Stefano Roddaro (stefano.roddaro@nano.cnr.it)

Fabio Taddei (fabio.taddei@nano.cnr.it)

References

- [1] Absorption refrigerators based on Coulomb-coupled single-electron systems. P. A. Erdman, B. Bhandari, R. Fazio, J. P. Pekola, and F. Taddei. *Phys. Rev. B* 98, 45433 (2018).
- [2] Thermal drag in electronic conductors. B. Bhandari, G. Chiriaco, P. A. Erdman, R. Fazio, and F. Taddei. *Phys. Rev. B* 98, 35415 (2018).
- [3] Nonlinear thermovoltage in a single-electron transistor. P. A. Erdman, J. T. Peltonen, B. Bhandari, B. Dutta, H. Courtois, R. Fazio, F. Taddei, and J. P. Pekola. *Phys. Rev. B* 99, 165405 (2019).
- [4] Optimal probabilistic work extraction beyond the free energy difference with a single-electron device. O. Maillet, P. A. Erdman, V. Cavina, B. Bhandari, E. T. Mannila, J. T. Peltonen, A. Mari, F. Taddei, C. Jarzynski, V. Giovannetti, and J. P. Pekola. *Phys. Rev. Lett.* 122, 150604 (2019).
- [5] Measurement of the thermoelectric properties of individual nanostructures. F. Rossella, F. Pennelli, and S. Roddaro. *Semiconductors and Semimetals* 98, 409 (2018).
- [6] Suspended InAs nanowire-based devices for thermal conductivity measurement using the 3ω method. M. Rocci, V. Demontis, D. Prete, D. Ercolani, L. Sorba, F. Beltram, G. Pennelli, S. Roddaro, and F. Rossella. *Jour. Mat. Eng. and Perf.* 27, 6299 (2018).

Universal quantum metrology with spins at equilibrium

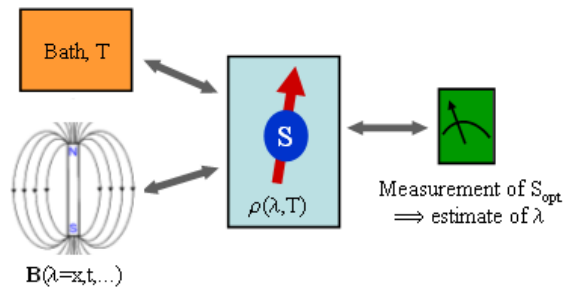
We propose metrological protocols for the estimation of the intensity and the orientation of a magnetic field, and show that quantum-enhanced precision may be achieved by probing the field with an arbitrary spin at thermal equilibrium. The optimal observable is shown to correspond to the spin projection along a temperature-dependent direction, and allows a maximally precise parameter estimation also through ensemble measurements. We prove the robustness of our scheme against deviations of the measured spin projection from optimality. Finally, we discuss parameter estimation based on dynamical strategies, and a number of specific applications.

Quantum sensing and metrology are the art of exploiting the quantum features of a probe for implementing precise estimation protocols. In quantum parameter estimation, the parameter of interest (λ) is encoded into the state of a physical system (the probe), and has to be inferred by suitably designed measurement schemes. In particular, the optimal observables allow one to achieve the ultimate quantum limit in terms of estimation precision.

A magnetic field is a typical quantity whose estimate can be obtained through a quantum probe. The most widely pursued approach ultimately relies on the measurement of the Larmor precession angle (or, more generally, of the quantum phase) accumulated by the spin due to its interaction with the field. This approach requires the coherent control and dynamics of the spin state. Systems at thermal equilibrium represent a possible alternative, whereby the state preparation, though less general, is greatly simplified, and decoherence no longer represents a limiting factor.

Fig. 1

Schematics of the proposed metrological protocol: a spin of arbitrary length S is coupled to a parameter-dependent field $B(\lambda)$ and in thermal equilibrium at a temperature T . The value of the unknown parameter λ is inferred from the outcome of a measurement of the optimal spin projection S_{opt} , whose (temperature-dependent) expression we derive within the framework of quantum parameter estimation.



Here, we consider the estimation of a magnetic field, obtained by measuring any possible observable of a spin of arbitrary length S in a thermal equilibrium state [1,2]. We find a general expression for the quantum Fisher information, which is also given in terms of common thermodynamic quantities, such as magnetization and magnetic susceptibility. Besides, the optimal observable is shown to coincide with the spin projection along a direction that depends on temperature but is independent on the spin length. In the low-temperature limit, optimality is obtained not only for a single spin projection, but rather for a whole plane of equivalent directions.

Remarkably, the upper bound for the estimation precision is also saturated by an ensemble measurement of the optimal spin projection, which is quantified by a different figure of merit. Finally, the dependence of the Fisher information on the measured spin projection demonstrates the robustness of the estimation protocol with respect to deviations from optimality.

Contact person

Filippo Troiani (filippo.troiani@nano.cnr.it)

References

- [1] Universal quantum magnetometry with spin states at equilibrium. F. Troiani and M. G. A. Paris. *Phys. Rev. Lett.* 120, 260503 (2018).
- [2] Quantum metrology at level anticrossing. L. Chirardi, I. Siloi, P. Bordone, F. Troiani, and M. G. A. Paris. *Phys. Rev. A* 97, 012120 (2018).

InAs/InP axial heterostructured nanowires: from the growth dynamics to quantum confined electronic devices

The nanowire geometry offers a high flexibility in combining semiconductors with different lattice parameters in high-quality heterostructures. As a consequence, axial nanowire heterostructures have become extremely interesting for both fundamental science and device applications. Here we report on the growth of InAs/InP axial heterostructured nanowires by means of Au-assisted Chemical Beam Epitaxy. A deep investigation of the growth dynamics of thin alternating InAs/InP segments has allowed to optimize the growth process and to obtain the desired structures (nanowire-quantum dots) with a precise control of the segments' thickness. The nanowires obtained have been used to realize quantum-confined electronic devices to study novel phenomena at the nanoscale.

The InAs/InP system is particularly suitable for the realization of axial heterostructured nanowires (NWs) in Au-assisted growth. Indeed, the very low solubility of both As and P into the Au nanoparticles (NPs) allows to obtain atomically sharp interfaces in both growth directions [1]. However, the chemical composition of the NP changes when the growth is switched from one material to the other one, and this affects the NP stability and the growth mode [1]. Therefore, the precise control of the thickness of InP and InAs alternating segments can be very challenging. In this context, we studied how the isothermal NP reconfiguration affects the growth dynamics of thin alternating InAs/InP segments, and we demonstrated a strategy to obtain an accurate control of the length/diameter dependence and of the segments' thickness [2]. These findings allowed us to grow InAs NWs with built-in InP tunneling barriers of well-defined thickness (~5 nm), separated by a thin (~20 nm) InAs segment, defining a quantum dot (QD). We used these NW-QDs to fabricate single electron transistors (SETs), and we demonstrated very regular Coulomb blockade resonances over a large gate voltage range (Fig. 1). By analyzing the resonance line shapes, we map the evolution of the tunnel couplings from the few to the many electron regime, with

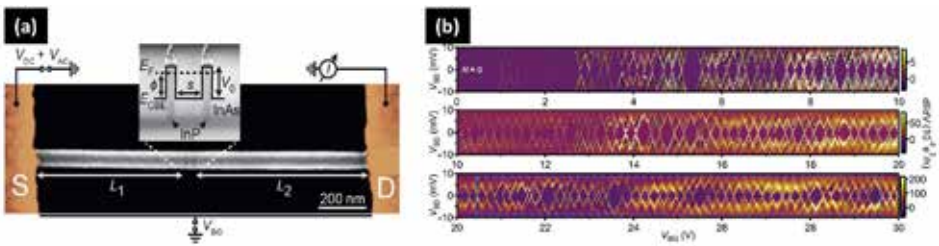


Fig. 1 (a) False colored scanning electron micrograph (SEM) of a typical SET device consisting of an InAs nanowire with two InP tunnel barriers (dark segments) of length $l_1 = l_2 = 5$ nm, separated by an InAs QD of 20 nm. (b) Differential conductance, $dI = dV_{SD}$, as a function of the bias V_{SD} , and the back gate voltage, V_{bc} showing regular and stable Coulomb diamonds over a gate range of 30V.

electrically tunable tunnel couplings from $<1\mu\text{eV}$ to $>600\mu\text{eV}$, and a transition from the temperature to the lifetime broadened regime. The InP segments form barriers with almost fully symmetric tunnel couplings and a barrier height of ~ 350 meV. The strong electronic confinement achievable in our InAs/InP NW-QDs can be used also for the investigation of novel thermoelectric effects in the quantum regime. Indeed, we demonstrated the full electrostatic control of the heat engine features of a thermally biased NW-QDs operating in high temperature regimes (Fig. 2). The electrical conductance and the thermopower were obtained from charge transport measurements and accurately reproduced with a theoretical model [3]. Finally, using the same kind of NW-QD, we fabricated SETs inside a high-temperature superconducting microwave (MW) cavity, and we investigated the influence of the electric field of the MW radiation on the transport characteristics of our devices (Fig. 3). We found that, above a threshold power, the MW field induces a broadening of the current peak and a current polarity reversal [4]. These effects are relevant for multi-photon assisted tunneling processes.

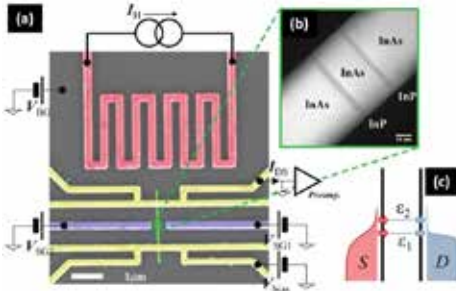


Fig. 2

(a) SEM of a typical thermoelectric device: a local heater (red) is used to establish a temperature difference between the two ends of the NW (green) embedding an InAs/InP heterostructured QD (b). A set of electrodes (yellow) is used both as electrical contacts to the NW and as local resistive thermometers. The QD electronic configuration (c) can be controlled with a pair of side gates (purple) or using the conductive substrate as a backgate electrode.

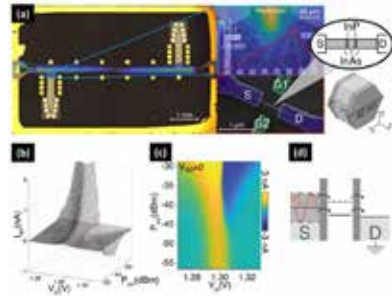


Fig. 3

(a) Optical (left) and SEM (right) images of a SET inside a MW cavity, realized with a InAs/InP NW-QD. (b-c) Evolution of the $I_{SD}(V_C)$ characteristics in the presence of a microwave drive of frequency ω_0 and increasing power P_{inc} . (d) Schematic energy diagrams showing the MW-assisted tunneling through the QD levels ϵ' and ϵ'' .

Contact persons

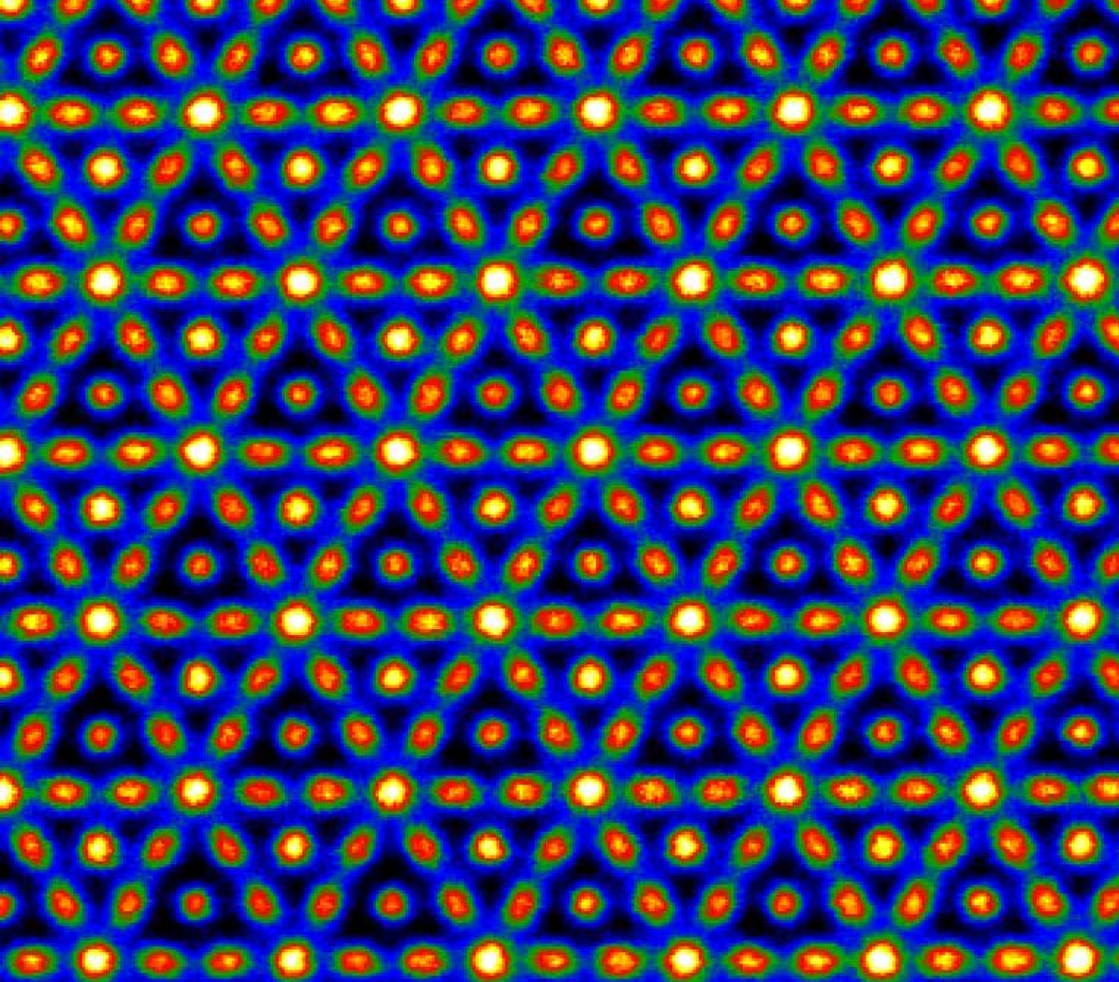
Lucia Sorba (lucia.sorba@nano.cnr.it)

Valentina Zannier (valentina.zannier@nano.cnr.it)

References

- [1] Nanoparticle Stability in Axial InAs–InP Nanowire Heterostructures with Atomically Sharp Interfaces. V. Zannier, F. Rossi, V. G. Dubrovskii, D. Ercolani, S. Battiato, and L. Sorba. *Nano Lett.* 18, 167–74 (2018).
- [2] Growth dynamics of InAs/InP nanowire heterostructures by Au-assisted chemical beam epitaxy. V. Zannier, F. Rossi, D. Ercolani, and L. Sorba. *Nanotechnology* 30, 094003 (2019).
- [3] Thermoelectric Conversion at 30 K in InAs/InP Nanowire Quantum Dots. D. Prete, P. A. Erdman, V. Demontis, V. Zannier, D. Ercolani, L. Sorba, F. Beltram, F. Rossella, F. Taddei, and S. Roddaro. *Nano Lett.* 19, 3033–3039 (2019).
- [4] Microwave-Assisted Tunneling in Hard-Wall InAs/InP Nanowire Quantum Dots. S. Cornia, F. Rossella, V. Demontis, V. Zannier, F. Beltram, L. Sorba, M. Affronte, and A. Ghirri. *Sci. Rep.* 9, 19523 (2019).





Highlights

-

**Surfaces and interfaces:
nanofabrication, imaging,
and spectroscopy**

Introduction to Surfaces and interfaces: nanofabrication, imaging, and spectroscopy

The Institute research activities concerning “Surfaces and Interfaces: nanofabrication, imaging, and spectroscopy” are focused on the use of nanotechnologies to design and realize materials and architectures with optimal properties for clean energy conversion and storage, nanomechanics, and molecular spintronics. The investigated systems include two-dimensional materials, oxides, supported organic molecules, plasmonic materials and many more. Most of them have been grown in the Institute laboratories using advanced techniques like reactive molecular beam epitaxy, magnetron sputtering, also combined with inert gas-aggregation, electron-beam lithography. The functionality of the investigated compounds is tuned by an accurate control of the properties at the atomic scale, assessed by high-spatial resolution imaging techniques, like scanning probe microscopies and transmission electron microscopies, coupled with advanced spectroscopies, exploiting also synchrotron radiation. Time-resolved studies by ultrafast spectroscopies allow to follow the dynamics of electronic and plasmonic excitations and to identify the corresponding decay channels. The possibility to combine scanning tunneling microscopy measurements and calorimetry has also been recently implemented. Simulations based on density functional theory provide an extremely important guide for material design and for the interpretation of the observed behavior.

The prototype 2D material, graphene, is modified by the introduction of deformations and defects, with the aim of tailoring its electronic states and as a consequence its absorption properties, reactivity and frictional properties. Hydrogen adsorption and intercalation is one of the main research focuses, in view of the importance of the investigated materials in the field of hydrogen storage. The combination of graphene and layered chalcogenides is also a subject of intensive studies, which point at inducing mechanical deformations and modifying frictional properties. Graphene and intercalated metal layers are also used to tune the superexchange interactions between organic molecules and ferromagnetic substrates. Black phosphorus is a further subject of intense research activities, which point at assessing the modifications induced by thermal treatments and by metal doping.

A topic, which attracts strong research efforts, is the study of the mutual interactions between plasmonic materials and other compounds, for applications in photocatalysis and photovoltaics. Mass-selected plasmonic nanoparticles with resonances in the visible light range are combined with wide band gap reducible oxides to increase reactivity, with transparent conductive oxides to tune charge carrier concentration and with hybrid perovskites in solar cells, to increase the optical path of solar radiation. Important in this context is the demonstrated possibility to directly measure localized surface plasmon resonances by scanning transmission electron microscopy combined with electron energy loss spectroscopy. Information on the plasmonic resonance de-excitations and consequent modification of the properties of the composite material have been obtained using ultrafast time-resolved spectroscopies.

Tailoring the magnetic coupling between magnetic molecules and a ferromagnetic surface: the role of graphene and its intercalation with gold atoms

Molecules with a magnetic core and an organic shell are prototypical systems to study magnetism and spintronics at the nanoscale. One intriguing issue is the possibility to tailor the hybrid interface between an organic layer and an inorganic (magnetic) surface that may lead to the so-called “spinterface” effects. We focus our attention to molecules comprising transition-metal (TM) or rare-earth ions (RE) and study how the magnetization of molecular layers deposited on magnetic substrates depends on the interposition of graphene and additional layers.

In order to control the magnetic interaction between a molecular system and magnetic inorganic substrate, we recently investigated the magnetic coupling of (RE- Pc_2 and Co-TPP) magnetic molecules with the ferromagnetic Ni substrate, when deposited on its (111) surface. More specifically, we are interested in studying how the magnetic coupling is influenced by interposing a graphene layer between molecules and the nickel surface and, furthermore, when a gold layer is intercalated between graphene and nickel. X-ray absorption spectroscopy (XAS), linear and magnetic circular dichroism (XLD and XMCD) were exploited to investigate a sub-monolayer of RE- Pc_2 or Co-TPP molecules. In both systems the molecules lay flat on the Ni(111)/SLG surface, with and without the Au intercalation.

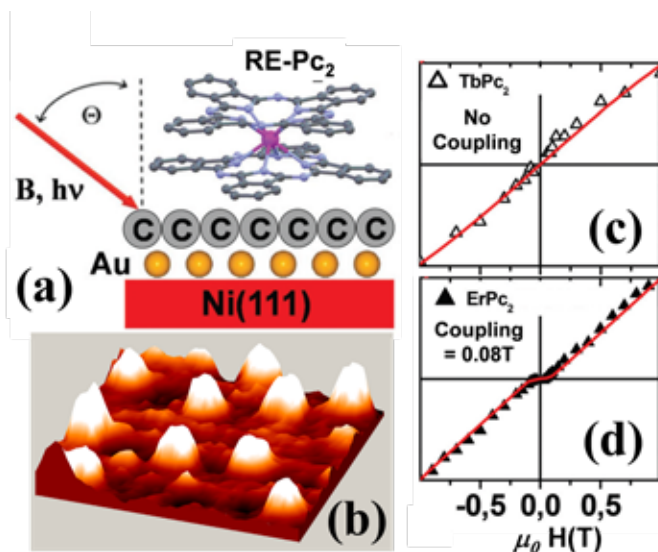


Fig. 1

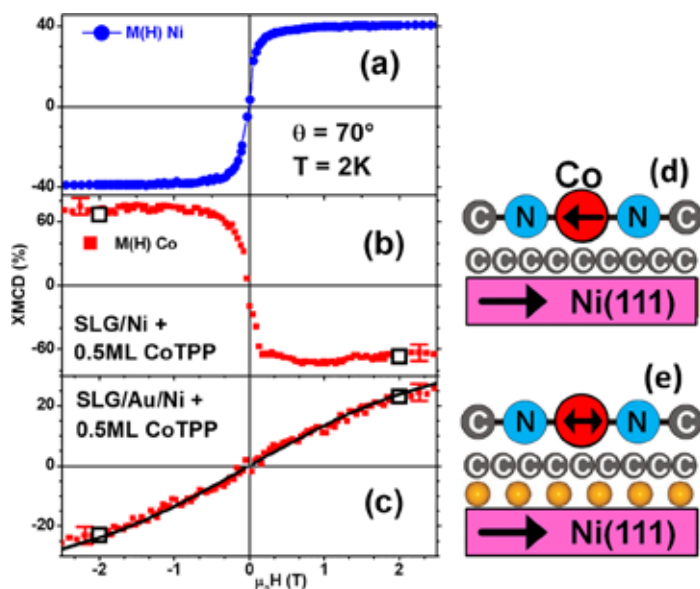
(a) Sketch of the measurements conditions with the RE- Pc_2 molecules lying flat on the Ni(111)/Au/SLG surface. The magnetic field B and the beam are collinear and oriented at an angle $\theta = 70^\circ$ with respect to the normal to the surface. (b) STM images (tunneling conditions: 2V, 20pA): 3D view of the isolated Pc_2Tb molecules deposited on SLG/Ni(111) surface ($25 \times 25 \text{ nm}^2$).

In first work [1], two types of RE-Pc₂ molecules (RE = Tb, Er) with a different magnetic anisotropy (easy-axis for Tb, easy-plane for Er) were considered. XMCD showed an antiferromagnetic coupling between RE and Ni(111) even in the presence of the graphene interlayer. Au intercalation, instead causes the vanishing of the interaction between Tb and Ni(111) (Fig. 1c). Conversely, in the case of ErPc₂, we found that the gold intercalation does not perturb the magnetic coupling (Fig. 1d). In a second work we have investigated a sub-monolayer of Co-TPP molecules [2] and we found that cobalt strongly couples antiferromagnetically to the Ni substrate, also through the graphene layer. The intercalation of graphene with gold leads to a complete removal of this coupling (see Fig. 2).

Overall, these studies give insights on the role of graphene and intercalated gold layers in the super-exchange coupling at metal-organic interface.

Fig. 2

Comparison between the magnetization curves for (a) Ni (blue circles), and Co (filled red squares) without (b) and with (c) Au-intercalation, measured at grazing incidence ($\theta = 70^\circ$, $T = 2$ K). The black line in (c) is the Brillouin curve of a pure paramagnet ($\lambda = 0$). Colour scheme: Co, red; N, blue; C, dark grey; Au, orange. The Co-TPP molecules lay flat on the Ni(111)/SLG surface, both with and without Au intercalation.



Contact persons

Valdis Corradini (valdis.corradini@nano.cnr.it)

Roberto Biagi (roberto.biagi@unimore.it)

References

- [1] Probing magnetic coupling between LnPc₂ (Ln=Tb, Er) molecules and graphene / Ni (111) substrate with and without Au-intercalation: role of the dipolar field. V. Corradini, A. Candini, D. Klar, R. Biagi, V. De Renzi, A. Lodi Rizzini, N. Cavani, U. del Pennino, S. Klyatskaya, M. Ruben, E. Velez-Fort, K. Kummer, N. B. Brookes, P. Gargiani, H. Wende, and M. Affronte. *Nanoscale* 10, 277-283 (2018).
- [2] CoTPP molecules deposited on Graphene/Ni (111): quenching of the antiferromagnetic interaction induced by gold intercalation. V. Corradini, A. Candini, D. Klar, R. Biagi, V. De Renzi, A. Lodi Rizzini, N. Cavani, U. del Pennino, H. Wende, E. Otero, and M. Affronte. *J. Appl. Phys.* 125, 142904 (2019).

Plasmonic-nanoparticle sensitization of oxides and plasmonic semiconductors for solar energy conversion

Transient modifications of the functionality of oxides are obtained by combining the materials with metallic nanoparticles, in which visible light absorption induces the excitation of localized surface plasmon resonances (LSPRs). We demonstrate that LSPRs can be tuned by changing the architecture of the oxide/metal system. Moreover, we identify an efficient and long-living plasmon-mediated transient charge transfer from the nanoparticles to the oxide, expected to influence the material redox properties. LSPRs can be directly imaged by scanning transmission electron microscopy coupled with electron energy loss spectroscopy. Here, we demonstrate for the first time the localization of two surface plasmon resonances on (vacancy) doped copper phosphide semiconducting nanocrystals.

The coupling of wide band gap oxides with plasmonic nanoparticles (NPs) has shown to be effective in providing materials with a light absorption range extending over the full solar radiation spectrum promising to convert solar into chemical or electric energy. The localized surface plasmon resonance (LSPR) decay, occurring on femtosecond time scales, involves a relevant energy transfer to the oxide, which may lead to modifications of the material properties on much longer time scales. A clear understanding of the mechanisms for plasmonic energy transfer in well-controlled systems is essential for a knowledge-driven optimization of this important class of functional materials. By fast transient absorption spectroscopy (FTAS) measurements, performed at EuroFEL Support Laboratory (EFSL – Cnr Ism), we identified a long-living excited state induced by LSPR decay, and we ascribed it to a transient occupation of 4f levels (Fig. 1) [1]. The state has a lifetime beyond 500 ps and it is expected to have an influence on the material redox properties (Fig. 1).

An additional contribution to NP activity and plasmonic response can come from the NP-oxide interaction via the charge transfer from/to the support. These excess charges induce a small shift of LSPR, modifies the dielectric properties, and influences the dynamic properties of plasmon losses and hot electron injection. We have recently demonstrated by means of XPS and UPS that an interfacial charge transfer occurs between the Fe core and Ag shell in well-ordered array of self-organized NPs on MgO films on Mo(001) [2]. As a consequence of the Fe@Ag morphology and composition the NP LSPR is modified with respect to pure Ag NPs (Fig. 2).

Direct imaging of LSPRs is nowadays possible making use of scanning transmission electron microscopy (STEM), coupled with energy loss spectroscopy (EELS), and it has been largely used for metallic NPs. However, similar LSPRs are expected in semiconductors, e.g. from hole carriers in the valence band generated from vacancies, and frequencies typically observed in the infrared (<1 eV). By making use of STEM-EELS, we demonstrated that Cu vacancies in hexagonal Cu_{3-x}P NPs (~50 nm size and ~10 nm thickness), can be directly quantified ($n_h = n_v = 5.0 \cdot 10^{21} \text{ cm}^{-3}$). These are responsible of two LSPRs localized at the centre and at the edge of the NPs, which are in agreement with the resonances calculated from the vacancy concentration obtained from the STEM analysis (Fig. 3) [3].

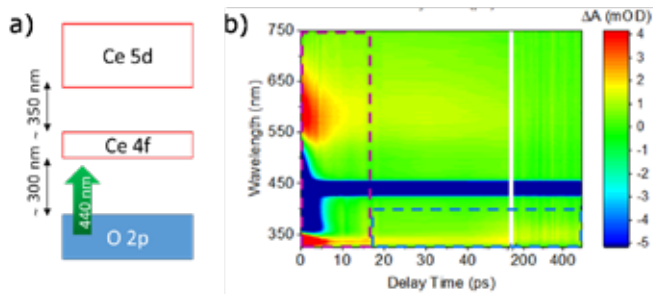


Fig. 1

a) Sketch of the CeO₂ electronic structure, showing the absence of transitions at the LSPR excitation wavelength of 440 nm. b) FTAS map of Ag NPs embedded in a CeO₂ matrix, obtained using a pump at the LSPR excitation wavelength (440 nm), below the CeO₂ band gap. The purple box highlights the Ag NPs LSPR-related features at ultrashort times, while the blue box marks the signal ascribed to electron injection from Ag NPs to the CeO₂ film [1].

Fig. 2

a) 100 × 100 nm² STM image 0.5 Å Ag/0.4 Å Fe/10 ML MgO on Mo(001) (I = 0.06 nA, U = 3.2 V). Inset shows the FFT of the image. (b) EELS spectra of Ag and Fe@Ag NPs on MgO film. The fits of the plasmon modes evidence the contribution to the response of the system. A sketch reports the charge transfer occurring in the core-shell NPs [2].

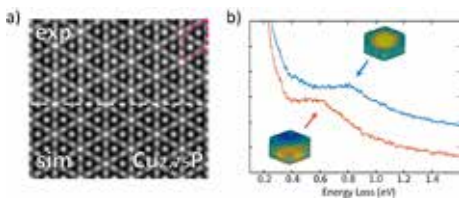
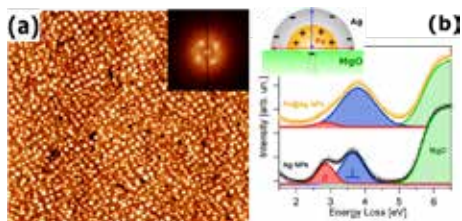


Fig. 3

a) STEM image (exp) compared with a simulated image (sim) from a [001] Cu_{3-x}P NP assuming x = 2.75, corresponding to 1.5 average Cu vacancies in the hexagonal cell (dashed magenta line). b) EELS spectra obtained from the edge (orange line) and from the center (blue line) of the NP, and calculated charge distributions of the two LSPRs.

Contact persons

Paola Luches (paola.luches@nano.cnr.it)
Giovanni Bertoni (giovanni.bertoni@nano.cnr.it)

References

- [1] Highly efficient plasmon-mediated electron injection into cerium oxide from embedded silver nanoparticles. J. S. Pelli Cresi, M. C. Spadaro, S. D'Addato, S. Valeri, S. Benedetti, A. di Bona, D. Catone, L. Di Mario, P. O'Keeffe, A. Paladini, G. Bertoni, and P. Luches. *Nanoscale* 11, 10282 (2019).
- [2] Core-Shell Charge Transfer in Plasmonic Fe@Ag Nanoparticles on MgO Film. S. Benedetti, I. Valenti, and S. Valeri. *The Journal of Physical Chemistry C* 123, 8206 (2019).
- [3] Direct Quantification of Cu Vacancies and Spatial Localization of Surface Plasmon Resonances in Copper Phosphide Nanocrystals. G. Bertoni, Q. Ramasse, R. Brescia, L. De Trizio, F. De Donato, and L. Manna. *ACS Materials Letters* 1, 665-670 (2019).

Strain engineering of two-dimensional materials

The control of mechanical deformations in 2D materials such as graphene, transition metal dichalcogenides, and other graphene-related materials opens exciting perspectives for the engineering of the electronic states and of the optoelectronic response. Artificial lattice studies have validated these concepts, but their implementation using actual 2D crystals remains today largely elusive. We investigate methods to induce and measure strain in 2D crystal and demonstrate how they can substantially modify their properties.

A first central and enabling target of the activities is the investigation different strategies to induce and measure strain in 2D. In particular, we demonstrate a novel method based polymeric actuators that can be nanopatterned with a great design freedom by electron-beam nanolithography [1]. The method provides an ideal platform to induce custom strain profiles, which would be challenging to obtain using more conventional techniques reported in the literature, and it can be easily combined with a variety of imaging and spectroscopic techniques [2,3]. All these are in fact crucial in order to measure and understand the mechanical configuration of the material (Fig. 1). Among these, an important part of the activities focuses on the development of atomic force methods for the investigation of the mechanical configuration and properties of suspended graphene membranes, which poses particularly challenging issue in terms of data interpretation, and is crucial for the progress of nanomechanical systems based on 2D materials.

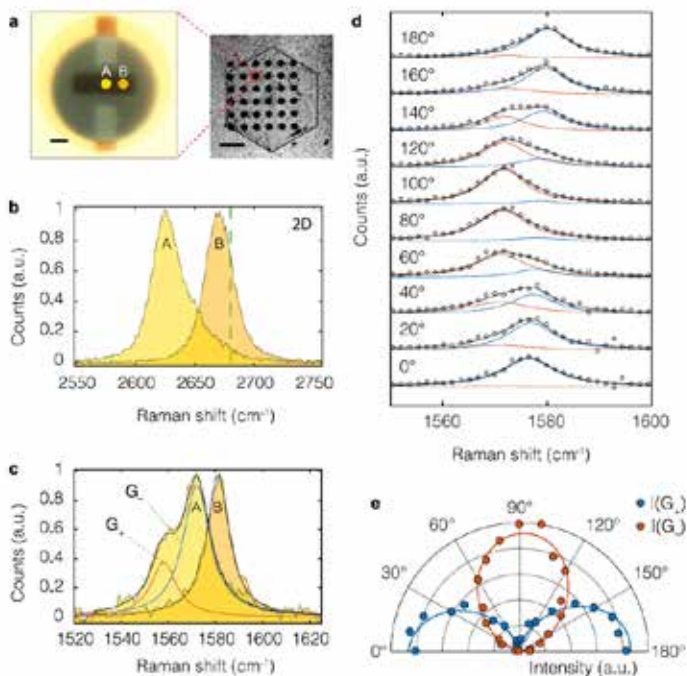
Different device architectures have been devised and explored to transfer strain to the 2D crystals. A first approach consists of using suspended atomic monolayers, where the material is completely free to expand or contract in the real space, also leading to intriguing phenomena such as the controlled nucleation of micro and nano-wrinkles [1], which can be associated with an interesting modulation of the chemical, mechanical, optical and electronic properties of the material. A further very promising approach we explore is the use of Van der Waals heterostructures, where mechanical deformation is allowed by the very low frictional forces that can be obtained between the stacked layers. In particular, in our activities we studied so far the deformation of WS_2 on top of graphene and its impact on the local photoluminescence of the dichalcogenide monolayer [4]. The same approach is expected to be a valid for many of the possible combinations of 2D materials that are currently studied within the scientific community.

Fig. 1

(a) Optical micrographs of one of our polymer-actuated suspended graphene devices. Scale bars correspond to 2 μm (left) and 50 μm (right).

(b) The 2D peak measured at the center of the membrane (yellow dot in panel (a)) is significantly shifted with respect to the one obtained 2 μm away (orange dot), in a region where no significant strain is expected. (c) The G peak displays the splitting of the G_+ and G_- Raman modes, as expected in the presence of anisotropic strain.

(d,e) The two components can be separated by taking advantage of polarized Raman, which can be also exploited to determine the crystalline orientation of the flake. (left) and 50 μm (right). (b) The 2D peak measured at the centre of the membrane (yellow dot in panel (a)) is significantly shifted with respect to the one obtained 2 μm away (orange dot), in a region where no significant strain is expected. (c) The G peak displays the splitting of the G_+ and G_- Raman modes, as expected in the presence of anisotropic strain. (d,e).



Contact persons

Alessandro Pitanti (alessandro.pitanti@nano.cnr.it)

Stefano Roddaro (stefano.roddaro@nano.cnr.it)

References

- [1] Controlling local deformation in graphene using micrometric polymeric actuators. F. Colangelo, A. Pitanti, V. Mišeikis, C. Coletti, P. Pingue, D. Pisignano, F. Beltram, A. Tredicucci, and S. Roddaro. *2D Materials* 5, 045032 (2018).
- [2] Mapping the mechanical properties of a graphene drum at the nanoscale. F. Colangelo, P. Pingue, V. Mišeikis, C. Coletti, F. Beltram, and S. Roddaro. *2D Materials* 6, 025005 (2019).
- [3] Microphotoluminescence (μPL) measurements of bidimensional materials in a custom-made setup. F. V. Di Girolamo, A. Di Lieto, A. Sottile, S. Roddaro, M. Tonelli, and A. Tredicucci. *Jour. of Phys* 1226, 012008 (2019).
- [4] Local tuning of WS₂ photoluminescence using polymeric micro-actuators in a monolithic van der Waals heterostructure. F. Colangelo, A. Morandi, S. Forti, F. Fabbri, C. Coletti, F. V. Di Girolamo, A. Di Lieto, M. Tonelli, A. Tredicucci, A. Pitanti, and S. Roddaro. *Appl. Phys. Lett.* 115, 183101 (2019).

Black Phosphorus: Pristine and doped surface investigations using Scanning Tunneling Microscopy

Exfoliated black phosphorus (bP) attracted great interest after its first realization in 2014 for its interesting properties such as a band gap tunable with layer number and electrical and optical properties anisotropic in plane. However, surface studies on this material have been hampered because of its high reactivity with oxygen and water. We developed a protocol to study the surface of exfoliated bP by Scanning Tunneling Microscopy (STM). After achieving atomic resolution, we applied this protocol to controlled desorption experiments and studied the anisotropic craters that form on the surface with annealing close to desorption temperature.

Within the Cnr Nano SEED project 2017 SURPHOS we developed a procedure to exfoliate bP and mount the samples under nitrogen atmosphere in a glove bag on the sample holder for STM measurements. As a conducting flat substrate suitable for this technique, we use graphene on silicon carbide. That allows us to avoid any fabrication step and therefore to minimize environmental contamination of the samples. With this method, we obtain high quality samples, as demonstrated by the atomic resolution obtained on the bP flakes, shown in Fig. 1.

We study the modification of the surface upon annealing up to 550 °C. In particular, our attention is focused on the temperature range 375 °C–400 °C, when sublimation starts, and a controlled desorption from the surface occurs alongside with the formation of characteristic well-aligned craters. There is an open debate in the literature whether the crystallographic orientation of these craters is along the zigzag or the armchair direction [X. Liu et al., *J. Phys. Chem. Lett.* 6, 773 (2015); M. Fortin-Deschènes et al., *J. Phys. Chem. Lett.* 7, 1667 (2016)]. Thanks to the atomic resolution provided by STM, we are able solve the controversy, stating that the craters are one monolayer deep and identifying the orientation of the craters with respect to the bP crystal: the long axis of the craters is aligned along the zigzag direction of bP, as shown in Fig. 2 [1].

We also evaporated sub-monolayer copper in situ onto these exfoliated bP samples. From transport measurements, copper is known to n-dope bP [S. P. Koenig et al., *Nano Lett.* 16, 2145 (2016)] but no study of the microscopic mechanism has been performed so far. We investigate the samples by STM and scanning tunneling spectroscopy (STS). We observe an n-type doping of bP due to Cu islands as well as a band gap opening. Ab initio simulations complement the experimental observations.

Further activities on bP at Cnr Nano regard the study of longitudinal magneto transport at very high fields (in collaboration with McGill University Montreal) and the characterization of nanocomposites in which bP flakes are embedded in a polymeric matrix [2,3] (in collaboration with Cnr Icom). This activity is part of the ERC Advanced grant PHOSFUN.

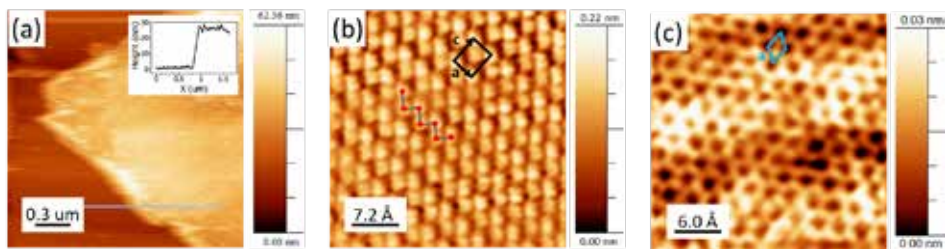


Fig. 1

STM images identifying bP flakes and graphene substrate. (a) STM image showing on the right a bP flake ~25 nm high above the graphene substrate on the left. The inset shows the height profile across the line shown in the STM image. Scan size: $2\mu\text{m} \times 2\mu\text{m}$, imaging parameters: (0.7 V, 300 pA). Annealing conditions: 200 °C, 2 h. (b) Atomic resolution image obtained on bP at room temperature showing the zigzag pattern with unit cell parameters $a = (3.45 \pm 0.43)$ Å and $c = (4.40 \pm 0.12)$ Å. Scan size: $3.6\text{ nm} \times 3.6\text{ nm}$, imaging parameters: (0.7 V, 25 pA). Annealing conditions: 400 °C, 10 min. (c) Atomic resolution image on graphene. Unit cell indicated. Scan size: $3\text{ nm} \times 3\text{ nm}$, imaging parameters: (0.1 V, 157 pA). Annealing conditions: 450 °C, 2 h.

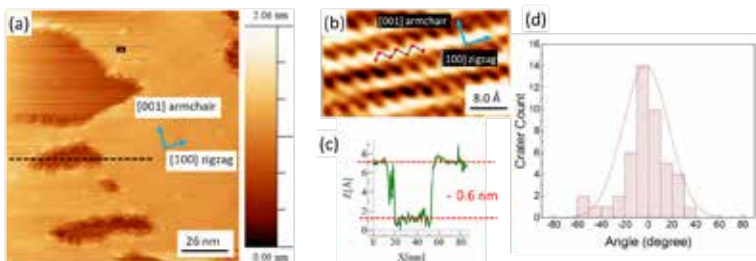


Fig. 2

Crystallographic direction of crater alignment. (a) STM image of a $130\text{ nm} \times 130\text{ nm}$ scan area, showing aligned craters on bP after annealing at 400 °C for 2 h; scanning parameters: (1.2 V, 100 pA). (b) Atomic resolution image obtained after zooming into the region marked in (a), providing information of the crystallographic directions of the bP flake; scanning parameters: (1.2 V, 100 pA). (c) Height profile across the crater along the dashed line in (a), showing ~0.5 nm step height, compatible with monolayer desorption. (d) Histogram showing the distribution of crater angle orientation in one of the areas measured after annealing at 375 °C, 10 min. 0° corresponds to the horizontal axis in the image.

Contact persons

Francesca Telesio (francesca.telesio@nano.cnr.it)
Stefan Heun (stefan.heun@nano.cnr.it)

References

- [1] STM study of exfoliated few layer black phosphorus annealed in ultrahigh vacuum. A. Kumar, F. Telesio, S. Forti, A. Al-Temimy, C. Coletti, M. Serrano Ruiz, M. Caporali, M. Peruzzini, F. Beltram, and S. Heun. 2D Mater. 6, 015005 (2019).
- [2] Polymer-Based Black Phosphorus (bP) Hybrid Materials by in Situ Radical Polymerization: An Effective Tool to Exfoliate bP and Stabilize bP Nanoflakes. E. Passaglia, F. Cicogna, F. Costantino, S. Colai, S. Legnaioli, G. Lorenzetti, S. Borsacchi, M. Geppi, F. Telesio, S. Heun, A. Ienco, M. Serrano-Ruiz, and M. Peruzzini. Chem. Mater. 30, 2036 (2018).
- [3] Hybrid nanocomposites of 2D black phosphorus nanosheets encapsulated in PMMA polymer material: New platforms for advanced device fabrication. F. Telesio, E. Passaglia, F. Cicogna, F. Costantino, M. Serrano-Ruiz, M. Peruzzini, and S. Heun. Nanotechnology 29, 295601 (2018).

Graphene engineering: new opportunities for controlled functionalization and energy storage

All amazing properties of graphene – high carrier mobility, robustness and flexibility, broadband transmittance, large surface to mass ratio, lubricity – rely on its being a perfect 2D hexagonal crystal. However, this brings also some drawbacks, such as null density of states at the Dirac point, weak interactions and reactivity, limiting its potential both in nano-electronics and in storage applications. These, in addition, require functionalization or building 3D graphene-based scaffolds. We combine Density Functional Theory (DFT), classical Molecular Dynamics (MD), Scanning Tunneling Microscopy (STM), Low Energy Electron Diffraction (LEED), and Nano-calorimetry to the aim of functionalizing and morphing supported graphene for energy applications.

To these aims, graphene imperfections acquire a new significance: the crystal symmetry breaking by chemical defects, structural deformations, or other types of disorder creates electron density inhomogeneities with an enhancement of reactivity and new interaction capabilities [1]. This is the case both for the buffer layer on SiC [1], obtained by Si evaporation and partially covalently bound to the substrate (Figs. 1a,b) and for quasi free-standing monolayer graphene (QFMLG) [2,3] obtained by metal or H intercalation (Figs. 1a,c). Both show possible “hot spots” of chemical reactivity located on nano-sized super lattices, which could be exploited for chemical nano-patterning.

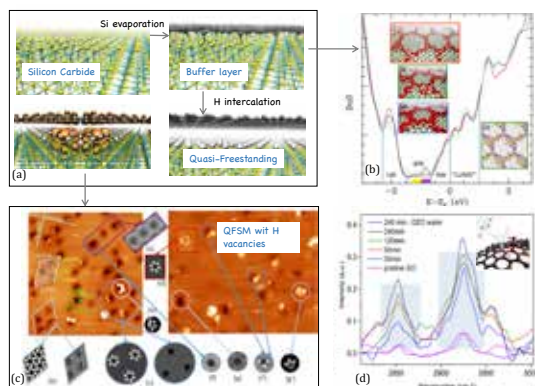


Fig. 1

(a) A scheme illustrating the production of different types of graphene on SiC and their main structural characteristics. From the SiC bulk (upper left) one obtains the buffer layer by Si evaporation. Intercalating metals or H, one obtains QFMLG. If the H coverage is not complete, localized electronic states form between the substrate and the graphene layer (orange surfaces in the bottom left image). The color-coding for atoms in structures is: yellow = Si, cyan = C in the substrate, grey = C in graphene, white = H. (b) Details of the total and local density of states of the buffer layer (from [2]). The total DoS is

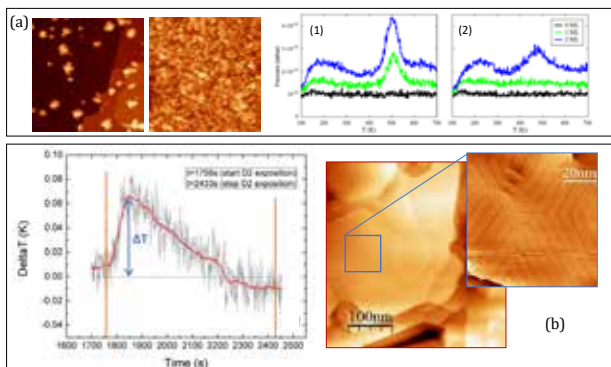
reported at the top for three slightly different model systems and shaded up to the Fermi level. The system appears a doped semiconductor with some localized states in the ~ 1 eV gap. The electronic density of the in-gap states is reported as insets in the enlarged DoS plot at the bottom, as red isosurfaces (total DoS integrated in the gap, for the three different models), and in yellow-purple, for two separated sets of in-gap states. (c) An illustration of the different types of localized vacancy states that can be found in QFSMG (orange = STM images, grey = STM simulated images). The experimental images show that vacancies are located over a nano-sized lattice, although not all sites are occupied. However, the sizes, shapes, and contrasts are various. The simulations show that these differences depend on the number and relative location of the H-vacant sites, allowing at the same time to classify a large number of different vacancy types. From [3,4]. (d) Raman spectrum of the C-H peak to determine the amount of chemisorbed H (images from [5]), as per the water splitting reaction path illustrated in the inset.

On the other hand, grain boundaries of supported nano-crystalline graphene are shown to pin Ti clusters more efficiently than single-crystalline graphene (Fig. 2a) [4]. Besides, electric or electrochemically driven functionalization is shown to be a viable route to control H adhesion, and is enhanced by the presence of structural defects such as epoxy or hydroxyl groups produced by oxidation (Fig. 1d) [5], so to allow the combination of H-storage with water splitting for new concept devices in the clean energy field.

Calorimetry is a powerful tool to investigate the energy exchange due, e.g., to chemisorption, but it usually requires macroscopic sample quantities. We have developed an original experimental setup able to detect temperature variations as low as 10 mK in a sample of ~10 ng using a thermometer device having physical dimensions of 5x5 mm², and used it to measure the enthalpy release during the adsorption of D₂ on a Ti-decorated monolayer graphene, involving an enthalpy release of ~ 23 μJ [6]. Further upgrades and combination with atomically resolved microscopy techniques show an improvement of sensitivity up to 4 mK at room temperature (Fig. 2b).

Fig. 2

H adhesion on graphene of different types. (a) STM images of single-crystalline graphene (1-left) and nano-crystalline graphene (2-left) after Ti deposition of 0.55 ML. TDS on (1-right) single-crystalline graphene and (2-right) nanocrystalline graphene, with Ti coverage of 0 ML (black), 1 ML (green), and 2 ML (blue). Hydrogen uptake is higher in single crystalline graphene [4]. (d) Heat release during the hydrogenation of a Ti-graphene sample (left) and surface analysis of a gold on mica thermometer (right) [6]. Zoom-in shows the gold “herringbone” reconstruction.



Contact persons

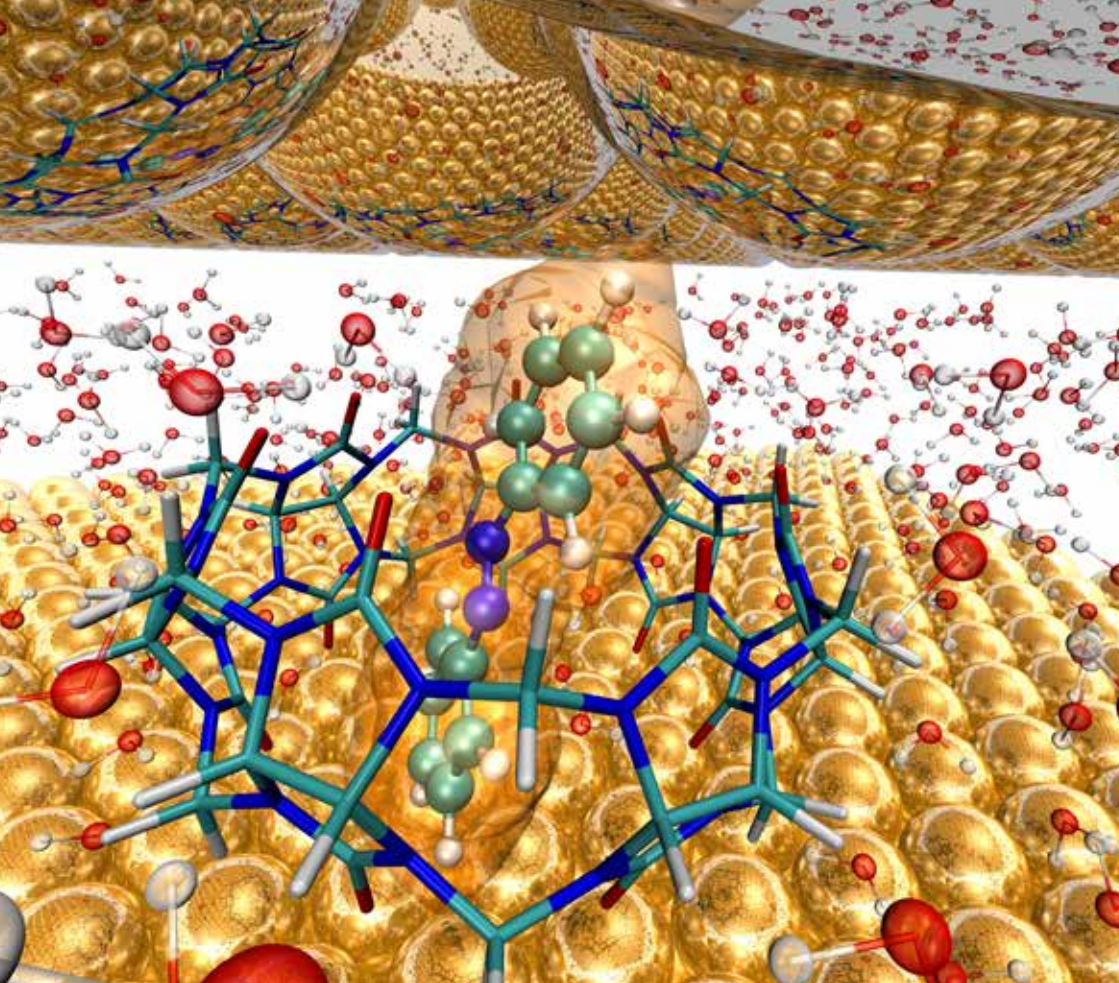
Valentina Tozzini (valentina.tozzini@nano.cnr.it)

Stefano Veronesi (stefano.veronesi@nano.cnr.it)

References

- [1] Intrinsic structural and electronic properties of the Buffer Layer on Silicon Carbide unraveled by Density Functional Theory. T. Cavallucci and V. Tozzini. *Sci Rep* 8, 13097 (2018).
- [2] Unraveling localized states in quasi free standing monolayer graphene by means of Density Functional Theory. T. Cavallucci, Y. Murata, M. Takamura, H. Hibino, S. Heun, and V. Tozzini. *Carbon* 130, 466-474 (2018).
- [3] Atomic and Electronic Structure of Si Dangling Bonds in Quasi-Free-Standing Monolayer Graphene. Y. Murata, T. Cavallucci, V. Tozzini, N. Pavliček, L. Gross, G. Meyer, M. Takamura, H. Hibino, F. Beltram, and S. Heun. *Nano Res* 11, 864–873 (2018).
- [4] Morphology of Ti on Monolayer Nanocrystalline Graphene and Its Unexpectedly Low Hydrogen Adsorption. Y. Murata, S. Veronesi, D. Whang, and S. Heun. *J Phys Chem C* 123, 1572-1578 (2018).
- [5] Water splitting for hydrogen chemisorbed in graphene oxide dynamically evolves into a graphene lattice. L. Ciapparuchi, L. Bellucci, G. C. Castillo, G. M. D. Sánchez, Q. Liu, V. Tozzini, and J. Martorell. *Carbon* 153, 234-241 (2019).
- [6] A sensitive calorimetric technique to study energy (heat) exchange at the nano-scale. L. Basta, S. Veronesi, Y. Murata, Z. Dubois, N. Mishra, F. Fabbri, C. Coletti, and S. Heun. *Nanoscale* 10, 10079-10086 (2018).





Highlights

- Nanoscale theory modelling and computation

Introduction to Nanoscale theory modelling and computation

Over the past recent years, the theoretical modelling and computation activities at Cnr Nano have been extended in scope and width, now ranging from development of theoretical methods and their implementation in large scale community codes, to the exploitation of state-of-the-art techniques for the study of cutting edge scientific problems relevant to nanoscience and nanomaterials. These include the development of advanced density functional theory methods to address ground and excited state properties as well as the theoretical framework to study molecular nanoplasmonic phenomena; large scale studies of electronic and optical properties of nanostructures. Quantum confinement and many-body effects in low dimensional structures are also extensively investigated. Overall, the impact of these studies spans from applications in nanomedicine to light harvesting and photocatalysis, and to the design of optoelectronic devices. Three main topics are outlined in the following.

Development of advanced methodologies. Formal developments of the theoretical framework of DFT have been put in place in order to further investigate the features of the so-called ensemble-DFT method, showing how it can impact the study of ground as well as excited state properties of matter. Also related to a variational formulation of the electronic structure problem, Koopmans compliant functionals, aimed at restoring the piece-wise linearity of the total energy, have been demonstrated and assessed for extended systems [N. L. Nguyen et al., *Phys. Rev. X* 8, 021051 (2018)]. Real-time quantum chemistry methods dedicated to molecular nanoplasmonic systems (where, e.g., molecular excitations are coupled to confined plasmons) have been developed and applied to scientific cases of interest (see below).

Jointly with activities related to the MaX Centre of Excellence, these developments represent key enablers for a large amount of future computational studies related to nanoscience and nanodevices. Importantly, a number of the studies presented here would have not been possible without the work done on codes [P. Giannozzi et al., *J. Phys.: Condens. Matter* 29, 465901 (2017); D. San-

galli et al., J. Phys.: Condens. Matter 31, 325902 (2019)] to enable the use of large scale high performance computing infrastructures.

Optics & Nanoplasmonics. STM-induced luminescence of graphene nanoribbons experimentally shows unexpected features that were investigated theoretically by large scale many-body perturbation theory calculations. The experimental results were then rationalized as connected to peculiar transitions arising from the nanoribbon termini, optically enhanced by the presence of the tip. Electronic and optical properties of doping centers (H and Nb) of rutile TiO₂ have also been investigated computationally. This analysis showed important defect-related features in the optical spectra, which can be relevant to understand photocatalytic properties of doped TiO₂. Nanoplasmonics simulations helped clarifying the interpretation of infrared absorption spectra of biological ion-channels supported on gold surfaces and also showed how photoisomerization of azobenzene can be manipulated by controlling strong coupling parameters.

Low dimensional structures. The distribution of dopants in hexagonal-diamond Si nanowires of different dimensions has been studied by using density functional theory methods. The study found out different trends depending on the diameter of the wires, highlighting the relevance of quantum confinement and shedding light on the role of crystal phase in the doping mechanism at the nanoscale. In a separate work, III-V core-shell nanowires were studied using an effective mass approach developed in-house. Carrier localization, electronic structure and optical spectra of the systems were simulated showing how density, localization, and spin-orbit interaction can be tailored. The interplay of quantum confinement and electron-electron interaction in Carbon nanotubes has also been the subject of a joint theoretical experimental study. By performing quasiparticle calculations, the authors showed that the giant magnetic moments found experimentally can only be captured by considering a self-energy correction to the electronic band structure due to electron-electron interactions.

Modeling of electron and spin states in core-shell nanowires

Multishell coaxial semiconductor nanowires are attracting much interest due to their possible application as light harvesting devices, nanophotonic sources, quantum computing gates, and nanoscale FETs with novel geometries.

We study electronic states of III-V core-shell nanowires, where carriers can be either strongly localized in the wire core, or form a curved 2D electron gas, possibly wrapped on the surface of the prismatic hexagonal interface between different materials. We compute the highly engineerable carrier localization, the electronic structure, the optical spectra and the value of spin-orbit coupling.

A predictive numerical modeling of carrier states in a complex structure as coaxial semiconductor nanowires must rely on a comprehensive simulation taking into account dimensions, material modulation, doping profiles and the effect of applied electric and magnetic fields. By using a 8-band k,p model and a self-consistent local density-functional simulation code, specifically developed in-house to tackle this class of systems, we show how free-carrier density, localization, and spin-orbit interaction can be tailored [1,2] by means of external fields (see, e.g., Fig. 1) and structure engineering. Also, Aharonov-Bohm like oscillations, Landau level formation and magnetic anisotropy of the magneto-conductance are predicted.

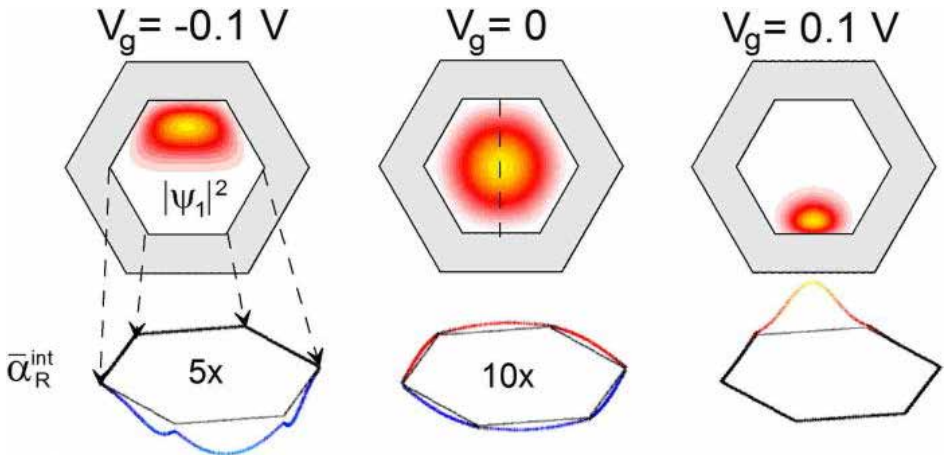


Fig. 1

Top row: Square of the ground state envelope function of electrons for three values of the bottom gate voltage V_g in an hexagonal section of a InAs-InAsP core-shell nanowire. The free-electron density is $n_e=10^7$ cm⁻³. Bottom row: linear density of the interfacial spin-orbit coupling at the core/shell interface. Results are obtained from a self-consistent simulation for the electronic states and a 8-band k,p model for the spin-orbit coupling [2].

Since core-shell nanowires are promising candidates for the realization of quantum gates in topologically-protected quantum computing platforms, due to the possibility of tailoring spin-orbit coupling by means of external fields, the assessment of spin-orbit spectra is technologically relevant. Additionally, electrical control of spin-orbit coupling is necessary in the realization of spintronic devices.

The prismatic geometry of core-shell nanowires leads to complex localization patterns of carriers in regimes where the mean-field approach fails. In this case, we describe the formation of optically active in-gap excitonic states by means of a multielectron numerical approach based on the exact solution of the multiparticle Hamiltonian for electrons in the valence and conduction bands, which includes the Coulomb interaction in a nonperturbative manner. We expose the formation of well-separated quasidegenerate levels, and analyze the electron localization in the corners or on the sides of the polygonal cross sections [3].

Indeed, the assessment of confined-exciton spectra in core-shell nanowires has been mostly focused on hexagonal structures. However, triangular or square core-shell nanowires have also shown unique properties, such as a broad range of emitted radiation observed even at room temperature which makes them perfect candidates as multicolor light sources.

Contact persons

Andrea Bertoni (andrea.bertoni@nano.cnr.it)

Guido Goldoni (guido.goldoni@unimore.it)

References

- [1] Tuning Rashba spin-orbit coupling in homogeneous semiconductor nanowires. P. Wójcik, A. Bertoni, and G. Goldoni. *Phys. Rev. B* 97, 165401 (2018).
- [2] Enhanced Rashba spin-orbit coupling in core-shell nanowires by the interfacial effect. P. Wójcik, A. Bertoni, and G. Goldoni. *Appl. Phys. Lett.* 114, 073102 (2019).
- [3] Excitons in Core-Shell Nanowires with Polygonal Cross Sections. A. Sitek, M. Urbaneja Torres, K. Torfason, V. Gudmundsson, A. Bertoni, and A. Manolescu. *Nano Lett.* 18, 2581 (2018).

Molecular nanoplasmonics: from spectroscopy to strong coupling effects

The investigation of the interaction between molecular excitations and plasmons confined at the nanoscale is a field of research of great scientific and technological interest. Such interaction may be used to enhance spectroscopic signals of molecules, down to the single molecule level. It can also be so large to allow the creation of hybrid molecule-plasmon excitation (strong coupling regime). Within the ERC project TAME Plasmons, we are developing and applying multiscale approaches for these systems, featuring an atomistic, quantum-mechanical description for the relevant molecular moiety. Thanks to these tools, we helped clarifying tip-enhanced infrared absorption spectra of biological ion channels, and we showed how the photoisomerization of azobenzene can be manipulated by strong coupling.

Localized surface plasmons (LSPs) are collective oscillations of the conduction electrons confined in a nanostructure. LSPs give origin to enhanced electromagnetic (EM) fields when excited at resonance frequency, that translate into enhanced optical properties of nearby molecules (e.g. Surface Enhanced Raman Scattering (SERS) or Infrared Absorption (SEIRA)), and that can be potentially used to launch a non-stationary, localized excitation in multichromophoric systems such as the protein LH2 [1]. The EM coupling between the molecular excitations and the LSPs can become so strong to create hybrid states, with a different excited state potential energy surface (PES), which then results in a different photochemistry.

We are developing multiscale models for such phenomena, that preserve the realism of atomistic, quantum mechanical description (e.g., DFT) for the molecule, combined with classical EM models for the nanostructures [2]. On the methodological side, we contributed developing ω FQ, a novel classical atomistic approach for plasmonic nanostructures, essentially based on the Drude model of conduction. We showed that ω FQ is able to reproduce the plasmonic behaviour of metal subnanometer junctions with quantitative fidelity to full ab initio calculations, at a much lower computational cost [3]. In parallel with such development, we have also extended to the strong coupling regime an established approach to simulate photochemistry of molecules, based on a specialized semi-empirical method. We have then simulated the azobenzene photoisomerization, showing how it can be manipulated by changing the strong coupling parameters [4].

We have also collaborated with the experimental group of L. Baldassarre and M. Ortolani (Sapienza Univ., Rome) who applied tip-enhanced infrared spectroscopy to characterize the light-induced changes in a mutated bacteriorhodopsin (BR) [5]. From the specific experimental plasmonic set-up, the polarization of the local EM field was inferred and plugged in a QM/MM method devised to simulate IR spectra of proteins [6] and specifically adapted to this set-up. A branching of the natural photocycle of the protein was identified for samples with thickness of ~ 2 lipid bilayers. The study is particularly relevant for BR-based optoelectronic and, more generally, for AFM-based IR spectroscopy studies of conformational changes of proteins embedded in intrinsically heterogeneous native cell membranes.

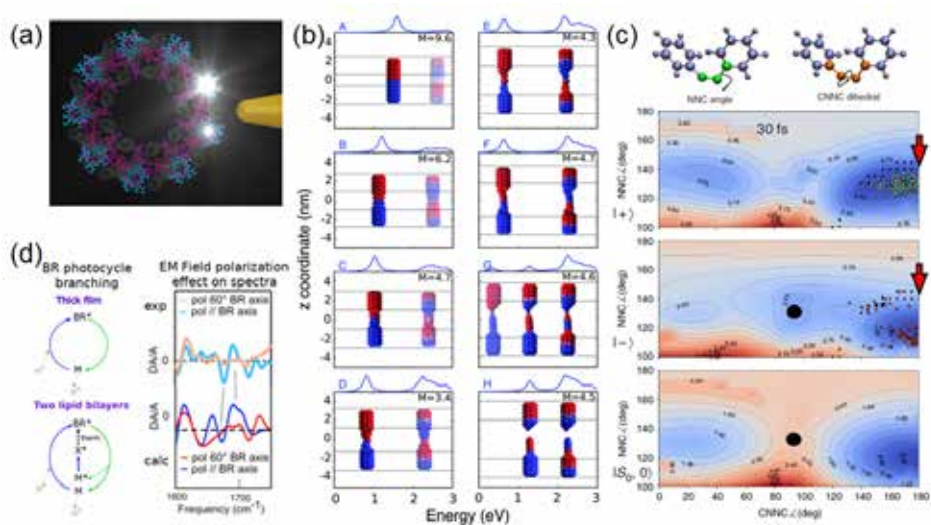


Fig. 1

(a) Pictorial representation of excitonic localization in LH2 obtained by a gold nanotip, simulated in [1]. (b) Absorption spectra of a Na nanojunction at different extent of stretching and the related oscillating charge distribution as obtained by ω FQ [3]; color scale: charge extent and sign. (c) Representation of azobenzene polaritonic PES as a function of the two internal coordinates relevant for photoisomerization [4]. Green/red dots: coordinates for the simulated trajectories after 30fs of dynamics, and their state. Black circle: electronic conical intersection. Red arrow: polaritonic conical intersection. (d) Left: Natural BR photocycle (up, thick film) and branched BR photocycle for samples with thickness of ~ 2 lipid bilayers (bottom). Right: Calculated and experimental difference spectra (M state - BR state) for different polarizations of the EM field. The polarization effects are highlighted with grey lines. Adapted from [5].

Contact persons

Stefano Corni (stefano.corni@nano.cnr.it)

Laura Zanetti Polzi (laura.zanettipolzi@nano.cnr.it)

References

- [1] Shaping excitons in light-harvesting proteins through nanoplasmonics. S. Caprasecca, S. Corni, and B. Mennucci. *Chem. Sci.* 9, 6219 (2018).
- [2] Multiscale modelling of photoinduced processes in composite systems. B. Mennucci and S. Corni. *Nat. Rev. Chem.* 3, 315 (2019).
- [3] A classical picture of subnanometer junctions: an atomistic Drude approach to nanoplasmonics. T. Giovannini, M. Rosa, S. Corni, and C. Cappelli. *Nanoscale* 11, 6004 (2019).
- [4] Manipulating azobenzene photoisomerization through strong light-molecule coupling. J. Fregoni, G. Granucci, E. Coccia, M. Persico, and S. Corni. *Nat. Comm.* 9, 4688 (2018).
- [5] Tip-Enhanced Infrared Difference-Nanospectroscopy of the Proton Pump Activity of Bacteriorhodopsin in Single Purple Membrane Patches. V. Gilberti, R. Polito, E. Ritter, M. Broser, P. Hegemann, L. Puskar, U. Schade, L. Zanetti-Polzi, I. Daidone, S. Corni, F. Rusconi, P. Biagioni, L. Baldassarre, and M. Ortolani. *Nano Lett.* 19, 3104 (2019).
- [6] A quantitative connection of experimental and simulated folding landscapes by vibrational spectroscopy. C. M. Davis, L. Zanetti-Polzi, M. Gruebele, A. Amadei, R. B. Dyer, and I. Daidone. *Chem. Sci.* 9, 9002 (2018).

Preferential positioning, stability and segregation of dopants in hexagonal Si nanowires

Considerable progresses in the growth of hexagonal-diamond (2H) group IV nanowires, also known as lonsdaleite nanowires, have once again proved the emerging role of crystal phase engineering in the design of novel nanostructures with well-tailored properties. Here we studied the physics of common p- and n- type dopants in hexagonal-diamond Si, a Si polymorph that can be synthesized in nanowire geometry without the need of extreme pressure conditions, by means of first-principles electronic structure calculations and compared our results with those for the well-known case of cubic-diamond nanowires (3C).

We performed ab initio DFT calculations to investigate the role of the crystal phase on p-type and n-type dopants stability in 2H- and 3C-Si nanowires (NWs). Calculations for bulk systems and larger diameter NWs revealed a clear preference for p-type dopants to be in the 2H phase as a consequence of the stronger tendency of this structure to stabilize a 3-fold coordination around the impurity. The robustness of our considerations is supported by a model which takes into account both structural and electronic effects in the stability of group III, group IV, and group V dopants in 2H-Si.

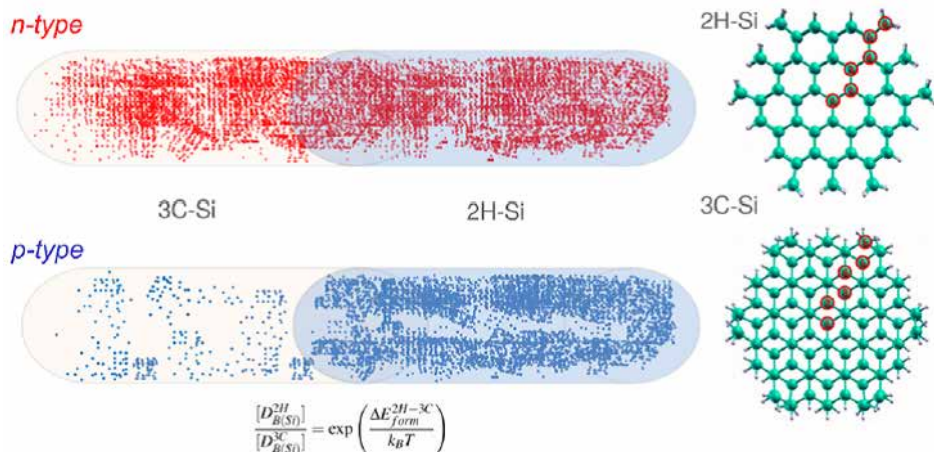


Fig. 1

Left panel: Qualitative distribution of B (bottom) and P (top) dopants in 3C/2H Si NW homo-junctions at large diameters. Right panel: Cross section of 2H and 3C Si NWs. © American Chemical Society (2019).

Our results confirm and complement the experimental observations of Fabbri et al. [1] where it was shown that B-doping helped retaining the hexagonal phase in 10 nm Si NWs. Additionally, although clean 2H/3C axial or radial interfaces have not been reported yet, the cubic/hexagonal multidomains reported by Vincent and coworkers [Nanotechnology 2018] are suitable samples to verify the accumulation of B-dopant on the hexagonal side of a 2H/3C grain boundary. The theoretical predictions could be verified by means of atom probe tomography measurements [Perea, Nat. Nanotechnology 2009]. In the case of ultrathin NWs, because of the lower symmetry with respect to bulk systems and the greater freedom of structural relaxation, there is only a moderate preference for both p- and n-dopants for 3C NWs. Furthermore, at such small diameters, both phases can induce segregation phenomena for p-type dopants due, again, to the tendency of trivalent atoms in group IV compounds to create a trigonal-like chemical environment, associated, in some cases, with large geometrical distortions. On the other hand, we show that segregation does not take place in the case of n-type dopants because of the high energy barriers that prevent diffusion to the surface. The novelty of these findings will likely impact future experimental works concerning the study of dopants in group IV polytype NWs.

Contact person

Stefano Ossicini (stefano.ossicini@unimore.it)

References

- [1] Preparing the way for doping wurtzite silicon nanowires while retaining the phase. F. Fabbri, E. Rotunno, L. Lazzarini, D. Cavalcoli, A. Castaldini, N. Fukata, K. Sato, G. Salviati, and A. Cavallini. *Nano Lett.* 13, 5900–5906 (2019).
- [2] Preferential positioning, stability and segregation of dopants in hexagonal Si nanowires. M. Amato, S. Ossicini, E. Canadell, and R. Rurali. *Nano Letters* 19, 866–876 (2019).

Advancing the theory and the computation of density functionals for mixed states of electrons

We know the fundamental equations to be solved in materials science but, except in special cases, we cannot solve them exactly, not even with the most powerful computers. To make an approximate solution practical and sufficiently accurate, the original problem must be reformulated, we may say, to carefully reduce any ‘dead wood’ in the calculations. Our work advances state-of-the-art generalized formulations of density functional theory, the most popular reformulation, to facilitate agile solutions of difficult chemical, biological, materials, and physics problems, such as those related to the charge transport through man-made nanostructures and charge transfers in molecules.

Density functional theory (DFT) is often referred to as ‘the workhorse’ of computational materials science. But its original formulation only applies to electronic ground states – i.e., states with the lowest energy— and only those with a filled shell. These limitations can be relaxed via proper generalizations. But in such generalizations, the formal properties of key quantities must be carefully revisited.

Mixed states (i.e., ensembles) of electrons can be tackled by means of Ensemble-DFT (EDFT). A first version of EDFT deals with systems that can gain and release electrons. A second version of EDFT deals with stationary states of higher energy mixed together with the ground state. Via these generalizations, for example, we can calculate important features of the charge transport through nanoelectronic devices as well as the charge-transfers that occur in important photochemical and photo-physical processes. In practice, however, this also requires to devise extended and improved approximate density functionals for ensembles.

Recently [1], we have shown that the energy gap for the charge transport through quantum dots – the artificial atoms of nanostructured semiconductors – can be estimated more cheaply and yet accurately than before. In a second work [2], we have proved that in mapping the real problems onto auxiliary simpler problems as allowed by the framework, there are central quantities implementing such a mapping that behave differently than expected, and that this must be taken into account to obtain improved results. In a third work [3], we have demonstrated that EDFT can indeed solve important prototypical charge-transfers in molecules.

Our latest work [4] exposed a component of the energy expressed via EDFT which is unique to ensembles and thus requires innovative approximations (see Figure 1). In the same work, we provided a proof-of-principle that the newly identified energy component can indeed be successfully approximated.

Works [2,3] have been highlighted by the Editors of the journals; work [4] appeared in the Cnr’s homepage as news.

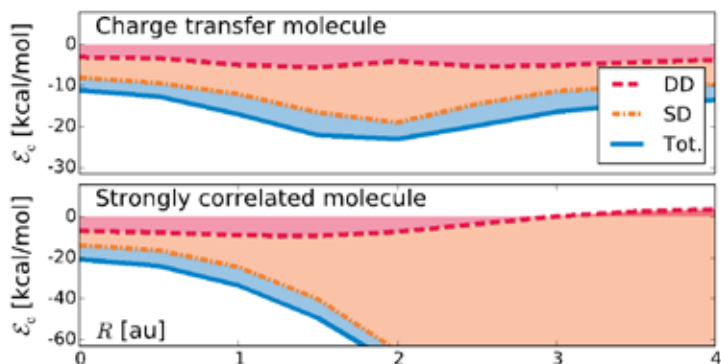


Fig. 1

Correlation energy (ϵ_c), which is an important component of the energies computed via (E)DFT, for ensembles of a diatomic-molecules model composed by the ground state and the first two excited states. SD (i.e., state-driven) denotes the part of the correlation energy that may be captured by conventional-like DFT approximations; DD (i.e., density-driven) is the correlation energy component, first identified in our work [4], that requires innovative approximations. R (horizontal axis) is the interatomic distance.

Contact person

Stefano Pittalis (stefano.pittalis@nano.cnr.it)

References

- [1] Fundamental gaps of quantum dots on the cheap. A. Guandalini, C. A. Rozzi, E. Räsänen, and S. Pittalis. Phys. Rev. B 99, 125140 (2019).
- [2] Asymptotic behavior of the Hartree-exchange and correlation potentials for fractional electron numbers in atoms. T. Gould, S. Pittalis, J. Toulouse, E. Kraisler, and L. Kronik. Phys. Chem. Chem. Phys. 21, 19805 (2019).
- [3] Charge transfer excitations from exact and approximate ensemble Kohn-Sham theory. T. Gould, L. Kronik, and S. Pittalis. J. Chem. Phys. 148, 174101 (2018).
- [4] Density-Driven Correlations in Many-Electron Ensembles: Theory and Application for Excited States. T. Gould and S. Pittalis. Phys. Rev. Lett. 123, 016401 (2019).

Light Emission Properties of Ultranarrow Graphene Nanoribbons

Thanks to their highly tunable band gaps, graphene nanoribbons (GNRs) with atomically precise edges are emerging as mechanically and chemically robust candidates for nanoscale light emitting devices of modulable emission color. We here combine ab-initio simulations and STM-induced light emission experiments to shed light on unpredicted, below-bandgap optical emission features in GNRs. Our theoretical findings, in addition to tracking the origin of the observed emission features, allow for a rationalization of other contradictory experimental observations, further opening the field for optical and optoelectronic applications.

While graphene is a promising material for a number of electronic applications, the absence of an optical gap limits its use for light emitting devices. Lateral confinement to form atomically precise, nanometer-wide graphene nanoribbons (GNRs) allows one to have a sizeable gap and prominent absorption features. A fine-tuning of the properties can be further achieved by exploiting more complex geometries and edge functionalization [1,2], as recently demonstrated by bottom-up fabrication techniques based on suitably designed molecular precursors. The reach of atomic precision has boosted this research line in the last decades, with an in-depth characterization of the GNR absorption properties. On the contrary, the investigation of their emission properties, which is relevant in the scope of future electroluminescent nanoscale devices, has been so far very limited.

We here investigate from first principles the electronic and optical response of infinite and finite-length armchair-edged graphene nanoribbons (A-GNRs), including the contact with an STM tip for the latter, within the framework of density functional theory and many-body perturbation theory. Ideal, infinite GNRs show an absorption spectrum dominated by excitonic excitations with Wannier-like character. For finite-length GNRs, we here identify additional low-energy, low-intensity excitations as a result of the explicit inclusion of zigzag termini. We find that these excitations coexist with bulk-like excitations, which have the same origin as the ones characterizing infinite AGNRs [3]. Moreover, they are shown to be almost independent of the GNR length due to their spatial localization at the termini. By investigating both the presence of defects and the effect of the STM tip, our simulations allow us to identify unpredicted optical transitions in GNRs and to elucidate the origin of below-bandgap STM-induced light emission [4]. This overall understanding contributes to opening the route for the realization of bright, robust and controllable graphene-based light emitting devices.

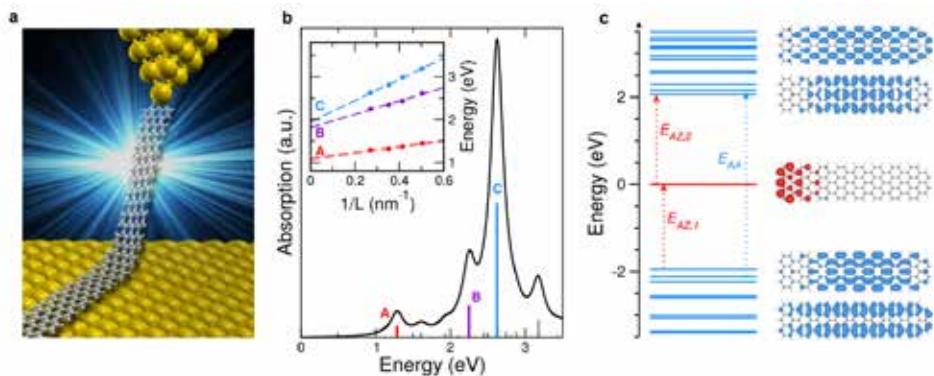


Fig. 1

(a) Schematics of the experimental configuration for STM-induced light emission from suspended GNRs. (b) Absorption spectrum and (c) energy level scheme computed for the self-standing (7,16)-AGNR according to the GW-BSE scheme. The main transitions corresponding to the peaks in (b) are displayed in (c), together with a few representative molecular orbitals around the Fermi level.

Contact person

Deborah Prezzi (deborah.prezzi@nano.cnr.it)

References

- [1] Bandgap Engineering of Graphene Nanoribbons by Control over Structural Distortion. Y. Hu, P. Xie, M. De Corato, A. Ruini, S. Zhao, F. Meggendorfer, L. A. Straaso, L. Rondin, P. Simon, J. Li, J. J. Finley, M. R. Hansen, J.-S. Lauret, E. Molinari, X. Feng, J. V. Barth, C.-A. Palma, D. Prezzi, K. Mullen, and A. Narita. *J. Am. Chem. Soc.* 140, 7803 (2018).
- [2] Multiwavelength Raman spectroscopy of ultranarrow nanoribbons made by solution-mediated bottom-up approach. D. Rizzo, D. Prezzi, A. Ruini, V. Nagyte, A. Keerthi, A. Narita, U. Beser, F. Xu, Y. Mai, X. Feng, K. Mullen, E. Molinari, and C. Casiraghi. *Phys. Rev. B* 100, 45406 (2019).
- [3] Termini effects on the optical properties of graphene nanoribbons. C. Cardoso, A. Ferretti, and D. Prezzi. *Eur. Phys. J. B* 91, 286 (2018).
- [4] Bright Electroluminescence from Single Graphene Nanoribbon Junctions. M. C. Chong, N. Afshar-Imani, F. Scheurer, C. Cardoso, A. Ferretti, D. Prezzi, and G. Schull. *Nano Lett.* 18, 175 (2018).

Interaction-driven giant orbital magnetic moments in carbon nanotubes

Carbon nanotubes are ideal systems to study many-body physics. This is particularly true in the case of ultraclean devices offering the study of quantum dots with extremely low disorder. The quality of such systems, however, has increasingly revealed glaring discrepancies between experiment and theory. Here, we address the outstanding anomaly of exceptionally large orbital magnetic moments in carbon nanotube quantum dots. We perform low temperature magnetotransport measurements of the orbital magnetic moment and find it is up to 7 times larger than expected from the conventional model. We carry out quasiparticle calculations and find the giant magnetic moments can only be captured by considering a self-energy correction to the electronic band structure due to electron-electron interactions.

We report on orbital magnetic moments, μ_{orb} , in ultraclean carbon nanotube quantum dots that deviate from existing theory both qualitatively and quantitatively. Instead of a magnetic moment which remains constant within a shell, we find that the orbital magnetic moment decreases monotonically with each added electron, as shown by dots with error bars in Fig. 1(c). Additionally, we analyze the magnitude of the moments and find that they are much larger than expected from semiclassical estimates based on a direct measurement of the nanotube radius R , according to the formula $\mu_{\text{orb}} = e v_F R / 2$, where e is the electron charge and v_F the Fermi velocity (empty squares in Fig. 1(c)). We further compare our results with other models taking into account a change in the size of the quantum dot with filling, a change in charging energy with magnetic field, and the orbital magnetic moment of a Wigner molecule [S. Pecker et al., *Nature Phys.* 9, 576 (2013)]. None of these models suffice to explain the magnitude or trend of our observations. It is only by treating electrons added to the dot as quasiparticles dressed by the Coulomb interaction with other electrons already present in the nanotube, including those in the filled valence band, that we are able to account for the enhanced orbital magnetic moment. A self-energy correction to the gap computed within the effective-mass approximation results in good agreement between observations and theory and is further validated by a first-principles GW calculation for a small nanotube. Finally, in agreement with previous studies, we show that our small band gap tubes present a residual gap at the Dirac field and we discuss the implications of our results in the context of the Mott [Deshpande et al., *Science* 323, 106 (2009)] and excitonic [D. Varsano et al., *Nature Commun.* 8, 1461 (2017)] insulating phases.

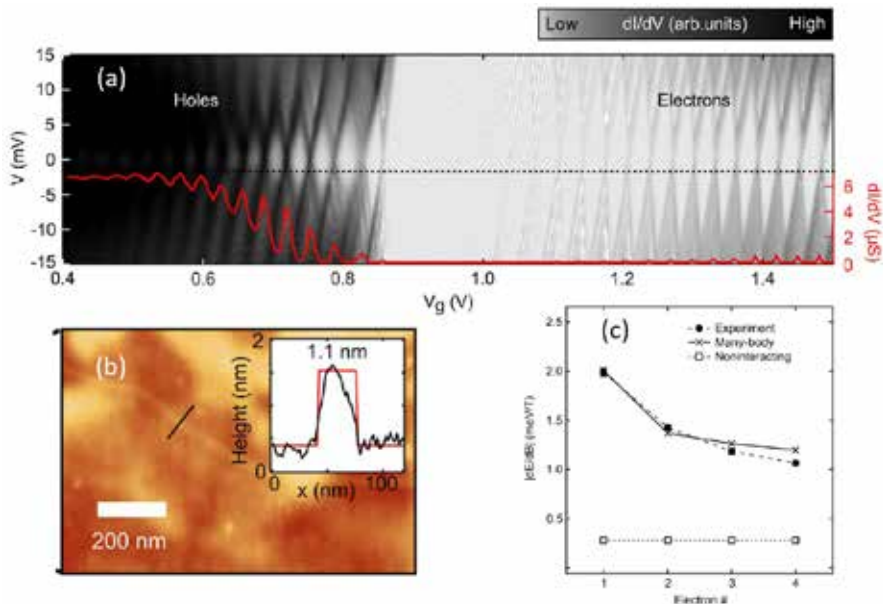


Fig. 1

Coulomb spectroscopy of a carbon nanotube quantum dot and orbital magnetic moment. (a) Coulomb diamonds of a representative ultraclean device at zero magnetic field. The gate voltage position V_g of Coulomb peaks at zero source-drain voltage V is converted into the chemical potential of each electron / hole added to the quantum dot. The chemical potential variation with the magnetic field gives the orbital magnetic moment. (b) AFM image of the device. The inset shows a line cut across the nanotube at the location of the black line in the AFM image, which provides an estimate of the radius. This is necessary to evaluate the orbital magnetic moment. (c) Measured (black dots with error bars) orbital magnetic moment vs number of electrons in the first orbital shell. The crosses are the values predicted within GW many-body perturbation theory, which explicitly includes electron-electron interaction. The empty squares are the prediction of the conventional semiclassical model.

Contact person

Massimo Rontani (massimo.rontani@nano.cnr.it)

Reference

[1] Interaction-driven giant orbital magnetic moments in carbon nanotubes. J. O. Island, M. Ostermann, L. Aspitarte, E. D. Minot, D. Varsano, E. Molinari, M. Rontani, and G. A. Steele. Phys. Rev. Lett. 121, 127704 (2018).

Electronic and optical properties of doped TiO₂ by many-body perturbation theory

Doping is one of the most common strategies for improving the photocatalytic and solar energy conversion properties of TiO₂, hence an accurate theoretical description of the electronic and optical properties of doped TiO₂ is of both scientific and practical interest. In this work we use many-body perturbation theory techniques to investigate two typical n-type dopants, niobium and hydrogen, in TiO₂ rutile. Using the GW approximation to determine band edges and defect energy levels, and the Bethe-Salpeter equation for the calculation of the absorption spectra, we find that the defect energy levels form nondispersive bands lying about 0.9 eV below the conduction bands of the pristine material. The defect states are also responsible for the appearance of low-energy absorption peaks that enhance the solar spectrum absorption of rutile. The spatial distributions of the excitonic wave functions associated with these low-energy excitations are very different for the two dopants, suggesting a larger mobility of photoexcited electrons in Nb-TiO₂.

Titanium dioxide is widely used in photocatalysis and solar energy conversion, but its efficiency is limited by the large band gap that severely reduces the photoabsorption of visible light. To improve the conductivity and photocatalytic properties, doping is often employed, and a large variety of dopants, both metals and non-metals, have been explored. Here we investigate the electronic structure and optical properties of Nb- and H-doped TiO₂, using a rigorous approach that goes beyond mean-field theory. We adopt MBPT, namely the GW approximation for the quasi-particle energies and the Bethe Salpeter equation for the optical spectra. The introduction of dopants into the rutile TiO₂ lattice leads to significant modification of the materials electronic and optical properties. Both interstitial Hydrogen and substitutional Niobium create a distortion of the crystal lattice around the defect and introduce electronic states localized mainly on adjacent Ti atoms. The resulting quasi-particle defect states form non dispersive bands that can be attributed to localized states with energies in the band gap (Fig. 1 top) that are found at about 0.9 eV below the conduction band minimum of pristine rutile. Comparing H- and Nb-doped TiO₂, a slightly higher degree of hybridization is apparent in TiO₂:H_i, which is consistent with the interstitial vs substitutional configuration of the defect. While the high energy part of the optical spectrum (> 3 eV) is little affected by the presence of the dopant states (Fig. 1 bottom), transition from the gap states to the conduction band give rise to new absorption peaks at low energy that enhance the absorption of rutile in the solar spectrum range. Interestingly, we found very different excitonic wavefunctions for the low energy excitations in H- and Nb doped rutile: while photoexcited electrons are largely delocalized in TiO₂:Nb_{Ti}, they remain localized close to the hole in TiO₂:H_i. These characteristics suggest a longer exciton lifetime and a larger mobility of photoexcited electrons in TiO₂:Nb_{Ti}, consistent with the use of Nb as an efficient dopant for improving the performance of TiO₂ in technological applications.

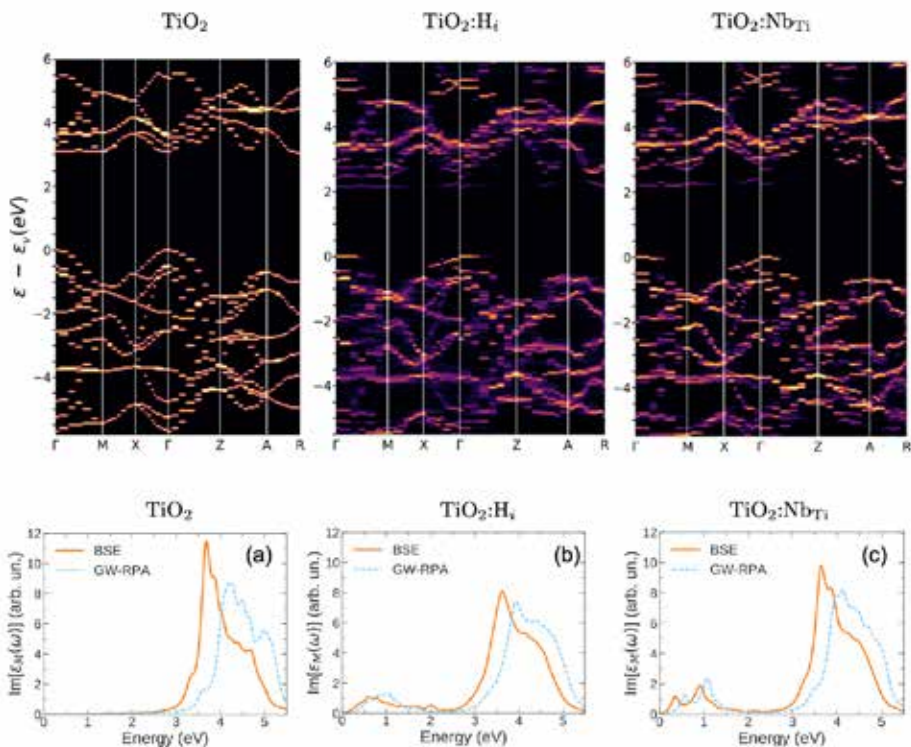


Fig. 1

Electronic and optical properties of pristine and doped TiO_2 : (Top): Unfolded quasi-particle band-structure for pristine, $\text{TiO}_2:\text{H}_i$ and $\text{TiO}_2:\text{Nb}_{\text{Ti}}$. Results for spin-up majority channels are shown. The more blurred the picture, the larger the hybridization induced by the defects. (Bottom): The imaginary part of the dielectric constant (averaged over x,y,z polarizations) for pristine, H-doped, and Nb-doped rutile, obtained by solving the BSE and the independent quasi-particle spectra (GW-RPA). Defect states are responsible for the absorption peaks in the low energy part of the spectra.

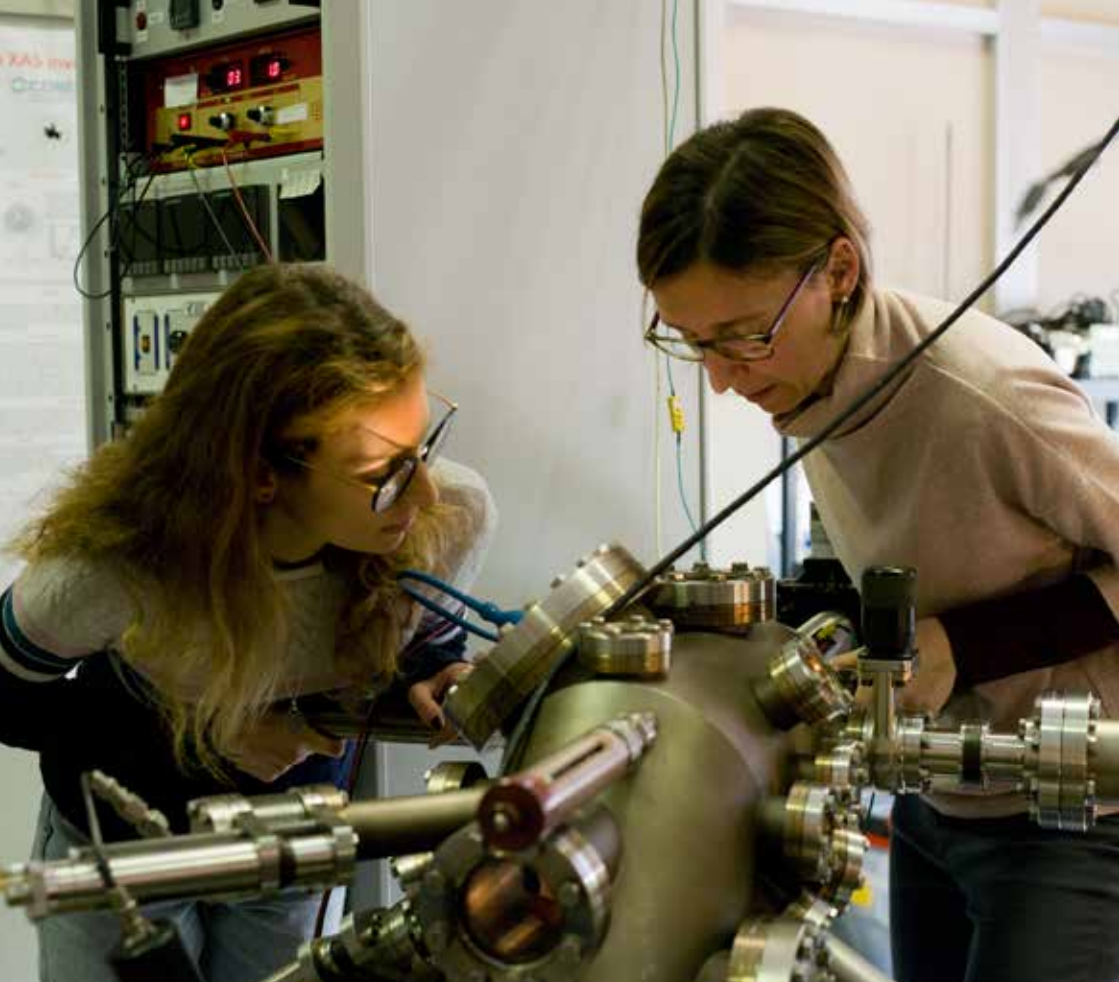
Contact person

Daniele Varsano (daniele.varsano@nano.cnr.it)

Reference

[1] Electronic and optical properties of doped TiO_2 by many-body perturbation theory. M. O. Atambo, D. Varsano, A. Ferretti, S. S. Ateeq, M. J. Caldas, E. Molinari, and A. Selloni. *Phys. Rev. Materials* 3, 045401 (2019).





Projects and grants

Cnr Nano research activity is mainly supported by funding obtained through competitive calls at different levels, from international to local. Projects running in 2018-2019 are listed below with the following details: project name, call details, project ID, coordinator, Cnr Nano principal investigator (if different), dates, website (if available). A short abstract is given for European-funded projects.

European projects



AndQC. Andreev qubits for scalable quantum computation. H2020-FETOPEN-2018-2020-01; GA 828948. Chalmers Tekniska Hogskola AB, SE (A. Geresdi); Cnr Nano Pisa (L. Sorba). 2019-2023. www.andqc.eu

Abstract. The goal is to establish the foundations of a radically new solid-state platform for scalable quantum computation, based on Andreev qubits. This platform is implemented by utilizing the discrete superconducting quasiparticle levels (Andreev levels) that appear in weak links between superconductors. Each Andreev level can be occupied by zero, one, or two electrons. The even occupation manifold gives rise to the first type of Andreev qubit. We will characterize and mitigate the factors limiting the coherence of this qubit to promote these proof-of-concept experiments towards a practical technology. The odd occupation state gives rise to a second type of qubit, the Andreev spin qubit, with an unprecedented functionality: a direct coupling between a single localized spin and the supercurrent across the weak link. Further harnessing the odd occupation state, we will investigate the so far unexplored scheme of fermionic quantum computation, with the potential of efficiently simulating electron systems in complex molecules and novel materials. The recent scientific breakthrough by the Copenhagen node of depositing of superconductors with clean interfaces on semiconductor nanostructures opened a realistic path to implement the Andreev qubit technology. In these devices, we can tune the qubit frequency by electrostatic gating. We will demonstrate single- and two-qubit control of Andreev qubits, and benchmark the results against established scalable solid-state quantum technologies, in particular semiconductor spin qubits and superconducting quantum circuits.

COMANCHE. Coherent manipulation and control of heat in solid-state nanostructures: the era of coherent caloritronics. FP7-IDEAS-ERC; GA 615187. Cnr Nano Pisa (F. Giazotto). 2014-2019.

Abstract. Electronic nanodevices have demonstrated to be versatile and effective tools for the investigation of exotic quantum phenomena under controlled and adjustable conditions. Yet, these have allowed giving access to the manipulation of charge flow with unprecedented precision. On the other hand, the wisdom dealing with control, measurements, storage, and conversion of heat in nanoscale devices, the so-called “caloritronics”, despite a number of recent advances, is still at its infancy. Although coherence often plays a crucial role in determining the functionalities of nanoelectronic devices, very little is known of its role in caloritronics. In such a context, coherent control of heat seems at present still very far from reach, and devising methods to phase-coherently manipulate the thermal current would represent a crucial breakthrough, which could open the door to unprecedented possibilities in several fields of science. Here we

propose an original approach to set the experimental ground for the investigation and implementation of a new branch of science, the “coherent caloritronics”.

EU-SUPER. Superconducting Magnetic RAM for Next Generation of Supercomputers. H2020-MSCA-IF-2017; GA 796603. Cnr Nano Pisa (F. Giazotto). 2018-2020.

Abstract. The ongoing demand for computing-power and data-storage is quickly approaching the physical limits of conventional silicon-based electronics. To overcome this limit different approaches beyond conventional complementary metal-oxide-semiconductor (CMOS) technology are nowadays under investigation. On the one hand, quantum computers, based on non-classical superposition of logic units (bit), offer bright perspectives. On the other hand, energy-efficient superconducting circuits based on Josephson junctions have already demonstrated a computational speed two orders of magnitude larger than conventional CMOS-based ones. The complete implementation of a supercomputer based on this technology is currently limited by the lack of memories operating at cryogenic temperatures, i.e. in close contact and compatible with the superconducting processor.

Starting from the growth of thin films of FI/S bilayers, the first objective of this project will be the design of new architectures to control the magnetic configuration of the FI/S interfaces. The successful miniaturization and patterning of these materials will enable the realization of a prototype of FI/S-based superconducting magnetic-RAM (SMRAM), thus providing the missing building block towards the implementation of the superconducting computer. The last objective of the project is to demonstrate the scalability (including all the write and read protocols) to make the SMRAM technology ready for the large-scale market.

GRANT (ATTRACT Seed project). GRaphene Golay micro-cell Arrays for a color-sensitive TeraHertz imaging sensor. H2020-INFRAINNOV-2017-1; GA 777222. Cnr Iom (M. Lazzarino); Cnr Nano Pisa (A. Pitanti). 2019-2020.

<https://attract-eu.com/selected-projects/graphene-golay-micro-cell-arrays-for-a-color-sensitive-terahertz-imaging-sensor-grant>

Abstract. Grant project aims at the realization of Golay micro-cells based on graphene suspended membranes. The pressure change in the cell due to the absorption of THz radiation will extremely push the ultralight membranes, improving the system detection sensitivity. Furthermore, a proper patterning of one cell side using metallic metasurfaces will enable selective absorption and the use of the micro-cells in color-sensitive arrays, building the base for an improved THz detection technology.

Graphene-based disruptive technologies - GrapheneCore1.

H2020-Adhoc-2014-20; GA 696656. Chalmers Tekniska Hoegskola AB, SE (J. Kinaret); Cnr Nano Pisa (V. Tozzini and M. S. Vitiello). 2016-2018.

www.grapheneflagship.eu



Abstract. This project is the second in the series of EC-financed parts of the Graphene Flagship, a 10 year research and innovation endeavour with a total project cost of 1 billion euros, funded jointly by the European Commission and member states and associated countries.

The mission of the Graphene Flagship is to take graphene and related layered materials from a state of raw potential to a point where they can revolutionize multiple industries. This will bring a new dimension to future technology – a faster, thinner, stronger, flexible, and broadband revolution. Our program will put Europe firmly at the heart of the process, with a manifold return on the EU investment, both in terms of technological innovation and economic growth.

Within the Optoelectronics work package Cnr Nano is involved in the development of photodetectors operating at Terahertz frequencies in the resonant plasma wave regime and exploiting graphene, black-phosphorus and related Van der Waals heterostructures. Within the hydrogen storage work package, it is involved in designing advanced graphene based materials for fast and efficient uptake, storage, and release.



Graphene Flagship Core Project 2. H2020-SGA-FET-GRAPHE-NE-2017; GA 785219. Chalmers Tekniska Hoegskola AB, SE (J. Kina-ret); Cnr Nano Pisa (V. Tozzini and M. S. Vitiello). 2018-2020.
www.grapheneflagship.eu

Abstract. The progress of the flagship follows the general plans set out in the Framework Partnership Agreement, and the second core project represents an additional step towards higher technology and manufacturing readiness levels. The Flagship is built upon the concept of value chains, one of which is along the axis of materials-components-systems; the ramp-up phase placed substantial resources on the development of materials production technologies, the first core project moved to emphasise components, and the second core project will move further towards integrating components in larger systems. This evolution is manifested, e.g., in the introduction of six market-motivated spearhead projects during the Core 2 project.

Within the Optoelectronics work package Cnr Nano is involved in the development of graphene high-speed photodetectors at THz frequencies, and saturable absorbers exploiting graphene, and graphene THz modulators. Within the energy storage work package, it is involved in computer modeling and design of graphene-based nano-porous materials to be used as smart electrodes in supercapacitors and batteries.



INTERSECT. Interoperable Material-to-Device simulation box for disruptive electronics. H2020-NMBP-TO-IND-2018; GA 814487. Cnr Nano Modena (A. Calzolari). 2019-2022.
www.intersect-project.eu

Abstract. Intersect wants to leverage European leadership in materials' modelling software and infrastructure to provide industry-ready integrated solutions that are fully compliant with a vision of semantic interoperability driven by standardized ontologies. The resulting IM2D framework - an interoperable material-to-device simulation plat-

form - will integrate some of the most used open-source materials modelling codes (Quantum ESPRESSO and SIESTA) with models and modelling software for emerging devices via the SimPhony infrastructure for semantic interoperability and ontologies, powered by the AiiDA workflow engine, and its data-on-demand capabilities and apps interface. API-compliance with established standards will allow pipelines to and from public repositories, and embedding into the front-end of materials hubs, such as MarketPlace, while testing, validation, and standardization will take place together with the industrial partners. Intersect will drive the uptake of materials modelling software in industry, bridging the gap between academic innovation and industrial novel production, with a goal of accelerating by one order of magnitude the process of materials' selection and device design and deployment.



IQubits. Integrated Qubits Towards Future High-Temperature Silicon Quantum Computing Hardware Technologies. H2020-FETOPEN-2018-2019-2020-01; GA 829005. Aarhus Universitet, DK (D. Zito); Cnr Nano Modena (F. Troiani). 2019-2023.
www.iqubits.eu

Abstract. The objectives of the interdisciplinary project IQubits are to (i) develop and demonstrate experimentally high-temperature (high-T) Si and SiGe electron/hole-spin qubits and qubit integrated circuits (ICs) in commercial 22nm Fully-Depleted Silicon-on-Insulator (FDSOI) CMOS foundry technology as the enabling fundamental building blocks of quantum computing technologies, (ii) verify the scalability of these qubits to 10nm dimensions through fabrication experiments and (iii) prove through atomistic simulations that, at 2nm dimensions, they are suitable for 300K operation. The proposed 22nm FDSOI qubit ICs consist of coupled quantum-dot electron and hole spin qubits, placed in the atomic-scale channel of multi-gate n- and p-MOSFETs, and of 60-240GHz spin control/readout circuits integrated on the same die in state-of-the-art FDSOI CMOS foundry technology. To assess the impact of future CMOS scaling, more aggressively scaled Si-channel SOI and nitride-channel qubit structures will also be designed and fabricated in two experimental processes with 10nm gate half pitch. The latter will be developed in this project. The plan is for the III-nitrides (III-N) qubits to be ultimately grown on a SOI wafer, to be compatible with CMOS.



MaX. Materials design at the exascale. H2020-EINFRA-2015-1; GA 676598. Cnr Nano Modena (E. Molinari). 2015-2018. Materials design at the exascale. European Centre of Excellence in materials modelling, simulations, and design. H2020-INFRAEDI-2018-1; GA 824143. Cnr Nano Modena (E. Molinari). 2018-2021.
www.max-centre.eu

Abstract. MaX aims at allowing the pre-exascale and exascale computers expected in Europe in the 2020's to meet the demands from a large and growing base of researchers committed to materials discovery and design. This goal will be achieved by: i) an innovative software development model, based on the concept of separation of concerns,

that will enable performance of the community codes on heterogeneous hardware architectures, without disrupting their internal structure, the richness of their simulation capabilities, and their distributed and open development model. In this way, the most important community codes for quantum mechanical materials modelling will be ready for pre-exascale machines by the completion of MaX programme, and prepared to be ported to new architectures as they will become available; ii) an integrated ecosystem enabling the convergence of HPC and HTPC, that will allow steering the millions to hundreds of millions of simulations that are needed to optimise the properties and performances of a material or a device, with robust and reproducible workflows, all contributing to an ever growing repository of curated data; iii) a new approach to scientific computing in which hardware and software are co-designed and co-developed taking into mutual account the constraints and goals; iv) innovative measures for easy access to materials science applications, for engaging academic and industrial communities and fostering a broader and diverse pool of well trained users and developers.



MIR-BOSE. Mid- and far-IR optoelectronic devices based on Bose-Einstein condensation. H2020-FETOPEN-1-2016-2017; GA 737017. Université Paris Sud, FR (R. Colombelli); Cnr Nano Pisa (M. S. Vitiello). 2017-2020.
www.mir-bose.eu

Abstract. The MIR-BOSE project will demonstrate disruptive optoelectronic devices operating in the strong coupling regime between light and matter. In particular: the first bosonic lasers operating in the mid-IR and THz frequency ranges of the electromagnetic spectrum. Second, a new concept of inverse-Q-switching leading to the generation of high power pulses in the mid-IR ranges, overcoming severe bottlenecks in current technology. Finally, non-classical/quantum light sources and devices based on ultra-fast modulation of the light-matter interaction, generating squeezed states of light in the mid-IR/THz spectral range for quantum optics applications. These new sources will have a major impact on a wide range of technologies and applications in the mid-IR and THz frequency ranges, being advantageous compared to current commercial solutions.



NANO-JETS. Next-generation polymer nanofibers: from electrified jets to hybrid optoelectronics. FP7-IDEAS-ERC; GA 306357. Cnr Nano Pisa (D. Pisignano). 2013-2018.
www.nanojets.eu

Abstract. This project ultimately targets the application of polymer nanofibers in new cavity-free lasers. To this aim, it wants to tackle the still unsolved problems of the process of electrospinning in terms of product control by the parameters affecting the dynamics of electrified jets. The electrospinning is based on the uniaxial elongation of polymeric jets with sufficient molecular entanglements, in presence of an intense electric field. It is a unique approach to produce nanofibers with high throughput. This project aims at elucidating and engineering the still unclear working principles of elec-

trospinning by solutions incorporating active materials, with a tight synergy among modelling, fast-imaging characterization of electrified jets, and process engineering. Once optimized, nanofibers will offer an effective, well-controllable and cheap material for building new cavity-free laser systems.



PHENOMEN. All-Photonic Circuits enabled by opto-mechanics. H2020-FETOPEN-2014-2015-RIA; GA 713450. ICN2, ES (C. Sotomayor Torres); Cnr Nano Pisa (A. Pitanti). 2016-2019.
www.phenomen-project.eu

Abstract. Phenomen aims at building a phononic chip platform, where coherent vibrations above 1 GHz can be generated, routed and detected via optomechanical devices operating at room temperature. Adding novel functionalities in phonon processing such as switching and modulation, the technology developed in Phenomen will enable the coupling of different physical (quantum) systems towards the realization of the ultimate hybrid platform, where photons, electrons, and phonons can be interchangeably used for information manipulation and control.

PHOSFUN. Phosphorene functionalization: a new platform for advanced multifunctional materials. ERC-2014-ADG; GA 670173. Cnr Iccom (M. Peruzzini) and Cnr Nano Pisa (S. Heun). 2015-2019.

Abstract. 2D materials have attracted a great deal of interest due to their variety of applications. Since its discovery in 2004, graphene has monopolized the attention given the unparalleled combination of outperforming structural and functional properties, which pave the way for a plethora of different applications. Its applicability in micro- and nanoelectronic has been later demonstrated to be strongly limited due to its inherent lack of a band gap. This limitation could be overcome using phosphorene, a recently discovered 2D sheet formed by phosphorus atoms prepared by exfoliation of black phosphorus and endowed with a natural band gap. The PHOSFUN proposal focuses on the unexplored chemical reactivity of phosphorene and gathers together chemists mastering the chemistry of phosphorus with physicists expert in advanced nanostructured systems. We aim, among others, to set-up a scalable and reproducible synthesis of mono and multilayer phosphorene.



Q-SORT. Quantum sorter. H2020-FETOPEN-1-2016-2017; GA 766970. Cnr Nano Modena (V. Grillo). 2017-2021.
www.qsort.eu

Abstract. Q-SORT introduces a revolutionary concept whereby the transmission electron microscope (TEM) is employed as a so-called Quantum Sorter, i.e., a device that can pick out and display detailed information about electron quantum states. This in turn provides researchers with precious new information about the sample being examined. The project -which includes applications in physics, biology, and bio-

chemistry- is expected to have a wide-ranging impact due to the ubiquitous adoption of TEM and STEM across many disciplines. Q-SORT also has foundational value in physics as it fosters its own kind of sparse-sensing approach to TEM, advancing the field in the direction of quantum measurement.

SOULMAN. Sound–Light Manipulation in the Terahertz. FP7-IDEAS-ERC; GA 321122. Università di Pisa, IT and Cnr Nano Pisa (A. Tredicucci). 2013-2018.

Abstract. The interaction of electromagnetic radiation with the mechanical vibrations of solids affects and determines many different physical phenomena. At the microscopic level, scattering of light with phonon excitations is a well-known process exploited in semiconductor devices like Raman amplifiers and acousto-optic modulators. At the macroscopic scale, the interaction is mediated by the radiation pressure and is raising considerable interest as a way to excite and control mechanical oscillators, allowing, for instance, the refrigeration of a macroscopic object near the quantum limit. This rich physics has been mostly developed in the visible or near-infrared spectral ranges. SouLMan aims at establishing the new field of THz opto-mechanics based on quantum cascade technology, at investigating the phenomena and concepts that become available in this spectral range and in optically active systems, and at using this knowledge to implement innovative device functionalities and applications.

SPRINT. Ultra-short pulse laser resonators in the Terahertz. H2020-ERC-CoG-2015; GA 681379. Cnr Nano Pisa (M. S. Vitiello). 2016-2021.

Abstract. Ultra-short light pulses with large instantaneous intensities can probe light-matter interaction phenomena, capture snapshots of molecular dynamics and drive high-speed communications. In a semiconductor laser, mode-locking is the primary way to generate ultrafast signals. Despite the intriguing perspectives, operation at Terahertz (THz) frequencies is facing fundamental limitations: engineering “ultrafast” THz semiconductor lasers from scratch or finding an integrated technology to shorten THz light pulses are currently two demanding routes. SPRINT aims to innovatively combine the ground-breaking quantum cascade laser (QCL) technology with graphene, to develop a new generation of passive mode-locked THz photonic laser resonators, combined with unexplored electronic nanodetectors for ultrafast THz sensing and imaging.

SUPERTEd. Thermoelectric detector based on superconductor-ferromagnet heterostructures. H2020-FETOPEN-1-2016-2017; GA 800923. Jyväskylän Yliopisto, FI (T. Heikkilä); Cnr Nano Pisa (F. Giazotto). 2018-2022.
www.superted-project.eu

Abstract. Superted proposes to study a new type of sensor based on the thermoelectric conversion of the radiation signal to electrically measurable one. This approach is based on the newly found giant thermoelectric effect taking place in superconductor/ferromagnet heterostructures. Utilizing this effect, the sensor pixels can be self-powered by

the measured radiation, and therefore extra bias lines are not needed (patent pending for the detector concept). Within the project, we aim to establish a proof of concept of this device by (i) fabricating such detector elements, and (ii) characterizing single pixels of thermoelectric detectors for X-ray and THz imaging via approaches that are scalable to large arrays.



SUPERTOP. Topologically protected states in double nanowire semiconductor hybrids. H2020 QuantERA ERA-NET Cofund in Quantum Technologies 2017. Budapest University of Technology and Economics, HU (S. Csonka); Cnr Nano Pisa (L. Sorba). 2018-2020.
<http://dept.physics.bme.hu/Supertop/>

Abstract. To realize fully topologically protected universal quantum computation, more exotic anyons, such as parafermions are required. Thus, the unambiguous demonstration of parafermion states will have a great impact on the development of universal quantum computation. The experimental realization of parafermions is challenging, since they are based on the combination of various ingredients, such as crossed Andreev reflection, electron–electron or spin-orbit interaction, and high quality quantum conductors. Thus, the investigation of all these ingredients is essential and timely to achieve further experimental progress.

The main objectives of SuperTop are: a) development of different DNW (double nanowire-based hybrid devices geometries), which consist of two parallel 1D spin-orbit nanowires coupled by a thin superconductor stripe, and b) investigation of the emerging exotic bound states at the superconductor/semiconductor interface of the DNW.



TAME-Plasmons. Theoretical chemistry Approach to tMEResolved molecular Plasmonics. H2020-ERC-CoG-2015; GA 681285. Università di Padova, IT and Cnr Nano Modena (S. Corni). 2016-2021.
www.tame-plasmons.eu

Abstract. Ultrafast spectroscopy is a powerful tool able to disclose the atomistic real-time motion picture of the basic chemical events behind technology and life, such as catalytic reactions or photosynthetic light harvesting. Nowadays, by cleverly harnessing the interaction of the studied molecules with plasmons (collective electron excitations supported, e.g., by metal nanoparticles) it is becoming possible to focus these investigations on specific nanoscopic regions, such as a portion of a catalytic surface or of a photosynthetic membrane. The goal of TAME-Plasmons is to develop a theoretical chemistry approach to directly simulate the real-time evolution of molecules interacting with plasmons and light.

T-CONVERSE (ATTRACT Seed project). Temperature-to-phase conversion THz radiation sensors. H2020-INFRAINNNOV-2017-1; GA 777222. INFN, IT (F. Paolucci); Cnr Nano Pisa (F. Gia-zotto). 2019-2020.

<https://attract-eu.com/selected-projects/temperature-to-phase-conversion-thz-radiation-sensors-t-converse/>

Abstract. T-CONVERSE proposes new class cryogenic radiation sensors characterized by operating broadband from 10GHz to 10THz, resolving power larger than 100, and unprecedented noise equivalent power of the order of 10-23W/Hz^{1/2}. These detectors are based on the innovative concept of temperature-to-phase conversion. In a TPC sensor, the latter can be due to the absorption of radiation by antenna coupled to the detection junction. Finally, j across the readout junction is measured by an integrated superconducting quantum interference transistor. Thanks to their unparalleled performances, the TPC detectors could be the cornerstone of novel technologies for THz imaging and spectroscopy. In particular, they could be extensively used for homeland, border and citizen security applications. THz sensors can detect in real-time weapons, illegal goods, drugs or explosives in packs; bringing the sensitivity, the quality and the level of checks beyond any currently existing system devoted to security. Furthermore, the TPC sensors could be employed for food security and citizen health in quality controls of food packaging/adulteration, suspect pharmaceutical freight and fraud inspections.



TeraApps. Doctoral Training Network in Terahertz Technologies for Imaging, Radar and Communication Applications. H2020-MSCA-ITN-2017; GA 765426. University of Glasgow, UK (E. Wasige); Cnr Nano Pisa (M. S. Vitiello). 2018-2021.

www.gla.ac.uk/research/az/teraapps/

Abstract. This network addresses the future societal need in Terahertz technologies, by addressing the training gap, and crystallizing world leading groups in a concentrated research effort. Emerging research areas in this field link e.g. semiconductor materials synthesis, high-speed electronic device physics and engineering, antenna design, THz optics, and a raft of diverse applications and a new generation of academic and industry leaders in developing these devices and systems in the terahertz spectral band is now required. In particular, the project focuses on tunneling devices that have been shown to be the leading candidate in realizing compact, low cost, high performance THz transmitters and receivers once coupled to suitable antennas. Also, new two-dimensional (2D) materials such as graphene or 1D nanowires are emerging as suitable platforms for realizing highly sensitive detectors of THz radiation.

TOPOCIRCUS. Simulations of Topological Phases in Superconducting Circuits. H2020-MSCA-IF-2018; GA 841894. Cnr Nano Pisa (F. Gia-zotto). 2019-2022.

Abstract. The discovery of topological order characterising novel exotic phases of matter has generated a breakthrough in the comprehension of complex condensed matter

phases. Topological invariants entirely determine the behaviour of certain observables and confer to the systems a strong robustness to perturbations. Going beyond condensed matter states, topological order can be engineered in different setups that can benefit from it and represent alternative platform for the simulation of exotic topological phases. Among the most promising candidates for such a plan are the superconducting circuits based on the Josephson effect. This project aims at studying the interconnections between the topological notion and the Josephson effect and to propose superconducting circuits as a platform for the simulation and manipulation of novel topological phases of matter.



ULTRAQCL. Ultrashort Pulse Generation from Terahertz Quantum Cascade Lasers. UE H2020-FETOPEN-2014-2015-RIA; GA 665158. CNRS-LPA, FR (S. Dhillon); Cnr Nano Pisa (M. S. Vitiello). 2015-2018.
www.ultraqcl.eu

Abstract. The generation of ultrafast and intense light pulses is an underpinning technology across the electromagnetic spectrum enabling the study of fundamental light-matter interactions, as well as industrial exploitation in a plethora of applications across the physical, chemical and biological sciences. However, in the terahertz (THz) frequency range, with its proven applications in imaging, metrology and non-destructive testing, a semiconductor based technology platform for intense and short pulse generation has yet to be realized. Ultrafast excitations of photoconductive switches or nonlinear crystals offer only low powers, low frequency modulation or broadband emission with little control of the spectral bandwidth. In the ULTRAQCL project we will breakthrough this technological gap, using THz quantum cascade lasers (QCLs) as a foundational semiconductor device for generating intense and short THz pulses.

xPRINT. 4-Dimensional printing for adaptive optoelectronic components. ERC-2015-COG; GA 682157. Cnr Nano Pisa (A. Camposeo). 2016-2021.

Abstract. Additive manufacturing of three-dimensional objects relies on depositing or curing materials in a layer-by-layer fashion, starting from computer assisted design. These technologies have rapidly evolved from laboratory research to commercially available desktop systems, with costs decreasing continuously. Notwithstanding such astonishing progress, the potentialities of three-dimensional printing are still poorly exploited in terms of both materials and process resolution. This project will shed new light on the fundamental aspects of three-dimensional polymerization, thus establishing new process design rules and predictive tools for printing resolution. It will also specifically engineer additive manufacturing for printing materials embedding active compounds, thus leading to four-dimensional objects, namely structures that have three-dimensional features and time-changing physical properties at the same time.

National projects

ARTES4.0. Advanced Robotics and enabling digital Technology and Systems. MISE D.D. del 29.01.2018. Cnr Nano Pisa (L. Persano). 2019-2022.

aSTAR. Attosecond transient absorption and reflectivity for the study of exotic materials. MIUR Prin 2017 nr. 2017RKWTMY. Politecnico di Milano (C. Vozzi); Cnr Nano Modena (S. Pittalis). 2019-2022.

Early dysfunctions of intercellular signalling in brain disorders. MIUR Prin 2017 nr. 20175C22WM. Cnr Ibcn (F. Mammano); Cnr Nano Pisa (G. M. Ratto). 2019-2022.

EXC-INS. Excitonic insulator in two-dimensional long-range interacting system. MIUR Prin 2017 nr. 2017BZPKSZ. Università di Modena e Reggio Emilia (E. Molinari); Cnr Nano Modena (M. Rontani). 2019-2022.

HARVEST. Learning from natural pigment-protein complexes how to design artificial light-harvesting systems. MIUR Prin 2017 nr. 201795SBA3. Politecnico di Milano (G. Cerullo); Cnr Nano Modena (D. Prezzi). 2019-2022.

MAXIMA. Bando Industria Sostenibile MISE. Cnr Nano Pisa (M. S. Vitiello). 2016-2019.

MONSTRE2D. Monolithic strain engineering platform for two-dimensional materials. MIUR Prin 2017 nr. 2017KFMJ8E. Università di Pisa (A. Tredicucci); Cnr Nano Pisa (V. Tozzini). 2019-2022.

NEMO. Next generation of molecular and supramolecular machines: towards functional nanostructured devices, interfaces, surfaces and materials. MIUR Prin 2017 nr. 20173L7W8K. Università degli Studi di Bologna (A. Credi); Cnr Nano Pisa (L. Persano). 2019-2022.

UTFROM. Understanding and Tuning Friction through nanostructure Manipulation. MIUR Prin 2017 nr. 20178PZCB5. Università di Genova (R. Ferrando); Cnr Nano Modena (G. Paolicelli). 2019-2022.

Cnr projects

Advanced characterization methods for the study of rare-earth single-ion magnets on oxide substrates. Cnr Bilateral project Czech Republic – CAS. Cnr Nano Modena (V. Bellini). 2019-2021.

Conversione di energia in dispositivi quantistici alla nanoscala. Cnr Bilateral project ARGENTINA CONICET. Cnr Nano Pisa (F. Taddei). 2017-2018.

Morphing graphene chemical properties: a Density Functional Approach. Cnr Bilateral project GEORGIA – SRNSF. Cnr Nano Pisa (V. Tozzini). 2018-2019.

Nanomax Nanobrain. Nanotechnology-based therapy and diagnostics of brain diseases. Cnr Progetto Bandiera. Cnr, IT; Cnr Nano Pisa (G. M. Ratto). 2016-2018.

Regional projects

CAPSULIGHT. Realizzazione di una capsula robotica a LED per il trattamento dei disordini gastrointestinali. Regione Toscana; Bando FAS Salute 2014. Scuola Superiore Sant'Anna, Pisa; Cnr Nano Pisa (A. Sgarbossa). 2016-2018. <http://capsulight.com/>

DIAMANTE. Diagnostica molecolare innovativa per la scelta terapeutica personalizzata dell'adenocarcinoma duttale pancreatico. Regione Toscana; Bando FAS Salute. Università di Pisa (U. Boggi); Cnr Nano Pisa (R. Bizzarri). 2016-2018.

DIAST. Sviluppo di un sistema diagnostico integrato per applicazioni spaziali terrestri. Regione Toscana; Bando FAR FAS 2014. AEROSPAZIO Tecnologie, Rapolani (FI); Cnr Nano Pisa (M. S. Vitiello). 2016-2018.

FELIX. Fotonica ed elettronica integrate per l'industria. Regione Toscana; Bando Por CREO FESR 2014-2020. Scuola Superiore Sant'Anna, Pisa (G. Prati); Cnr Nano Pisa (L. Sorba). 2016-2018. www.santannapisa.it/it/ricerca/progetti/fotonica-ed-elettronica-integrate-industria-felix

NIPROGEN. La natura ispira processi innovativi per lo sviluppo di impianti per la medicina rigenerativa a elevato grado di vascolarizzazione e performance meccaniche. Regione Emilia Romagna; Bando POR-FESR 2014-2020. Cnr Istec (A. Tampieri); Cnr Nano Modena (A. Alessandrini). 2016-2018. <http://niprogen.it/>

RIMMEL - Rivestimenti Multi-funzionali e multi-scala, per componenti MEccanici in acciaio e Leghe di alluminio fabbricati con additive manufacturing. Regione Emilia Romagna; Bando POR FESR 2014-2020 - Azione 1.2.2. Cnr Nano Modena (S. Valeri). <https://rimmel.nano.cnr.it/>

SCIADRO. Utilizzo di flotte e sciame di droni dotati di sensori e tecnologie abilitanti innovative per la sicurezza del territorio e degli aeroporti. Regione Toscana; Bando FAR-FAS 2014. Cnr Nano Pisa (F. Giazotto; M. S. Vitiello). 2016-2018. <http://www.sciadro.it/>

SENSOR. Nuovi Sensori Real Time per la Determinazione di Contaminazioni Chimiche e Microbiologiche in Matrici Ambientali e Biomedicali. Regione Toscana; Bando POR CREO FESR Toscana 2014-2020. Laboratori ARCHA S.R.L., Pisa; Cnr Nano Pisa (M. Cecchini). 2018-2020.

SUPER Supercomputing Unified Platform. Regione Emilia Romagna; Bando POR-FESR 2014-2020, Asse 1 - Ricerca e Innovazione, Azione 1.5.1. Cineca, IT (S. Bassini); Cnr Nano Modena (E. Molinari). 2019-2020.

Other funding agencies

ANCIENT_ROME. Study of many body excitations in defective titanium dioxide materials by ab-initio Methods. PRACE Project Access (Call 19). 30M core hours. Cnr Nano Modena (C. Cardoso). 2019-2020.

Balzan Research Project. Fondazione Internazionale Premio Balzan. Cnr Nano Pisa (M. S. Vitiello). 2017-2022.

EXTEND. Excitonic instability in two dimensional tungsten Ditelluride. PRACE Project Access (Call 19). 45M core hours. Cnr Nano Modena (D. Varsano). 2019-2020.

Intracellular chloride dynamics in autistic brain: a better understanding is needed for tailored cures. Telethon 2018. Cnr Nano Pisa (G. M. Ratto). 2019-2022.

Molecular Spins for Quantum Technologies. AOARD 2017-2020. Osaka City University, JP; Cnr Nano Modena (M. Affronte).

Nanotecnologie per la determinazione di marker molecolari tumorali e per la diagnostica precoce. Fondazione Pisa Bando 2016. Cnr Nano Pisa (G. M. Ratto). 2017-2020.

Pre-clinical testing of Lithium treatment in Krabbe disease. Fondazione Cassa di Risparmio di Lucca. Cnr Nano Pisa (M. Cecchini). 2017-2018.

Pre-clinical testing of single and combined autophagy modulation by Lithium and Rapamycin in Globoid Cell Leukodystrophy. European Leukodystrophy Association (ELA) International Fellowship Grant, ELA 2018-008F2. Cnr Nano Pisa (M. Cecchini). 2019-2020.

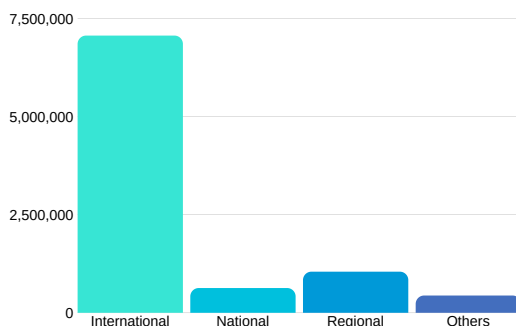
SENT_TO_NY. Study of Covered and functionalized TiO₂ nanostructures: The role of many-body effects. PRACE Project Access (Call 18) n. 2018194573. 30M core hours. Cnr Nano Modena (I. Marri). 2018-2019.

SIDEX. Size DEpendence of the EXcitonic properties of MoS₂ nanoribbons from many-body perturbation theory. PRACE Project Access (Call 15). 590M core hours. Cnr Nano Modena (P. D'Amico). 2017-2018.

STREET_OF_NY. Study of optoelectronic properties of titanium dioxide nanosystems in the frame of the many body perturbation theory. PRACE Project Access (Call 14). 38M core hours. Cnr Nano Modena (I. Marri). 2017-2018.

TERAX. Carbon-nanotube excitons in the THz frequency range from first-principles many-body perturbation theory. PRACE Project Access (Call 14). 58M core hours. Cnr Nano Modena (D. Varsano). 2017-2018.

2018-2019 external fundings (in €)



QUANTUM | GRAPHENE | FIELD | PROPE
RTIES | SINGLE | OPTICAL | SPIN | DYN
AMICS | TERAHERTZ | ELECTRONS | MO
LECULAR | JOSEPHSON | NANOPARTIC
LES | DOPED | EFFECT | INTERACTION |
LASER | NANOWIRES | SYSTEMS | THE
RMAL | CELLS | INAS | MAGNETIC | COU
PLING | CHARGE | HYBRID | LIGHT | MO
DEL | ULTRAFAST | PHOSPHORUS | PLA
SMONIC | WAVE | CASCADE | CRYSTAL
S | OXIDE | PROTEINS | SURFACES

Publications

A list of publications from journals with $IF \geq 9.227$ (i.e., Physical Review Letter's IF in 2018) ordered by their JCR 2018 IF is given. A full and updated list of publications is available on the Institute website at the page "Publications" (<http://www.nano.cnr.it/?mod=men&id=502>). Publications marked with © earned a cover in the corresponding journal. Covers are displayed at the end of this section.

Colloquium: Nonequilibrium effects in superconductors with a spin-splitting field.
F. S. Bergeret, M. Silaev, P. Virtanen, and T. T. Heikkilä. *Rev Mod Phys* 90, 41001 (2018).

Metallic supercurrent field-effect transistor.
G. De Simoni, F. Paolucci, P. Solinas, E. Strambini, and F. Giazotto. *Nat Nanotechnol* 13, 802-805 (2018).

Anisotropic Nanoscale Wrinkling in Solid-State Substrates.
M. C. Giordano and F. B. de Mongeot. *Adv Mater* 30, 1801840 (2018).

Twisting neutrons may reveal their internal structure.
H. Larocque, I. Kaminer, V. Grillo, R. W. Boyd, and E. Karimi. *Nat Phys* 14, 1-2 (2018).

An Intravascular Magnetic Catheter Enables the Retrieval of Nanoagents from the Bloodstream.
V. Iacovacci, L. Ricotti, E. Sinibaldi, G. Signore, F. Vistoli, and A. Menciassi. *Advanced Science* 5, 1800807 (2018).

Energy Conversion at the Cuticle of Living Plants.
F. Meder, I. Must, A. Sadeghi, A. Mondini, C. Filippeschi, L. Beccai, V. Mattoli, P. Pingue, and B. Mazzolai. *Adv Funct Mater* 28, 1806689 (2018).

Bandgap Engineering of Graphene Nanoribbons by Control over Structural Distortion.
Y. Hu, P. Xie, M. De Corato, A. Ruini, S. Zhao, F. Meggendorfer, L. A. Straaso, L. Rondin, P. Simon, J. Li, J. J. Finley, M. R. Hansen, J.-S. Lauret, E. Molinari, X. Feng, J. V. Barth, C.-A. Palma, D. Prezzi, K. Mullen, and A. Narita. *J Am Chem Soc* 140, 7803-7809 (2018).

Hierarchical Order in Dewetted Block Copolymer Thin Films on Chemically Patterned Surfaces.
F. Ferrarese Lupi, T. J. Giammaria, A. Miti, G. Zuccheri, S. Carignano, K. Sparnacci, G. Seguini, N. De Leo, L. Boarino, M. Perego, and M. Laus. *ACS Nano* 12, 7076-7085 (2018).

The ultrafast dynamics and conductivity of photoexcited graphene at different Fermi energies.
A. Tomadin, S. M. Hornett, H. I. Wang, E. M. Alexeev, A. Candini, C. Coletti, D. Turchinovich, M. Klaui, M. Bonn, F. H. L. Koppens, E. Hendry, M. Polini, and K.-J. Tielrooij. *Sci Adv* 4, eaar5313 (2018).

Mapping the Coulomb Environment in Interference-Quenched Ballistic Nanowires.
D. Gutstein, D. Lynall, S. V. Nair, I. Savelyev, M. Blumin, D. Ercolani, and H. E. Ruda. *Nano Lett* 18, 124-129 (2018).

Nanoparticle Stability in Axial InAs-InP Nanowire Heterostructures with Atomically Sharp Interfaces.

V. Zannier, F. Rossi, V. G. Dubrovskii, D. Ercolani, S. Battiato, and L. Sorba. *Nano Lett* 18, 167-174 (2018).

Bright Electroluminescence from Single Graphene Nanoribbon Junctions.

M. C. Chong, N. Afshar-Imani, F. Scheurer, C. Cardoso, A. Ferretti, D. Prezzi, and G. Schull. *Nano Lett* 18, 175-181 (2018).

Phase-Tunable Josephson Thermal Router.

G. F. Timossi, A. Fornieri, F. Paolucci, C. Puglia, and F. Giazotto. *Nano Lett* 18, 1764-1769 (2018).

Ferromagnetic and Antiferromagnetic Coupling of Spin Molecular Interfaces with High Thermal Stability.

G. Avvisati, C. Cardoso, D. Varsano, A. Ferretti, P. Gargiani, and M. G. Betti. *Nano Lett* 18, 2268-2273 (2018).

Excitons in Core-Shell Nanowires with Polygonal Cross Sections.

A. Sitek, M. Urbaneja Torres, K. Torfason, V. Gudmundsson, A. Bertoni, and A. Manolescu. *Nano Lett* 18, 2581-2589 (2018).

Ultra-Efficient Superconducting Dayem Bridge Field-Effect Transistor.

F. Paolucci, G. De Simoni, E. Strambini, P. Solinas, and F. Giazotto. *Nano Lett* 18, 4195-4199 (2018).

Controlling the Quality Factor of a Single Acoustic Nanoresonator by Tuning its Morphology.

F. Medeghini, A. Crut, M. Gandolfi, F. Rossella, P. Maioli, F. Vallée, F. Banfi, and N. Del Fatti. *Nano Lett* 18, 5159-5166 (2018).

Toward the Absolute Spin-Valve Effect in Superconducting Tunnel Junctions.

G. De Simoni, E. Strambini, J. S. Moodera, F. S. Bergeret, and F. Giazotto. *Nano Lett* 18, 6369-6374 (2018).

Koopmans-Compliant Spectral Functionals for Extended Systems.

N. L. Nguyen, N. Colonna, A. Ferretti, and N. Marzari. *Phys Rev X* 8, 21051 (2018).

Continuous-wave highly-efficient low-divergence terahertz wire lasers.

S. Biasco, K. Garrasi, F. Castellano, L. Li, H. E. Beere, D. A. Ritchie, E. H. Linfield, A. G. Davies, and M. S. Vitiello. *Nat Commun* 9, 1122 (2018).

Electrically reconfigurable terahertz signal processing devices using liquid metal components.

K. S. Reichel, N. Lozada-Smith, I. D. Joshipura, J. Ma, R. Shrestha, R. Mendis, M. D. Dickey, and D. M. Mittleman. *Nat Commun* 9, 4202 (2018).

Narrow bounds for the quantum capacity of thermal attenuators.

M. Rosati, A. Mari, and V. Giovannetti. *Nat Commun* 9, 4339 (2018).

- Manipulating azobenzene photoisomerization through strong light-molecule coupling.
J. Fregoni, G. Granucci, E. Coccia, M. Persico, and S. Corni. *Nat Commun* 9, 4688 (2018).
- Nanowire-Intensified Metal-Enhanced Fluorescence in Hybrid Polymer-Plasmonic Electrospun Filaments.
A. Camposeo, R. Jurga, M. Moffa, A. Portone, F. Cardarelli, F. Della Sala, C. Ciraci, and D. Pisignano. *Small* 14, 1800187 (2018).
- Magnetic Shape Memory Turns to Nano: Microstructure Controlled Actuation of Free-Standing Nanodisks.
M. Campanini, L. Nasi, S. Fabbrici, F. Casoli, F. Celegato, G. Barrera, V. Chiesi, E. Bedogni, C. Magén, V. Grillo, G. Bertoni, L. Righi, P. Tiberto, and F. Albertini. *Small* 14, 1803027 (2018).
- Polymer-Based Black Phosphorus (bP) Hybrid Materials by in Situ Radical Polymerization: An Effective Tool to Exfoliate bP and Stabilize bP Nanoflakes.
E. Passaglia, F. Cicogna, F. Costantino, S. Coiai, S. Legnaioli, G. Lorenzetti, S. Borsacchi, M. Geppi, F. Telesio, S. Heun, A. Ienco, M. Serrano-Ruiz, and M. Peruzzini. *Chem Mater* 30, 2036-2048 (2018).
- Shaping excitons in light-harvesting proteins through nanoplasmonics.
S. Caprasecca, S. Corni, and B. Mennucci. *Chem Sci* 9, 6219-6227 (2018).
- Phase-sensitive terahertz imaging using room-temperature near-field nanodetectors.
M. C. Giordano, L. Viti, O. Mitrofanov, and M. S. Vitiello. *Optica* 5, 651-657 (2018).
- Squeezing Enhances Quantum Synchronization.
S. Sonar, M. Hajdusek, M. Mukherjee, R. Fazio, V. Vedral, S. Vinjanampathy, and L.-C. Kwek. *Phys Rev Lett* 120, 163601 (2018).
- Perfect Diode in Quantum Spin Chains.
V. Balachandran, G. Benenti, E. Pereira, G. Casati, and D. Poletti. *Phys Rev Lett* 120, 200603 (2018).
- Universal Quantum Magnetometry with Spin States at Equilibrium.
F. Troiani and M. G. A. Paris. *Phys Rev Lett* 120, 260503 (2018).
- Interfacial Charge Density and Its Connection to Adhesion and Frictional Forces.
M. Wolloch, G. Levita, P. Restuccia, and M. C. Righi. *Phys Rev Lett* 121, 26804 (2018).
- Boundary Time Crystals.
F. Iemini, A. Russomanno, J. Keeling, M. Schiro, M. Dalmonte, and R. Fazio. *Phys Rev Lett* 121, 35301 (2018).
- Thermodynamic Bound on Heat-to-Power Conversion.
R. Luo, G. Benenti, G. Casati, and J. Wang. *Phys Rev Lett* 121, 80602 (2018).

Interaction-Driven Giant Orbital Magnetic Moments in Carbon Nanotubes.
J. O. Island, M. Ostermann, L. Aspitarte, E. D. Minot, D. Varsano, E. Molinari, M. Rontani, and G. A. Steele. *Phys Rev Lett* 121, 127704 (2018).

Geometrical Bounds on Irreversibility in Open Quantum Systems.
L. Mancino, V. Cavina, A. De Pasquale, M. Sbroscia, R. I. Booth, E. Roccia, I. Gianani, V. Giovannetti, and M. Barbieri. *Phys Rev Lett* 121, 160602 (2018).

2019

Ultrafast generation and control of an electron vortex beam via chiral plasmonic near fields.

G. M. Vanacore, G. Berruto, I. Madan, E. Pomarico, P. Biagioni, R. J. Lamb, D. McGrouther, O. Reinhardt, I. Kaminer, B. Barwick, H. Larocque, V. Grillo, E. Karimi, F. J. García de Abajo, and F. Carbone. *Nat Materials* 18, 573-579 (2019).

Multiscale modelling of photoinduced processes in composite systems.

B. Mennucci and S. Corni. *Nat Rev Chem* 3, 315-330 (2019).

Charge Transfer between [4Fe4S] Proteins and DNA Is Unidirectional: Implications for Biomolecular Signaling.

R. D. Teo, B. J. G. Rousseau, E. R. Smithwick, R. Di Felice, D. N. Beratan, and A. Migliore. *Chem* 5, 122-137 (2019).

© Ionic-Liquid Gating of InAs Nanowire-Based Field-Effect Transistors.

J. Lieb, V. Demontis, D. Prete, D. Ercolani, V. Zannier, L. Sorba, S. Ono, F. Beltram, B. Sacépé, and F. Rossella. *Adv Funct Mater* 29, 1804378 (2019).

Lineage-Specific Commitment of Stem Cells with Organic and Graphene Oxide-Functionalized Nanofibers.

A. Portone, M. Moffa, C. Gardin, L. Ferroni, M. Tatullo, F. Fabbri, L. Persano, A. Piattelli, B. Zavan, and D. Pisignano. *Adv Funct Mater* 29, 1806694 (2019).

Frequency-tunable continuous-wave random lasers at terahertz frequencies.

S. Biasco, H. E. Beere, D. A. Ritchie, L. Li, A. G. Davies, E. H. Linfield, and M. S. Vitiello. *Light Sci Appl* 8, 43 (2019).

Capturing Metabolism-Dependent Solvent Dynamics in the Lumen of a Trafficking Lysosome.

F. Begarani, F. D'Autilia, G. Signore, A. Del Grosso, M. Cecchini, E. Gratton, F. Beltram, and F. Cardarelli. *ACS Nano* 13, 1670-1682 (2019).

Josephson Field-Effect Transistors Based on All-Metallic Al/Cu/Al Proximity Nanojunctions.

G. De Simoni, F. Paolucci, C. Puglia, and F. Giazotto. *ACS Nano* 13, 7871-7876 (2019).

Charge localization and reentrant superconductivity in a quasi-ballistic InAs nanowire coupled to superconductors.

J. C. Estrada Saldana, R. Zitko, J. P. Cleuziou, E. J. H. Lee, V. Zannier, D. Ercolani, L. Sorba, R. Aguado, and S. De Franceschi. *Sci Adv* 5, eaav1235 (2019).

Brain-targeted enzyme-loaded nanoparticles: A breach through the blood-brain barrier for enzyme replacement therapy in Krabbe disease.

A. D. Grosso, M. Galliani, L. Angella, M. Santi, I. Tonazzini, G. Parlanti, G. Signore, and M. Cecchini. *Sci Adv* 5, eaax7462 (2019).

Pushing down the lateral dimension of single and coupled magnetic dots to the nanometric scale: Characteristics and evolution of the spin-wave eigenmodes.

G. Carloti. *Appl Phys Rev* 6, 031304 (2019).

Direct Probe of the Seebeck Coefficient in a Kondo-Correlated Single-Quantum-Dot Transistor.

B. Dutta, D. Majidi, A. Garcia Corral, P. A. Erdman, S. Florens, T. A. Costi, H. Courtois, and C. B. Winkelmann. *Nano Lett* 19, 506-511 (2019).

© Vectorial Control of the Spin-Orbit Interaction in Suspended InAs Nanowires.

A. Iorio, M. Rocci, L. Bours, M. Carrega, V. Zannier, L. Sorba, S. Roddaro, F. Giazotto, and E. Strambini. *Nano Lett* 19, 652-657 (2019).

Preferential Positioning, Stability, and Segregation of Dopants in Hexagonal Si Nanowires.

M. Amato, S. Ossicini, E. Canadell, and R. Rurali. *Nano Lett* 19, 866-876 (2019).

Fast and Sensitive Terahertz Detection Using an Antenna-Integrated Graphene pn Junction.

S. Castilla, B. Terres, M. Autore, L. Viti, J. Li, A. Y. Nikitin, I. Vangelidis, K. Watanabe, T. Taniguchi, E. Lidorikis, M. S. Vitiello, R. Hillenbrand, K.-J. Tielrooij, and F. Koppen. *Nano Lett* 19, 2765-2773 (2019).

Thermoelectric Conversion at 30 K in InAs/InP Nanowire Quantum Dots.

D. Prete, P. A. Erdman, V. Demontis, V. Zannier, D. Ercolani, L. Sorba, F. Beltram, F. Rossella, F. Taddei, and S. Roddaro. *Nano Lett* 19, 3033-3039 (2019).

Tip-Enhanced Infrared Difference-Nanospectroscopy of the Proton Pump Activity of Bacteriorhodopsin in Single Purple Membrane Patches.

V. Giliberti, R. Polito, E. Ritter, M. Broser, P. Hegemann, L. Puskar, U. Schade, L. Zanetti-Polzi, I. Daidone, S. Corni, F. Rusconi, P. Biagioni, L. Baldassarre, and M. Ortolani. *Nano Lett* 19, 3104-3114 (2019).

Single Electron Precision in the Measurement of Charge Distributions on Electrically Biased Graphene Nanotips Using Electron Holography.

L. Vicarelli, V. Migunov, S. K. Malladi, H. W. Zandbergen, and R. E. Dunin-Borkowski. *Nano Lett* 19, 4091-4096 (2019).

Field-Effect Controllable Metallic Josephson Interferometer.

F. Paolucci, F. Vischi, G. De Simoni, C. Guarcello, P. Solinas, and F. Giazotto. *Nano Lett* 19, 6263–6269 (2019).

A nanophotonic laser on a graph.

M. Gaio, D. Saxena, J. Bertolotti, D. Pisignano, A. Camposeo, and R. Sapienza. *Nat Commun* 10, 226 (2019).

Fully phase-stabilized quantum cascade laser frequency comb.

L. Consolino, M. Nafa, F. Cappelli, K. Garrasi, F. P. Mezzapesa, L. Li, A. G. Davies, E. H. Linfield, M. S. Vitiello, P. De Natale, and S. Bartalini. *Nat Commun* 10, 2938 (2019).

Activation of PKA via asymmetric allosteric coupling of structurally conserved cyclic nucleotide binding domains.

Y. Hao, J. P. England, L. Bellucci, E. Paci, H. C. Hodges, S. S. Taylor, and R. A. Maillard. *Nature Commun* 10, 3984 (2019).

Wafer-Scale Synthesis of Graphene on Sapphire: Toward Fab-Compatible Graphene.

N. Mishra, S. Forti, F. Fabbri, L. Martini, C. McAleese, B. R. Conran, P. R. Whelan, A. Shivayogimath, B. S. Jessen, L. Buß, J. Falta, I. Aliaj, S. Roddaro, J. I. Flege, P. Bøggild, K. B. K. Teo, and C. Coletti. *Small* 15, 1904906 (2019).

Directed Functionalization Tailors the Polarized Emission and Waveguiding Properties of Anthracene-Based Molecular Crystals.

A. Camposeo, D. B. Granger, S. R. Parkin, D. Altamura, C. Giannini, J. E. Anthony, and D. Pisignano. *Chem Mater* 31, 1775–1783 (2019).

Black Phosphorus/Palladium Nanohybrid: Unraveling the Nature of P-Pd Interaction and Application in Selective Hydrogenation.

M. Vanni, M. Serrano-Ruiz, F. Telesio, S. Heun, M. Banchelli, P. Matteini, A. M. Mio, G. Nicotra, C. Spinella, S. Caporali, A. Giaccherini, F. D'Acapito, M. Caporali, and M. Peruzzi. *Chem Mater* 31, 5075–5080 (2019).

Fast-diffusing p75(NTR) monomers support apoptosis and growth cone collapse by neurotrophin ligands.

L. Marchetti, F. Bonsignore, F. Gobbo, R. Amodeo, M. Calvello, A. Jacob, G. Signore, C. S. Spagnolo, D. Porciani, M. Mainardi, F. Beltram, S. Luin, and A. Cattaneo. *PNAS* 116, 21563–21572 (2019).

Bow-Tie cavity for terahertz radiation.

L. Consolino, A. Campa, D. Mazzotti, M. S. Vitiello, P. De Natale, and S. Bartalini. *Optica* 6, 1 (2019).

Failure of Conductance Quantization in Two-Dimensional Topological Insulators due to Nonmagnetic Impurities.

P. Novelli, F. Taddei, A. K. Geim, and M. Polini. *Phys Rev Lett* 122, 16601 (2019).

Orthogonality Catastrophe in Dissipative Quantum Many-Body Systems.

F. Tonielli, R. Fazio, S. Diehl, and J. Marino. *Phys Rev Lett* 122, 40604 (2019).

Extractable Work, the Role of Correlations, and Asymptotic Freedom in Quantum Batteries.

G. M. Andolina, M. Keck, A. Mari, M. Campisi, V. Giovannetti, and M. Polini. Phys Rev Lett 122, 47702 (2019).

Exciting a Bound State in the Continuum through Multiphoton Scattering Plus Delayed Quantum Feedback.

G. Calajó, Y.-L.L. Fang, H. U. Baranger, and F. Ciccarello. Phys Rev Lett 122, 73601 (2019).

Optimal Probabilistic Work Extraction beyond the Free Energy Difference with a Single-Electron Device.

O. Maillet, P. A. Erdman, V. Cavina, B. Bhandari, E. T. Mannila, J. T. Peltonen, A. Mari, F. Taddei, C. Jarzynski, V. Giovannetti, and J. P. Pekola. Phys Rev Lett 122, 150604 (2019).

Quantum Martingale Theory and Entropy Production.

G. Manzano, R. Fazio, and E. Roldan. Phys Rev Lett 122, 220602 (2019).

Density-Driven Correlations in Many-Electron Ensembles: Theory and Application for Excited States.

T. Gould and S. Pittalis. Phys Rev Lett 123, 16401 (2019).

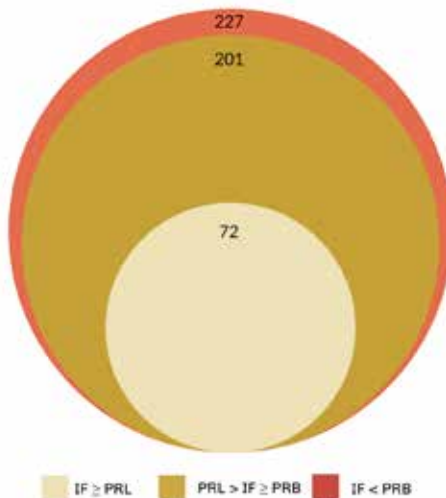
Synchronization of Optomechanical Nanobeams by Mechanical Interaction.

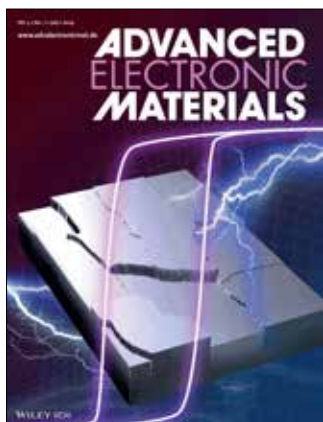
M. F. Colombano, G. Arregui, N. E. Capuj, A. Pitanti, J. Maire, A. Griol, B. Garrido, A. Martinez, C. M. Sotomayor-Torres, and D. Navarro-Urrios. Phys Rev Lett 123, 17402 (2019).

Many-Body Synchronization in a Classical Hamiltonian System.

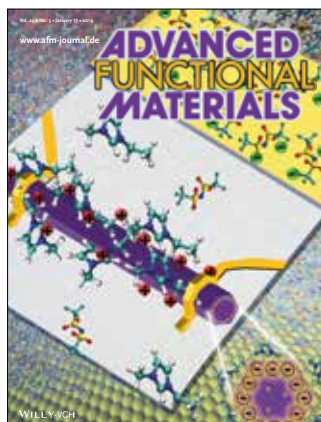
R. Khasseh, R. Fazio, S. Ruffo, and A. Russomanno. Phys Rev Lett 123, 184301 (2019).

2018-2019 Cnr Nano publications sorted by IF

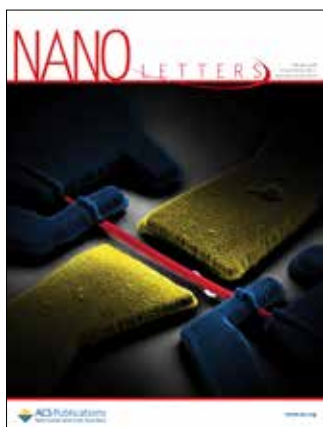




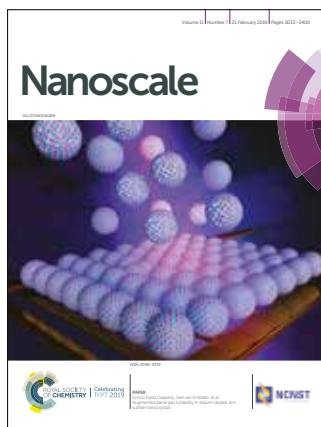
Advanced Electronic Materials 5 (7), 2019.



Advanced Functional Materials 29 (3), 2019.
[Inside Front Cover]



Nano Letters 19 (2), 2019.



Nanoscale 11 (7), 2019.



Cnr Nano Life



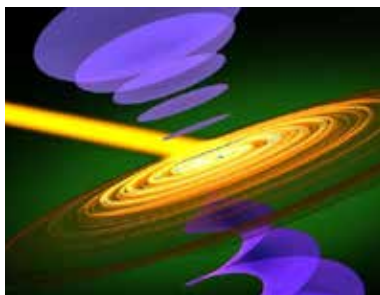
FEBRUARY Into the Future

For the second year Cnr Nano Modena opened its doors to many high-school students who embarked in a journey of discovery of science and technology. Thanks to the guidance project Into the Future, aimed at showing what researchers actually do to high schools students, more than 100 students had the chance to enter our labs, have a sneak peek at where science is actually done and meet people who work in research, listen to their career stories, and make questions.



APRIL A new state of matter in nanotubes

After being published in Nature Communications, Varsano, Rontani, and Molinari's research about the possibility of realising in zero-gap carbon the excitonic insulator, speculated fifty years ago by the Nobel prize Walter Kohn, hit the media being mentioned, among others, in the cultural insert of the Italian leading newspaper Corriere della Sera.



MAY Twisting whirlpools of electrons

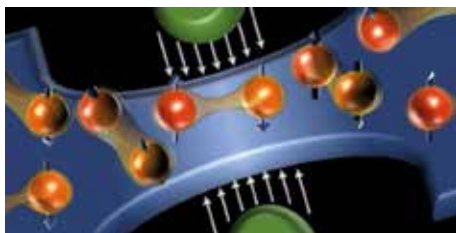
"Electron vortices will lead to faster computers and future therapies" was the featured news in the main Italian press agency ANSA reporting about the article published in Nature Materials by Vincenzo Grillo (Cnr Nano) and colleagues.



MAY

Innovation award to M.S. Vitiello

More than 180 researchers applied to the 16th edition of the Sapio Award for Research and Innovation. Cnr Nano researcher Miriam S. Vitiello received the Innovation prize for her work on the usage of Terahertz spectroscopy and its development towards commercial exploitation.



JULY

Transistors go metal

The fully metallic superconducting field-effect transistor developed by Francesco Giazotto's group (published on NanoLetters) received a featured article in the Research Highlights section of the Nature Electronics July issue. The superconductive device uses a configuration known as a Dayem bridge and can be fabricated by a one-step electron beam lithography process.

JULY

The ultimate nanosculptors

From 10 to 13 July, the international scientific community of nanofabrication gathered in Modena to attend the FEBIP international conference dedicated to the Focused Electron Beam-Induced Processing techniques. The meeting, organized by Cnr Nano (G.C. Gazzadi and S. Frabboni) which has cutting-edge facilities and skills in this sector, hosted over 70 scientists from 17 countries and leading companies in the field of electron microscopy.

Cnr Nano events in 2018



SEPTEMBER

A bright science night

On Sept. 28 all over Europe researchers meet citizens to raise awareness of science, for the EU Researchers Night. Our researchers participated in the Pisa event: Simone Zanotto and Gian Michele Ratto took the stage with the two bright short talks "Taming light" and "A view on the brain", and Andrea Camposeo's group showed a 4D-printing set up.

OCTOBER

Physics Nobel prize explained

On the occasion of the Nobel Prize for Physics 2018, Cnr Nano Modena and the FIM Department of Unimore organized a presentation to illustrate the "groundbreaking inventions in the field of laser physics" with a focus on the "optical tweezers and their application to biological nanosystems" (the object of Nobel Prize award) such as the ones studied in our labs.

OCTOBER

Ci vuole il fisico!

Inspired by scientific research developed in the laboratories of Cnr Nano and Unimore, the event "Ci vuole il fisico!" discussed the importance of Physics careers and the role of physicists in the technological development of our society. A full house of physics students, high school students and teachers attended the event.

OCTOBER

3rd Cnr Nano Meeting

Researchers from Cnr Nano gathered together for the 3rd Nanoscience Institute Meeting in Pisa on 29-30 October. About one hundred people between researchers and technologists convened in the stunning blue room of the Scuola Normale Superiore for this periodic in-person meeting to discuss scientific results and interests, start and strengthen collaborations. The dense program encompassed 22 oral presentations, 45 posters, all from Cnr Nano staff, and a focus on technology transfer by Cnr TT officer Giulio Bollino.



DECEMBER

A revolutionizing transistor

In this month our SQEL group's research hit the media twice! "Transistors that can change quantum hi-tech" and "Superconducting transistors for supercomputers that consume as a light bulb" were the headlines in the press and the radio about the fully metallic superconducting field-effect transistor developed by the Superconducting Quantum Electronics Lab researchers, led by Francesco Giazotto in Pisa.

DECEMBER

The future of materials science...

...hosted again in Modena, where the kick-off meeting of the MAX European Centre of Excellence was held on 13-14 December. MAX (MATERIALS design at the eXascale) is a European Centre of Excellence dedicated to the materials modelling, simulations and design at the frontiers of the current and future High Performance Computing. The network, coordinated by Cnr Nano, stars the main HPC centres, research groups, training and dissemination groups, industries active in Europe in the field.





JANUARY Printing beyond 3D

Ever thought of adding a D to 3D printing? In a featured article about frontiers of 3D printing, published in the tech magazine of La Repubblica, Andrea Camposeo speaks about 4D printing, such as printing 3-dimensional objects with properties that change over time and adapt to the environment. He coordinates the XPrint Erc Grant project dedicated to 4D printing.

JANUARY Cnr Nano goes on air

Pisa unit was in the spot of Aula40, a weekly radio program dedicated to sciences. In a one-hour long episode named "Miniature science", Marco Cecchini, Elia Strambini, Francesca Telesio, Valentina Tozzini, and Valentina Zannier talked in a live broadcast and in front of high-school students of nanoscience and of the frontier research going on at Cnr Nano.



1938 2018

JANUARY

Academia at the time of racial laws

On the occasion of the 80th anniversary of the Italian racial laws, professor Stefano Ossicini from Unimore and Cnr Nano held in Modena two seminars dedicated to the cultural origins and consequences of the Italian racial laws of 1938. The seminars focused in particular on the attitude of science, universities and academia, before and after the racial laws.

FEBRUARY

Talking of ourselves

By this time of the year the seminars series "Cnr Nano Colloquia" were in full swing both in the Pisa and Modena units. Cnr Nano Colloquia are delivered periodically by our researchers in order to increase interaction between their research groups as well as expose doctoral students to the institute's rich array of research activities. All talks can be attended by video conference in the other institute unit and presentation can be downloaded from our website to help the spreading of new ideas and common projects.



FEBRUARY

Intersecting the future

A kick-off meeting held on February 4-5 in the beautiful Accademia delle Scienze, Arti e Lettere in Modena launched the H2020 project Intersect, coordinated by Arrigo Calzolari from Cnr Nano. Intersect will drive the uptake of materials modelling software in industry, bridging the gap between academic innovation and industrial novel production, with a goal of accelerating by one order of magnitude the process of materials' selection and device deployment.

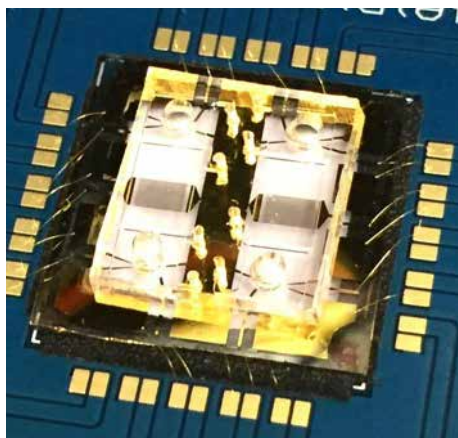
Cnr Nano events in 2019



MARCH

Space Girls land on Cnr Nano

On March 5, scientists from Cnr Nano and Unimore welcomed the Space girls, a group of secondary-school students with a passion for science and technology – whose project of an anti-radiation space suit was awarded by the Ministry of Education, University and Research. The visit was an opportunity to introduce Space girls to the world of nanosciences and labs.



MARCH

Lab-on-a chip, patented

A novel biomedical device capable of detecting a biomarker related to traumatic brain injuries and glioblastoma multiforme cancer has been developed and patented by Marco Cecchini (Cnr Nano) and Matteo Agostini, (Scuola Normale Superiore). The lab-on-a-chip, named Braiker, contains a series of nano-sensors that exploits the principles of nano-acoustics for detection.

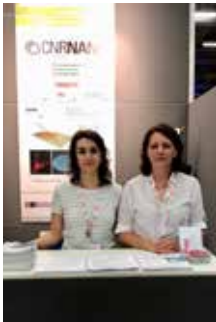
MAY

Nano gets bigger

The local television TRC newscast reported about the Cnr Nano Modena unit, focusing in particular on its new resources and people, such



as seven new national- and European-funded research projects and nine new permanent researchers and staff. The coordinator Massimo Rontani pointed out that "these results underline the quality of the research conducted in our laboratories and our ability to capitalize on resources in cutting-edge projects".



JUNE

Technological innovation on the booth

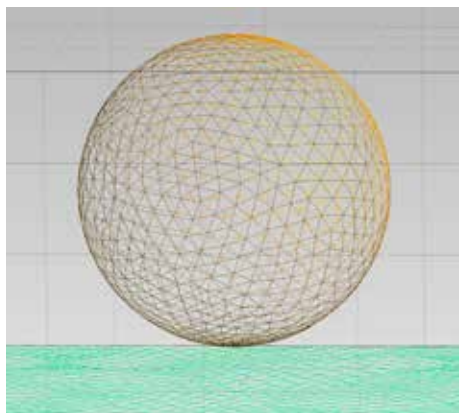
On June 6-7, Cnr Nano participated in the R2B Research to Business fair in Bologna. At the booth researchers presented a range of services with high-technological content dedicated to industrial research, made up of advanced skills for the study of materials and nanoscale devices at the border between basic and industrial research, in sectors ranging from mechanics to biomedicine to energy.

JUNE

First year parafermions

Cnr Nano Pisa organized and hosted the first-year annual meeting of the Super-Top QuantERA project. Six international leading groups with strong background in semiconductor nanodevices and new topological state of matter gathered on June 24-25 to present the first results of the project, whose ambitious aim is the realization of parafermions in double nanowire-based hybrid devices (DNW) never observed before.

Cnr Nano events in 2019



JUNE

The blender, the better

In an effort to improve the quality of its scientific visual communication, Cnr Nano and the MaX European Centre of Excellence organized in Modena a one-day course on Blender, a free and open source 3D creation suite. 26 PhD students and researchers attended the course aimed to provide hands-on knowledge of making great images and animations from 3D scientific data.



JULY

The ultimate coatings

The project RIMMEL was officially launched on July 1st in Modena by its Cnr Nano coordinator prof. Sergio Valeri and all the partners. The Emilia-Romagna Region funded project (POR-FESR 2014-2020) is dedicated to develop multi-functional and multi-scale coatings for mechanical components manufactured with additive manufacturing.



JULY

Celebrating Federico Capasso

To celebrate the 70th birthday of the eminent scientist Federico Capasso and his enthusiastic scientific vision, the symposium “Harnessing Light with Structured Materials” brought together worldwide renowned experts in a broad range of subjects, including flat optics and metamaterials, photonics, high energy lasers, ultra-cold matter, nano-optics, opto-genetics and biological science. The meeting, organized and chaired by Paolo De Natale from Cnr Ino and Miriam Vitiello from Cnr Nano, took place on July 10-11 in Arcetri, where also Galileo Galilei and Enrico Fermi had worked.



SEPTEMBER

Cnr Nano goes OPEN

Cnr Nano Modena opened its labs and to take part in the Emilia Romagna OPEN event, an initiative dedicated to students and citizens of all ages to discover the industrial and research heritage of the Emilia-Romagna region. On Sept. 26, more than 30 people visited the labs discovering the nanoworld and its technological perspectives.

Cnr Nano events in 2019



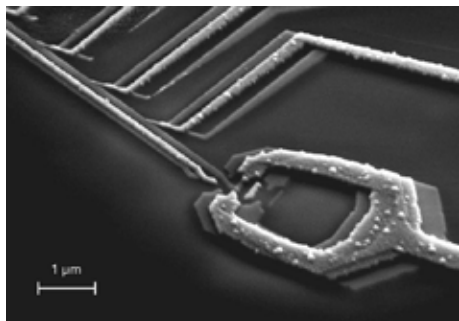
SEPTEMBER **Researchers on stage**

The Researchers' Night is back! Every year in more than 30 European countries researchers simultaneously leave their lab and meet people to talk about science. Cnr Nano joined the appointment in both Modena and Pisa events: our scientists engaged people with passionate talks, intriguing games and fascinating experiments on a science-full night.

SEPTEMBER **Nanowire week**

The Nanowire Week 2019 was held in Pisa from September 23 to 27, merging two well-established and highly successful annual workshops - Nanowires and the Nanowire Growth Workshop, organized by Lucia Sorba and Francesco Rossella. The lively program and the beautiful venue of Pisa and the Tuscany countryside attracted more than 250 researchers to discuss all topics of nanowire-related research, from fabrication and fundamental properties to applications.

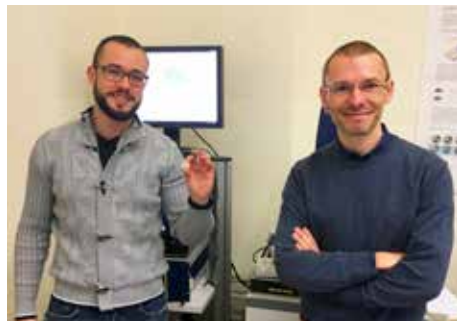




NOVEMBER

An award-winning micrograph

Picturing her cutting-edge research Nadia Ligato won the RAITH Micrograph Award 2019. The winning micrograph pictures a superconducting quantum interference proximity transistor with multi-tunnel junctions nanofabricated using electron beam lithography technique and shadow-angle evaporation.



DECEMBER

A business 'triple'

The Cnr Nano and Scuola Normale Superiore entrepreneurial project Inta System got awarded three times in a few weeks. After winning the 2019 edition of the PhD+, the innovation program of the University of Pisa, and the Tuscany Start Cup challenge in October, the business plan Inta System won the "Innovation Health Care" Prize, among the almost 1,000 business ideas presented at this year's National Innovation Prize. Inta System wants to market the lab-on-a-chip Braiker, developed by Matteo Agostini and Marco Cecchini, which allows to identify brain trauma from blood analysis.



People

The list below includes all researchers and staff
who worked at Cnr Nano in the years 2018-2019

Cnr Nano researchers

Valerio Bellini
Luca Bellucci
Stefania Benedetti
Andrea Bertoni
Giovanni Bertoni
Federica Bianco
Ranieri Bizzarri
Alessandro Braggio
Giorgia Brancolini
Arrigo Calzolari
Andrea Camposeo
Matteo Carrega
Alessandra Catellani
Marco Cecchini
Andrea Ciavatti
Valdis Corradini
Alessandro Crippa
Pino D'Amico
Giorgio De Simoni
Alessandro di Bona
Rosa Di Felice
Alessandra Di Gaspare
Filippo Fabbri
Riccardo Farchioni
Andrea Ferretti
Gian Carlo Gazzadi
Francesco Ghetti
Alberto Ghirri
Francesco Giazotto
Maria Caterina Giordano
Vincenzo Grillo
Stefan Heun
Nadia Ligato
Paola Luches
Ivan Marri
Francesca Matino
Francesco Paolo Mezzapesa
Yuya Murata
Riccardo Nifosi
Guido Paolicelli

Federico Paolucci
Claudia Maria Pereira Cardoso
Luana Persano
Marco Pieruccini
Alessandro Pitanti
Stefano Pittalis
Eva Arianna Aurelia Pogna
Deborah Prezzi
Gian Michele Ratto
Kimberly Reichel
Massimo Rontani
Enzo Rotunno
Carlo Andrea Rozzi
Melissa Santi
Johannes Schmidt
Antonella Sgarbossa
Lucia Sorba
Barbara Storti
Elia Strambini
Fabio Taddei
Ilaria Tonazzini
Valentina Tozzini
Filippo Troiani
Daniele Varsano
Stefano Veronesi
Leonardo Viti
Miriam Vitiello
Laura Zanetti Polzi
Valentina Zannier
Simone Zanotto

Cnr Nano Post Docs

Bamidele Ibrahim Adetunji
Lucia Angella
Matteo Archimi
Mahdi Asgari
Seyedehsamaneh Ataei
Michael Ontita Atambo
Lorenzo Baldacci
Antonella Battisti

Luca Chirolli
Rajiv Kumar Chouhan
Elena Corradi
Eugenio Damiano
Ambra Del Grosso
Nils Dessmann
Mariacristina Gagliardi
Katia Garrasi
Gabriel José Gil Pérez
Claudio Guarcello
Stefano Guiducci
Silvia Landi
Stefano Lumetti
Giampiero Marchegiani
Maria Celeste Maschio
Luca Masini
Andrea Mescola
Pierpaolo Minei
Aldo Moscardini
Gabriele Parlanti
Vinoshene Pillai
Alberto Portone
Mirko Rocci
Luca Salemi
Sedighe Salimian
Laura Sercia
Alberto Sottile
Nicola Spallanzani
Adam Dominik Szukalski
Francesca Telesio
Francesco Trovato
Leonardo Vicarelli
Avinash Vikatakavi
Pauli Virtanen
Francesco Vischi
Jihua Xu

Affiliated researchers

Marco Affronte
Andrea Alessandrini

Maria Allegrini
Pier Alberto Benedetti
Giuliano Benenti
Roberto Biagi
Pietro Bonfà
Paolo Bordone
Marilia Junqueira Caldas
Francesco Cardarelli
Franco Carillo
Giovanni Carlotti
Ciro Cecconi
Francesco Ciccarello
Stefano Corni
Sergio D'Addato
Elena Degoli
Valentina De Renzi
Alberto Di Lieto
Sebastiano Di Pietro
Daniele Ercolani
Rosario Fazio
Stefano Frabboni
Anna Maria Garbesi
Marco Gibertini
Vittorio Giovannetti
Guido Goldoni
Giuseppe Grosso
Khatuna Kakhiani
Alessandro Lascialfari
Stefano Luin
Rita Magri
Franca Manghi
Claudia Menozzi
Elisa Molinari
Stefano Ossicini
Gioacchino Massimo Palma
Pasqualantonio Pingue
Dario Pisignano
Maria Clelia Righi
Rosaria Rinaldi
Stefano Roddaro
Francesco Rossella
Davide Rossini

Alberto Rota
Alice Ruini
Alessandra Toncelli
Mauro Tonelli
Giovanni Tosi
Alessandro Tredicucci
Sergio Valeri
Giampaolo Zuccheri

Affiliated Post Docs

Matteo Agostini
Claudio Bonizzoni
Vittorio Buccheri
Francesco Colangelo
Francesco Delfino
Antonella De Pasquale
Mariagrazia Di Luca
Sutapa Dutta
Dayong Fan
Elisa Giovannetti
Andrea Mari
Cecilia Masciullo
Paola Morici
Enrico Pracucci
Paolo Restuccia
Luigi Romano
Giovanni Signore

Affiliated PhD students

Alina Adamow
Omer Arif
Luca Basta
Bibek Bhandari
Simone Biasco
Gianmichele Blasi
Miki Bonacci
Lennart Bours
Tommaso Cavallucci

Nicola Cavani
Dhawal Choudhary
Luigi Cigarini
Dario Cilluffo
Samuele Cornia
Olga Cozzolino
Stefano Cusumano
Naeimeh Eghbali Fam
Paolo Andrea Erdman
Giulio Fatti
Giulia Fiaschi
Jacopo Fregoni
Davide Giambastiani
Gina Greco
Alberto Guandalini
Michele Guerrini
Sara Khorshidian
Abhishek Kumar
Didi Lamers
Dario Alejandro Leon Valido
Nicola Melchioni
Roberta Mezzena
Gabriele Nardi
Andrea Ottomaniello
Jacopo Stefano Pelli Cresi
Francesco Pisani
Domenic Prete
Claudio Puglia
Frank Ernesto Quintela Rodriguez
Gregorio Ragazzini
Giulia Righi
Paolo Rosi
Cinzia Scorzoni
Giacomo Sesti
Eleonora Spurio
Simone Vacondio
Federico Venturi
Isha Verma
Matteo Zanfrognini

Administrative staff

Maria Grazia Angelini
Michela Balderi
Elisa Bognesi
Michele Corradi
Giovanna Diprima
Sandro Guerrazzi
Patrizia Pucci
Federica Sighinolfi
Anna Grazia Stefani

Technical staff

Maria Bartolacelli
Davide Calanca
Daniele Desiati
Maria Jesus Rodriguez Douton
Luisa Neri
Riccardo Pallini
Maddalena Scandola
Sureeporn Uttiya

Support Staff in Genova

Alberto Arnone
Matilde Bolla
Barbara Cagnana
Enrico Camauli
Marco Campani
Paolo Ciocia
Paola Corezzola
Monica Dalla Libera
Roberta De Donatis
Piero Di Lello
Fabio Distefano
Francesca Fortunati
Maria Carla Garbarino
Giuseppe Genovese
Danilo Imperatore Antonucci
José Carlos Manganaro
Diletta Miceli
Elisabetta Narducci
Marco Punginelli
Liliana Sciacaluga
Simone Spinozzi

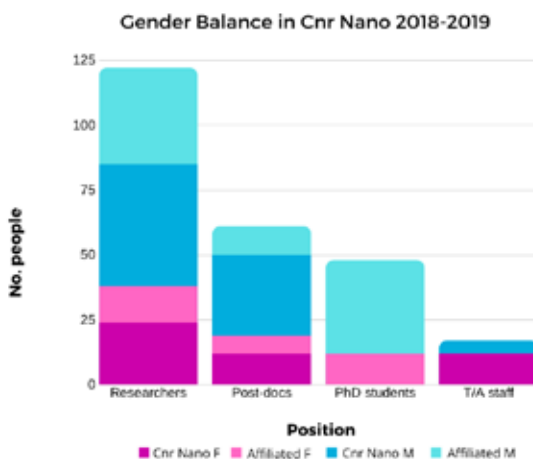


Image credits

Cover image **PeakForce Tapping® AFM image of surface-assembled amyloid fibrils obtained with a model peptide for Alzheimer disease.**

Courtesy of Giampaolo Zuccheri (Cnr Nano Modena).

p. 5 (FTBIO) **Confocal image of mouse hippocampal neurons grown on 10 µm tracks of fluorescent poly-L-lysine; the biochemical gratings were fabricated by micro-contact printing.**

Courtesy of Ilaria Tonazzini (Cnr Nano Pisa).

p. 19 (PHOTO) **SEM image of Free-standing single crystal InSb Nanoflags grown by Au-assisted Chemical Beam Epitaxy.**

Courtesy of Isha Verma (Cnr Nano Pisa).

p. 33 (SSQT) **InAs/InP/GaAsSb Core dual-shell NW based multifunctional devices with two parallel opposite doped channel separated with InP barrier.**

Courtesy of Sedighe Salimian (Cnr Nano Pisa).

p. 55 (SURF) **Atomic resolution image of a Cu_{3-x}P nanocrystal in [001] orientation.**

Courtesy of Giovanni Bertoni (Cnr Nano Modena).

p. 69 (THEO) **Azobenzene chromophore brought to the strong light-molecule coupling regime by the resonance with a plasmonic nanocavity.**

Courtesy of Jacopo Fregoni (Cnr Nano Modena).

p. 87 (Projects) Courtesy of William Guerrieri.

Finito di stampare nel mese di aprile 2020.

Progetto editoriale: Luisa Neri, Cnr Nano.

Progetto grafico: mediamo.net, Modena.

